I. THE KINETICS OF THE REACTIONS OF SILVER, LEAD, AND THALLIUM WITH THIOACETAMIDE

II. THE DISTRIBUTION OF BARIUM, TITANIUM, MANGANESE, CHROMIUM, IRON, NICKEL AND COBALT IN STONY METEORITES

Thesis by

Carleton Bryant Moore

In Partial Fulfillment of the Requirements
for the Degree of
Doctor of Philosophy

California Institute of Technology
Pasadena, California

1960

Acknowledgments

I wish to express my appreciation to Professors Ernest H. Swift and Harrison Brown for the advice and interest that they have given me during the experimental work and the preparation of this thesis.

I sincerely thank Professor E. C. Krinov of the USSR Academy of Sciences and Mr. E. P. Henderson of the United States National Museum for providing samples of many of the chondrites studied.

I am deeply indebted to the California Institute of Technology for teaching assistantships for the academic years 1955-1957, and to the Atomic Energy Commission for research assistantships for the academic years 1957-1959. I appreciate the 1958 summer fellowship provided by E. I. duPont de Nemours and Company, and the summer grants provided by Dr. Brown in 1957 and 1959.

Special thanks are due Miss Elisabeth Godijn and Mr. Arthur Chodos for their aid in developing the analytical procedures used in the last two parts of this thesis. I extend my thanks to Dr. Dwight M. Smith and other members of the Chemistry and Geological Sciences Divisions for their help and enlightening discussions.

To

Lesley B. Hoyer

Ludlum School, Hempstead, New York

and

Louis A. Weinland

Alfred University

Abstract

The precipitation of silver from acid solutions by thioacetamide at 60°C was investigated. Below pH 2 the reaction takes place predominantly by the hydrolysis of thioacetamide to form hydrogen sulfide. Above pH 2 a direct reaction between the silver and thioacetamide has a significant effect. The direct reaction rate equation was found to be

$$-\frac{d[Ag(I)]}{dt} = \frac{k''[Ag(I)]}{[H^+]^{1/2}\,[CH_3CSNH_2]^3} \quad .$$

At 60°C in a malonic acid - 0.1 VF sodium hydrogen malonate buffer k'' is 8.6×10^{-7} mole$^{7/2}$ liter$^{7/2}$ minute^{-1}.

The presence of chloride ion inhibits the rate of direct reaction between lead and thioacetamide. The reaction is first order with respect to $PbCl^+$ and about 50% slower than with Pb^{++} at 90°.

Thallous sulfide is precipitated by thioacetamide by both hydrolysis and direct reactions. The direct reaction is second order with respect to thallium, first order with respect to thioacetamide and probably inverse half order with respect to hydrogen ion.

The concentrations of barium, manganese and titanium have been determined spectrographically in 94 stony meteorites. There appear to be four barium concentration groups with median barium concentrations of 5, 10, 25 and 150 ppm. For the falls the average concentrations of manganese and titanium are 0.260 $\pm$ 0.028% and 0.064 $\pm$ 0.008%. For the finds the manganese content is 0.235 $\pm$ 0.023% and the titanium

content is 0.059 $\pm$ 0.007%. The presence of grouping in chondrites has been confirmed by X-ray fluorescence spectroscopic analysis.

Table of Contents

PART	TITLE	PAGE
Acknowledgments		i
Abstract		iii
Table of Contents		v
I	The precipitation of silver from acid solutions by thioacetamide	1
II	The effect of chloride ion on the direct reaction between lead and thioacetamide	24
III	The precipitation of thallous sulfide by thioacetamide	35
IV	The spectrographic determination of barium, manganese and titanium in stony meteorites	42
V	The determination of manganese, chromium, iron, nickel and cobalt in chondrites by X-ray fluorescence spectroscopy	64
References		103
Propositions		105
References to Propositions		107

Part I. The precipitation of Silver from Acid Solutions by Thioacetamide

In previous investigations of the precipitation of metal sulfides from acid solutions by thioacetamide, Swift and Butler (1) found that the precipitation can proceed by two mechanisms. In solutions with hydrogen ion concentrations greater than about 10^{-3}M., the rate of precipitation of lead sulfide was controlled by the hydrolysis of thioacetamide. However, the precipitation of lead sulfide at lower hydrogen ion concentrations was governed by a direct reaction which was dependent upon the lead ion and upon the thioacetamide concentration to the first order, and on the hydrogen ion concentration to the inverse half order. In the precipitation of arsenic(III) only evidence for the hydrolysis controlled reaction was found (2). This investigation was undertaken to observe the effect of substituting a unipositive element, Ag^{+}, on the reaction rate expressions, and to determine the optimum conditions in which thioacetamide can be used to precipitate and separate silver.

Experimental

Reagents:

Thioacetamide solutions, 1.0 VF (volume formal) were prepared by weight from Arapahoe reagent (lot 1402). The white solid dissolved to give clear, colorless solutions.

Reagent grade chemicals were used for all solutions.

A standard 0.1 VF silver nitrate solution was prepared by weight.

A 0.010 VF potassium thiocyanate solution was standardized against the silver nitrate solution.

A sodium hydrogen malonate-malonic acid buffer was prepared from sodium hydroxide solution and malonic acid. The buffer solution was 1 VF in sodium hydrogen malonate.

Sodium sulfate-sodium hydrogen sulfate buffer solutions were prepared by adding sulfuric acid to one formula weight of sodium sulfate and diluting the solution to one liter.

A 1.0 VF sulfuric acid solution was prepared from concentrated acid and standardized against standard sodium hydroxide.

Apparatus:

The apparatus used for the rate measurements is shown in Figure 1. The reaction tube consisted of a stoppered 38 x 200 mm. lipless test tube. Leading into and reaching to the bottom of the reaction tube was a sintered glass bubbling tube through which samples were forced out. Air drawn in through the bubbling tube aided in mixing the sample and bringing it to thermal equilibrium more rapidly at the start of the reaction. A rubber bulb attached to a short tube passing through the stopper was used to force samples out or pull air in.

The reaction tube was surrounded with a water bath which kept the temperature of the reaction solution at 60 ± 0.5°C. The temperature was controlled by a heating and thermostating unit composed of a bimetallic thermoregulator and a knife heater.

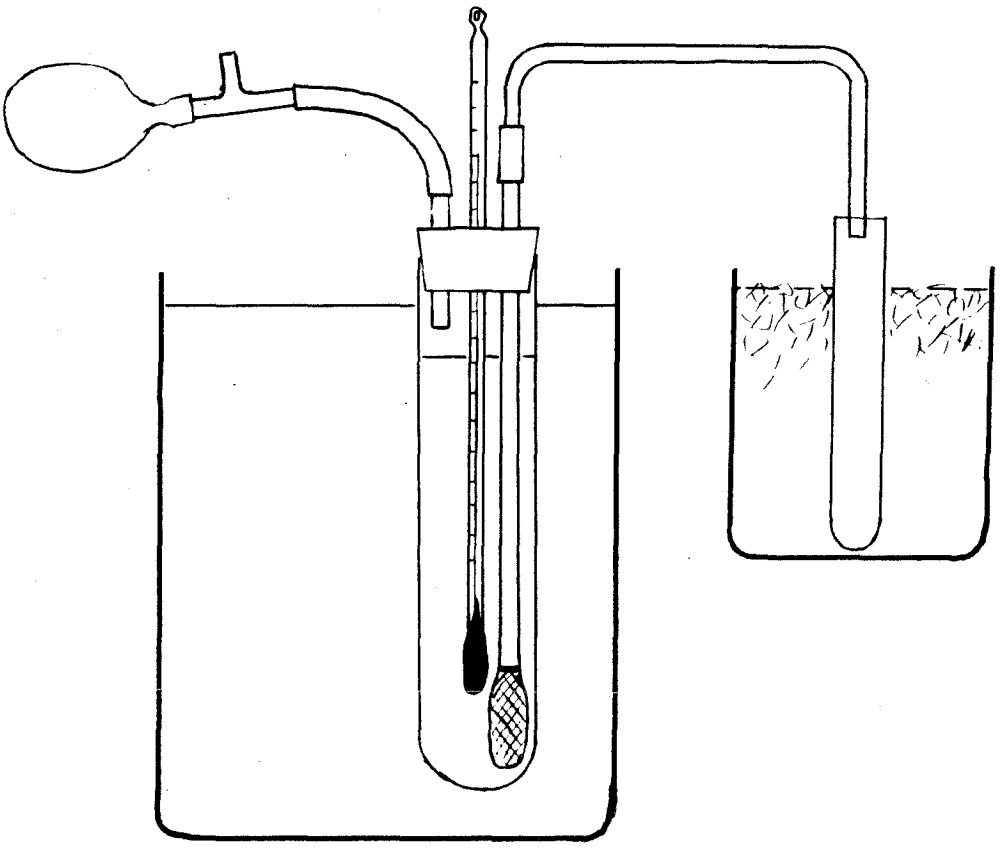

Figure 1. Apparatus.

Procedure:

The reaction solutions were prepared by mixing measured volumes of stock solutions of thioacetamide, buffer and silver nitrate and diluting to 100 ml. with distilled water. The reaction solution was heated to 60°C. in the constant temperature bath.

At timed intervals approximately 10 ml. of solution were forced through the sintered glass bubbler into a sample tube surrounded by an ice bath which quenched the reaction.

The sample was left in the ice bath for 1 to 2 minutes then centrifuged to remove any silver sulfide which passed through the sintered glass. A 5.00 ml. portion of the sample was pipetted from the centrifugate and transferred to a 15 x 125 mm. test tube which contained 1.5 millimoles of sodium hydroxide; this precipitated the silver quantitatively and rapidly. The precipitate of silver sulfide was removed by centrifugation and washed with 2 ml. of hot water which contained 0.1 millimole of sodium hydrogen sulfide.

The silver sulfide was then treated with 2 ml. of 6 VF nitric acid and was heated until it all dissolved. The nitric acid solution was transferred to a 150 ml. beaker, cooled, 1 ml. of 1/3 VF ferric nitrate added, and the solution diluted to 13 ml. A microburet was used to titrate the solution with 0.01 VF potassium thiocyanate.

The pH values of the reaction solutions were determined by preparing a simulated reaction solution without the silver nitrate, heating to 60°C, and measuring the pH with a pH meter.

Data and Discussion

Qualitative experiments indicated that silver, like lead, was precipitated as sulfide by thioacetamide in acid solutions by both the hydrolysis and direct mechanisms. However, the direct mechanism becomes predominant for silver at approximately pH 2 as compared to 3.5 for lead. This is caused by the fact that under the same experimental conditions the rate of the direct reaction of silver with thioacetamide is faster than that of lead. The measurements were made at 60°C. and at pH's from 2.5 to 3.8 in order that the rate of silver sulfide precipitation could be followed conveniently.

Hydrolysis Controlled Precipitation of Silver:

The rate of precipitation of silver was investigated at 60°C. in a solution initially 0.01 VF in silver nitrate, 0.1 VF in thioacetamide, and 0.1N in sulfuric acid. The plot in figure 2 shows that under these conditions, the hydrolysis of thioacetamide is the mechanism predominating in the precipitation of the silver.

If it is assumed that all of the hydrogen sulfide resulting from the hydrolysis reacts rapidly with the silver(I), it is possible to calculate from the rate measurements a value for the hydrolysis reaction rate constant, k', in the reaction rate equation

$$-\frac{d[CH_3CSNH_2]}{dt} = k'[H^+][CH_3CSNH_2] + \frac{k''}{2}\frac{[Ag(I)]}{[H^+]^{1/2}[CH_3CSNH_2]^3},$$

if the effect of the direct reaction is subtracted from the overall rate.

The calculated value for k' is 0.020 ± 0.002 liter $mole^{-1}$ $minute^{-1}$. The value found by Swift and Butler (1) was 0.019 liter $mole^{-1}$ $minute^{-1}$.

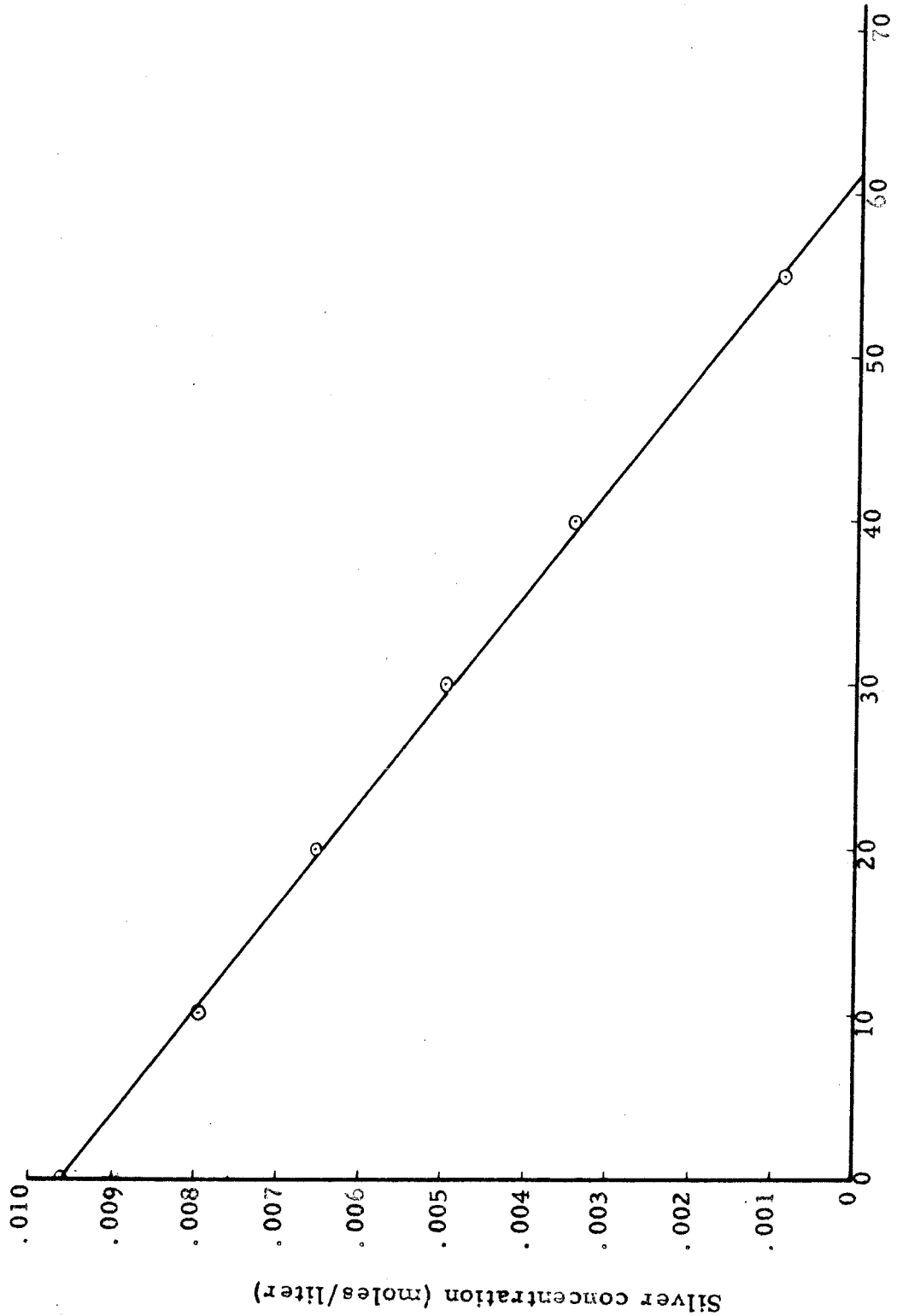

Figure 2. Rate of precipitation of silver in 0.1 NH_2SO_4 and 0.1 VF thioacetamide at 60°C.

Precipitation by the Direct Reaction:

Sodium sulfate-sodium hydrogen sulfate buffers were used in experiments at pH values of 2.47, 2.7, 3.45, and 3.8. The results were checked in a malonic acid-sodium hydrogen malonate buffer at a pH of 2.8.

At these hydrogen ion concentrations both the direct and hydrolysis mechanisms are significant. The data were analyzed by the differential method.

The reaction rate equation was assumed to be the sum of the direct and hydrolysis mechanisms and have the form

$$-\frac{d[Ag(I)]}{dt} = \frac{k_1[Ag(I)]^n[CH_3CSNH_2]^m}{[H^+]^p} + 2k'[H^+][CH_3CSNH_2] \quad (1)$$

where k' is the second order hydrolysis rate constant, 0.019 liter $mole^{-1}$ $minute^{-1}$ at 60°C., found by Swift and Butler. The experimental rate data were plotted on rectangular coordinate paper, and the slopes of the tangents to the resulting curves were determined at appropriate points. The rate of the hydrolysis reaction was calculated and subtracted from the overall rate to find the rate of the direct reaction at each point desired.

Effect of Silver Ion Concentration:

The rate of the direct reaction was taken at several silver concentrations on each concentration-time plot. Figure 3 is a plot of the logarithm of the direct reaction rate against the logarithm of silver concentration for two typical experiments.

It can be seen that the initial slope of the curves is one, indicating that n = 1 in equation 1 above. After about half the silver(I) has been precipitated the slope becomes greater, and in run No. 10 even reaches a value of two. For this reason, if the data are treated by the integral method, the reaction appears to be second order, while in reality the initial rate of reaction is first order.

In order to determine the initial direct rate of reaction, the direct rate of reaction calculated by subtracting the calculated hydrolysis reaction rate from the total rate of reaction was plotted vs Ag(I) at several Ag(I) concentrations for each experimental run. The straight line through the points was extrapolated to the initial silver concentration and the initial direct reaction rate determined. This initial direct reaction rate is used in all following calculations.

The Effect of Hydrogen Ion Concentration:

The effect of the hydrogen ion concentration was studied with solutions in which the concentrations of thioacetamide and buffer were essentially constant. Figure 4 is a plot of the logarithm of the hydrogen ion concentration. The slope of the line is -0.52 which indicates that the hydrogen ion concentration has a half order inhibition effect on the direct rate of precipitation of silver sulfide. This is the same effect that Swift and Butler observed in the precipitation of lead sulfide.

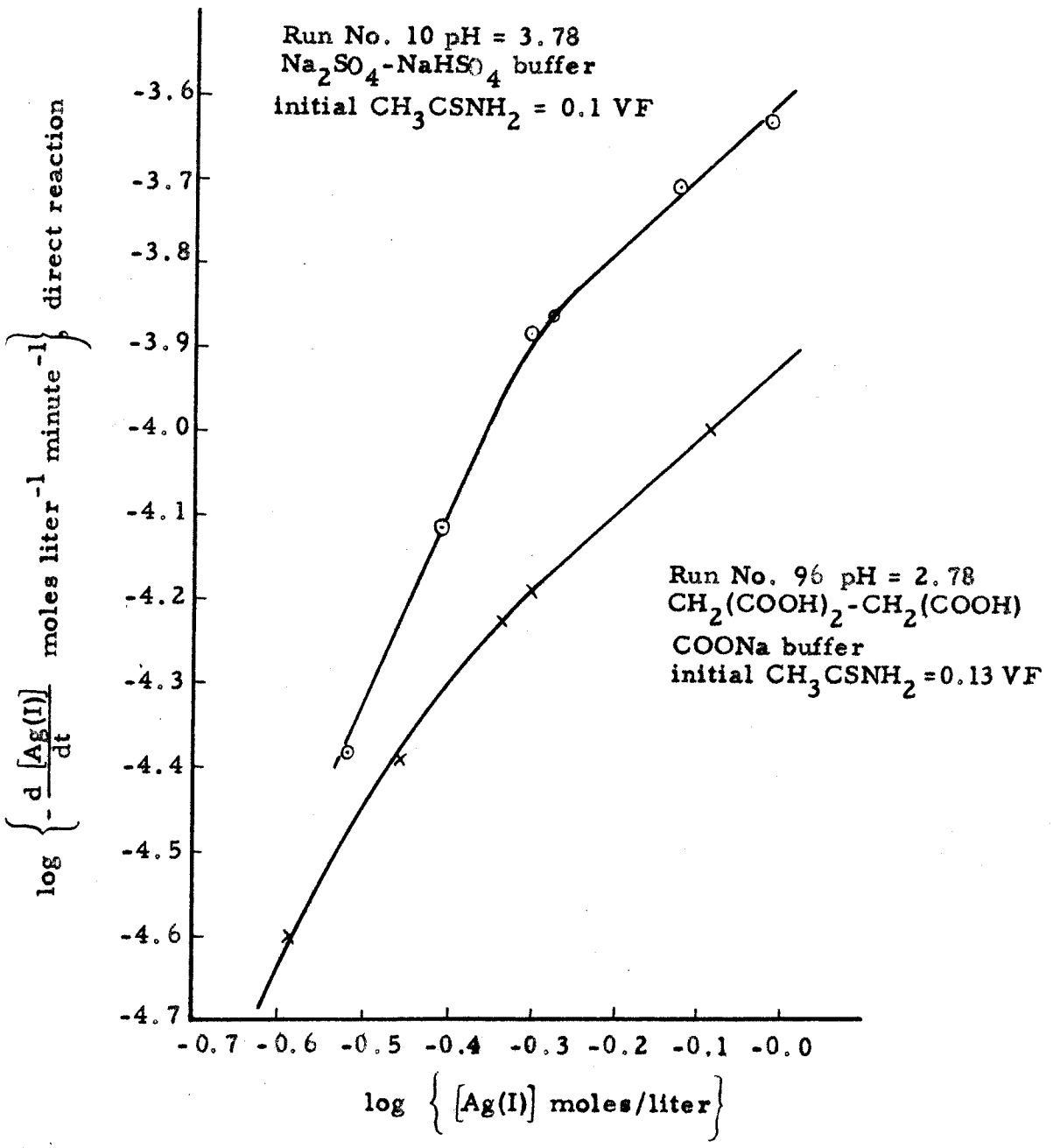

Figure 3. Effect of Silver (I) concentration on the direct rate of silver sulfide precipitation.

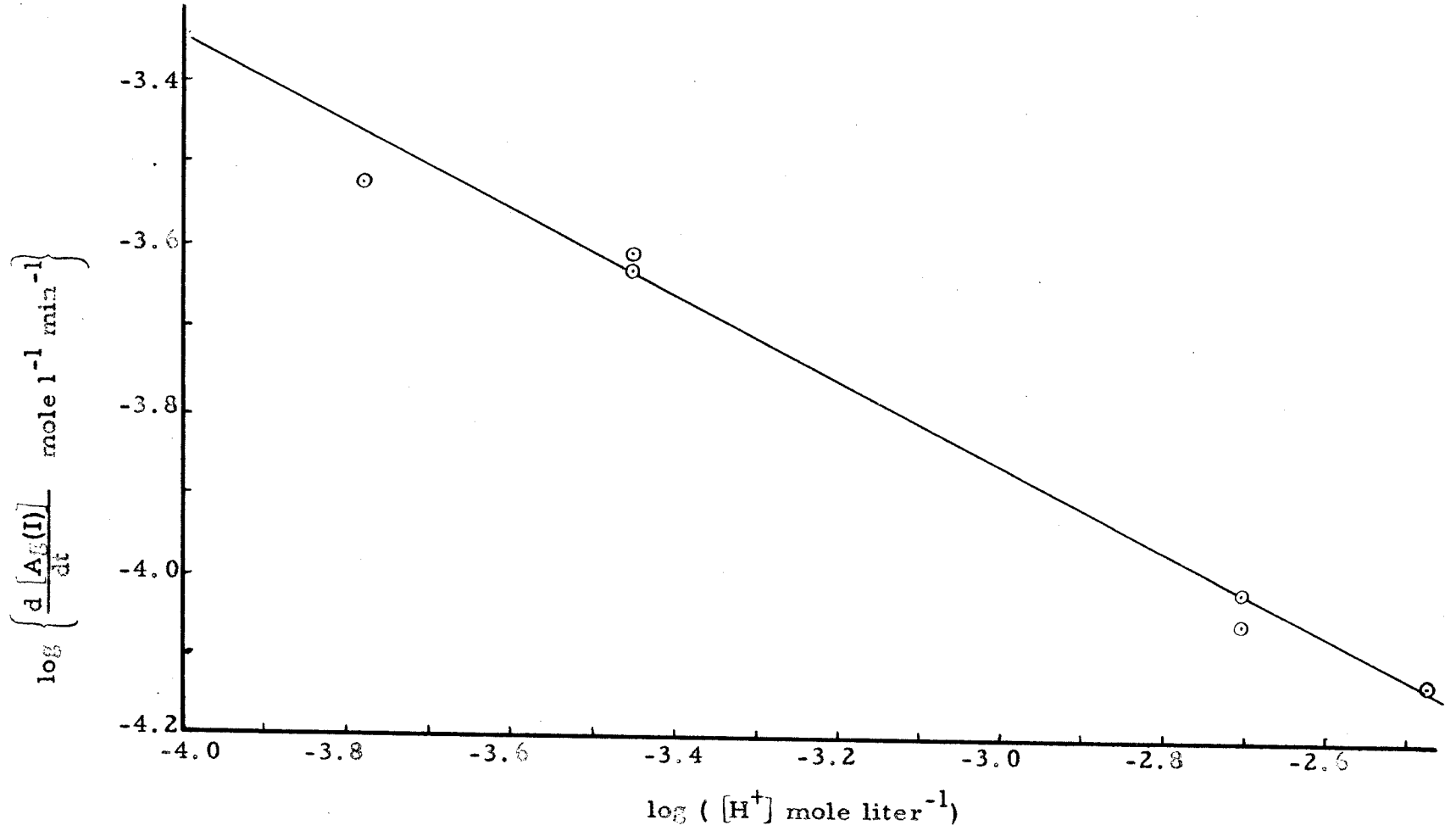

Figure 4. Effect of hydrogen ion concentration on the direct rate of silver sulfide precipitation.

Calculated values of velocity constants for the expression

$$\frac{-d\left[Ag(I)\right]}{dt} = \frac{k_2\left[Ag(I)\right]}{\left[H^+\right]^{1/2}}$$

are presented in Table I, and are constant within the limits of experimental accuracy.

Table I. The effect of hydrogen ion concentration on the rate of precipitation of silver sulfide

pH	$\frac{-d\left[Ag(I)\right]}{dt}$	k_2 (a)
	mole l^{-1} min^{-1}	mole$^{-1/2}$ $l^{1/2}$ min^{-1}
2.47	7.5×10^{-5}	4.4×10^{-4}
2.70	9.2×10^{-5}	4.1×10^{-4}
3.45	2.4×10^{-4}	4.6×10^{-4}
3.78	2.7×10^{-4}	3.7×10^{-4}
	avg	$4.2 \times 10^{-4} \pm 0.3 \times 10^{-4}$

(a) Calculated from $\frac{-d\left[Ag(I)\right]}{dt} = \frac{k_2\left[Ag(I)\right]}{\left[H^+\right]^{1/2}}$

The Effect of Thioacetamide Concentration:

Experiments made with constant initial concentrations of silver nitrate and sodium sulfate-sodium hydrogen sulfate buffer, and different initial concentrations of thioacetamide, showed that the thioacetamide had an inhibiting effect on the reaction rate.

The data on the thioacetamide effect in Table II are plotted in Figure 5 as the logarithm of the initial direct reaction rate vs. logarithm of thioacetamide concentration. At thioacetamide concentrations above 0.05 VF, the curve appears to be a straight line with a slope of -2.7. This indicates that the thioacetamide has a 2.7 order inhibition effect. At concentrations below 0.05 VF thioacetamide the slope of the line decreases indicating a decrease in the inhibition effect of the thioacetamide.

Table II. The Effect of Thioacetamide Concentration on the Direct Reaction Rate

Initial Ag(I) 0.01 VF, pH 2.70, sodium sulfate-sodium hydrogen sulfate buffer, 60°C.

CH_3CSNH_2 moles/liter	-dAg/dt total	-dAg/dt hydrolysis	-dAg/dt direct
	moles liter^{-1} minute^{-1}		
0.02	2.24×10^{-3}	1.4×10^{-6}	2.24×10^{-3}
0.04	9.33×10^{-4}	2.8×10^{-6}	9.30×10^{-4}
0.05	6.06×10^{-4}	3.6×10^{-6}	6.1×10^{-4}
0.08	1.51×10^{-4}	5.9×10^{-6}	1.45×10^{-4}
0.10	1.09×10^{-4}	7.4×10^{-6}	9.2×10^{-5}
0.15	4.29×10^{-5}	1.12×10^{-5}	3.17×10^{-5}

The above results were checked using a malonic acid-sodium hydrogen malonate buffer at pH 2.78. A similar curve was obtained for the thioacetamide dependence. The data are given in Table III and shown in Figure 6. For this buffer system, the thioacetamide dependence is inverse 3.1 order at 0.05 VF thioacetamide and above.

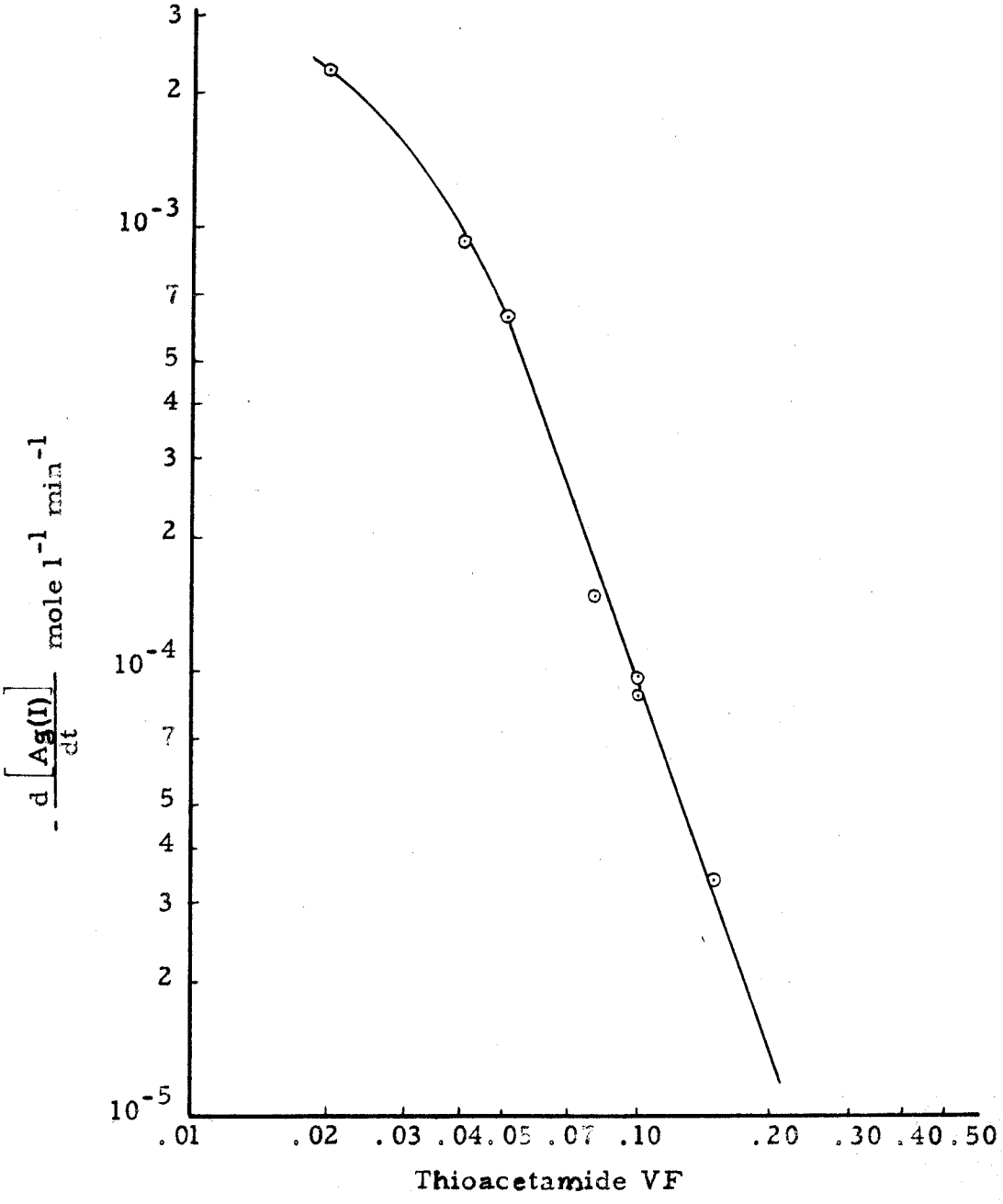

Figure 5. The effect of thioacetamide on the direct rate of precipitation of silver sulfide.

sodium sulfate-sodium hydrogen sulfate buffer pH= 2.72

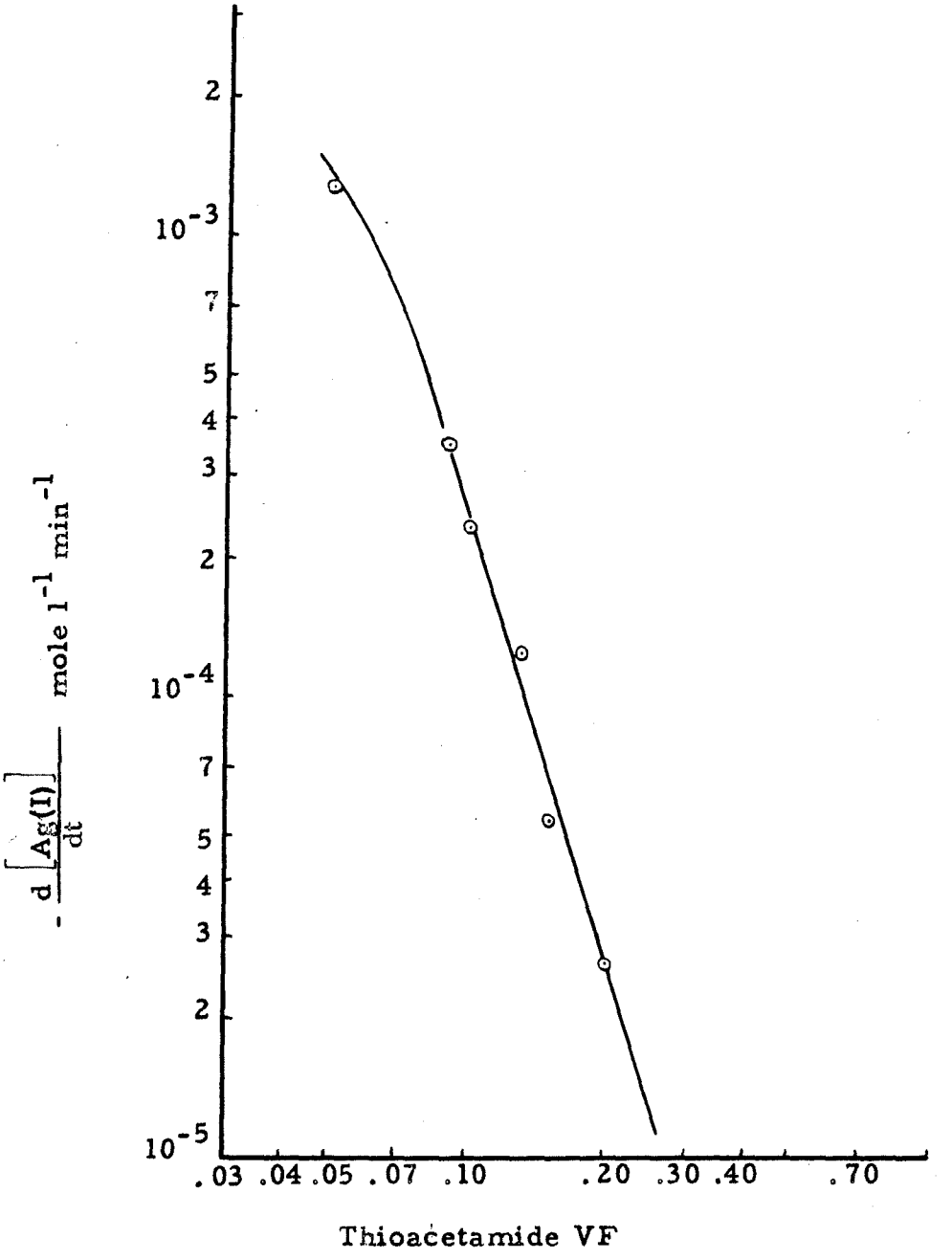

Figure 6. The effect of thioacetamide on the direct rate of precipitation of silver sulfide.

malonic acid-sodium hydrogen malonate buffer pH = 2.78

Table III. The Effect of Thioacetamide Concentration on the Direct Reaction Rate

Initial Ag(I) 0.01 VF, pH 2.78, malonic acid-sodium hydrogen malonate buffer, 60°C.

CH_3CSNH_2 moles/liter	-dAg/dt total	-dAg/dt hydrolysis	-dAg/dt direct
	moles liter^{-1} minute^{-1}		
0.05	1.26×10^{-3}	3.1×10^{-6}	1.26×10^{-3}
0.08	3.51×10^{-4}	4.9×10^{-6}	3.46×10^{-4}
0.10	2.36×10^{-4}	6.2×10^{-6}	2.3×10^{-4}
0.13	1.30×10^{-4}	8.1×10^{-6}	1.22×10^{-4}
0.15	6.27×10^{-5}	9.3×10^{-6}	5.37×10^{-5}
0.20	3.90×10^{-5}	1.25×10^{-5}	2.65×10^{-5}

Complex Formed with Silver and Thioacetamide:

The reaction of silver with thioacetamide is the only sulfide precipitation reaction studied so far in which thioacetamide has an inhibiting effect on the reaction rate. This could be caused by the formation of a stable complex of silver with thioacetamide. The following experiments were done in order to indicate the nature of such a complex.

Effect of Acetamide:

In order to estimate the effect of complexing silver by the $-NH_2$ group, a solution was made up 0.2 VF in acetamide, 0.01 VF in silver nitrate, and 0.1 VF in thioacetamide, at a pH of 2.78 with a malonic acid-sodium hydrogen malonate buffer. The direct rate of reaction

was 2.54×10^{-4} mole liter^{-1} minute^{-1} compared to 2.3×10^{-4} mole liter^{-1} minute^{-1} for the same solution without acetamide. No significant effect was noted.

Chloride Ion Effect:

A series of experiments was planned in order to observe what effect complexing the silver with chloride ion had upon the reaction rate. However, when a solution 5 VF in sodium chloride, 0.005 VF in silver nitrate, and 0.1 VF in thioacetamide was made up, an insoluble precipitate was formed. A semi-quantitative analysis indicated that this precipitate was the complex $Ag[SC(NH_2)CH_3]_4Cl$ described by Cox et al. (3).

It is interesting to note that this complex is so stable that the solution of sodium chloride and thioacetamide will convert freshly precipitated silver sulfide into the complex. If the complex is separated from the precipitating solution and placed in distilled water, decomposition takes place with the formation of silver sulfide.

In order to study the complex under conditions more nearly like those in which the earlier experiments were run, solutions containing varying amounts of thioacetamide and buffer were made up and mixed with freshly precipitated silver sulfide. The mixtures were allowed to stand overnight. Samples of the clear solutions above the silver sulfide were taken and sodium hydroxide was added to each in order to precipitate the silver in solution by its reaction with the excess thioacetamide. The solutions and results are listed in Table IV.

Table IV. The Solubility of Silver Sulfide in Thioacetamide Solutions

CH_3CSNH_2	Buffer pH=2.7	Result of adding NaOH
1.0 VF	none	very light brown color
0.4 VF	0.1 VF SO_4	light brown precipitate
0.8 VF	0.1 VF SO_4	brown precipitate
none	0.1 VF SO_4	none
0.8 VF	0.1 VF $HClO_4$	very light brown color

The silver sulfide appears to be dissolved by the formation of a complex of the silver with thioacetamide. This complex is stabilized by anions present in the buffer. The experiment with perchloric acid shows that ionic strength of effects alone cannot account for the differences in solubility.

A solution initially 0.01 VF in silver nitrate, 0.8 VF in thioacetamide, with a sodium sulfate-sodium hydrogen sulfate buffer of pH 2.5 was made up at room temperature. Upon mixing, a slow precipitation of silver sulfide took place. After ten days the solution was 0.006 VF in silver(I), and no further precipitation of silver was noticeable. All of the silver should have been precipitated by the hydrolysis reaction alone by this time. Hydrogen sulfide could be swept out of the solution by passing air through it. After forty days silver was still in solution and the odor of hydrogen sulfide could easily be detected above it.

These observations indicate that there is a stable complex formed between silver and thioacetamide.

Initial Direct Reaction Rate:

The initial direct reaction rate expression appears to be

$$-\frac{d[Ag(I)]}{dt} = \frac{k''\,[Ag(I)]}{[H^+]^{1/2}[CH_3CSNH_2]^3}$$

at thioacetamide concentrations above 0.05 VF thioacetamide. Values for k'' for the malonic acid buffer are given in Table V.

Table V. Effect of Thioacetamide Concentration on the Rate of Silver at 60°C.

Initial Ag(I) 0.01 VF, pH 2.78 malonic acid-sodium hydrogen malona-te buffer.

CH_3CSNH_2 mole l^{-1}	$\frac{-d[Ag(I)]}{dt}\frac{[H^+]^{1/2}[CH_3CSNH_2]^3}{[Ag(I)]} = k''$ mole$^{3/2}$ $l^{-3/2}$ min^{-1}
0.08	7.2×10^{-7}
0.10	9.4×10^{-7}
0.13	10.6×10^{-7}
0.15	7.4×10^{-7}
0.20	8.6×10^{-7}
	avg $8.6 \pm 1.0 \times 10^{-7}$

The observed inhibition of the reaction by thioacetamide may be explained by assuming that the reacting species is $Ag(CH_3CSNH_2)^+$, that the predominant form of silver in solution is $Ag(CH_3CSNH_2)_4^+$, and that the following reactions occur in solution:

$$Ag(CH_3CSNH_2)_4^+ \rightleftharpoons Ag(CH_3CSNH_2)_3^+ + CH_3CSNH_2 \quad \text{fast,}$$

$$Ag(CH_3CSNH_2)_3^+ \rightleftharpoons Ag(CH_3CSNH_2)_2^+ + CH_3CSNH_2 \quad \text{fast,}$$

$$Ag(CH_3CSNH_2)_2^+ \rightleftharpoons Ag(CH_3CSNH_2)^+ + CH_3CSNH_2 \quad \text{fast,}$$

$$Ag(CH_3CSNH_2)^+ \longrightarrow\longrightarrow Ag_2S \quad \text{slow,}$$

To a first approximation the concentration of the reacting species would be

$$[Ag(CH_3CSNH_2)^+] = \frac{k[Ag(CH_3CSNH_2)_4^+]}{[CH_3CSNH_2]^3} = \frac{k[Ag(I)]}{[CH_3CSNH_2]^3}.$$

Since

$$\frac{-d[Ag(I)]}{dt} = \text{const. } [Ag(CH_3CSNH_2)^+], \text{ then}$$

$$\frac{-d[Ag(I)]}{dt} = \frac{\text{const. } k\ Ag(I)}{(CH_3CSNH_2)^3}$$

The decrease in the thioacetamide inhibition effect at lower thioacetamide concentrations occurs because there is not enough thioacetamide present for $Ag(CH_3CSNH_2)_4^+$ to be the predominant species.

Effect of Buffer Concentration:

In addition to the runs made with the malonic acid-sodium hydrogen malonate and sodium sulfate-sodium hydrogen sulfate buffers, a run was made with double the concentration of sodium sulfate-sodium hydrogen sulfate buffer. The conditions and results are shown in Table VI.

Table VI. The Effect of Buffer on the Direct Reaction Rate

Buffer	pH	dAg/dt initial	k'' (a)
malonic acid-0.1M $NaHC_3H_2O_4$	2.78	2.3×10^{-4}	9.4×10^{-7}
$NaHSO_4$-0.1M Na_2SO_4	2.70	9.6×10^{-5}	4.3×10^{-7}
$NaHSO_4$-0.2M Na_2SO_4	2.70	6.4×10^{-5}	2.9×10^{-7}

(a) Calculated from

$$-\frac{d\left[Ag(I)\right]}{dt} = k'' \frac{\left[Ag(I)\right]}{\left[H^+\right]^{1/2}\left[CH_3CSNH_2\right]^3}$$

It is apparent from this data that the type and concentration of buffer used has a significant effect on the reaction rates.

Temperature Effect:

The rates of the direct reaction in solutions initially 0.02 VF in silver nitrate and 0.10 VF in thioacetamide with the same buffer solution were determined at 31, 45 and 61°C. Differences in the pH of the buffer at the different temperatures were taken into account in calculating the velocity constant k'' for the reaction.

Values of the hydrolysis constant for thioacetamide were found by extrapolating Swift and Butler's data to lower temperatures. In Table VII are shown the results and calculations for these experiments. Figure 7 is a plot of logarithm k'' vs temperature^{-1} and shows an Arrhenius temperature dependence. The activation energy is calculated from the slope to be 22.4 kcal. per mole.

Table VII. Temperature Effect on the Rate of Reaction of Silver with Thioacetamide

Temp °C.	H mole/l	k'[(a)] hydrolysis	dAg/dt[(b)] total	dAg/dt hydrolysis	dAg/dt direct	k''[(c)]
			mole liter^{-1} minute^{-1}			mole$^{1/2}$ l$^{-1/2}$ min^{-1}
31	3.3×10^{-4}	9×10^{-4}	7.5×10^{-6}	6×10^{-8}	7.4×10^{-6}	1.35×10^{-8}
45	2.5×10^{-4}	4.3×10^{-3}	3.0×10^{-5}	2×10^{-7}	3.0×10^{-5}	4.75×10^{-8}
61	1.6×10^{-4}	1.9×10^{-2}	2.4×10^{-4}	6×10^{-7}	2.4×10^{-4}	3.0×10^{-7}

(a) hydrolysis constant from equation $\frac{d\left[CH_3CSNH_2\right]}{dt} = k'\left[H^+\right]\left[CH_3CSNH_2\right]$ values from Swift and Butler (1).

(b) At Ag = 0.01 VF, CH_3CSNH_2 = 0.1 VF.

(c) Reaction rate constant for expression

$$-\frac{d\left[Ag(I)\right]}{dt} = k'' \frac{\left[Ag(I)\right]}{\left[H^+\right]^{1/2}\left[CH_3CSNH_2\right]^3} .$$

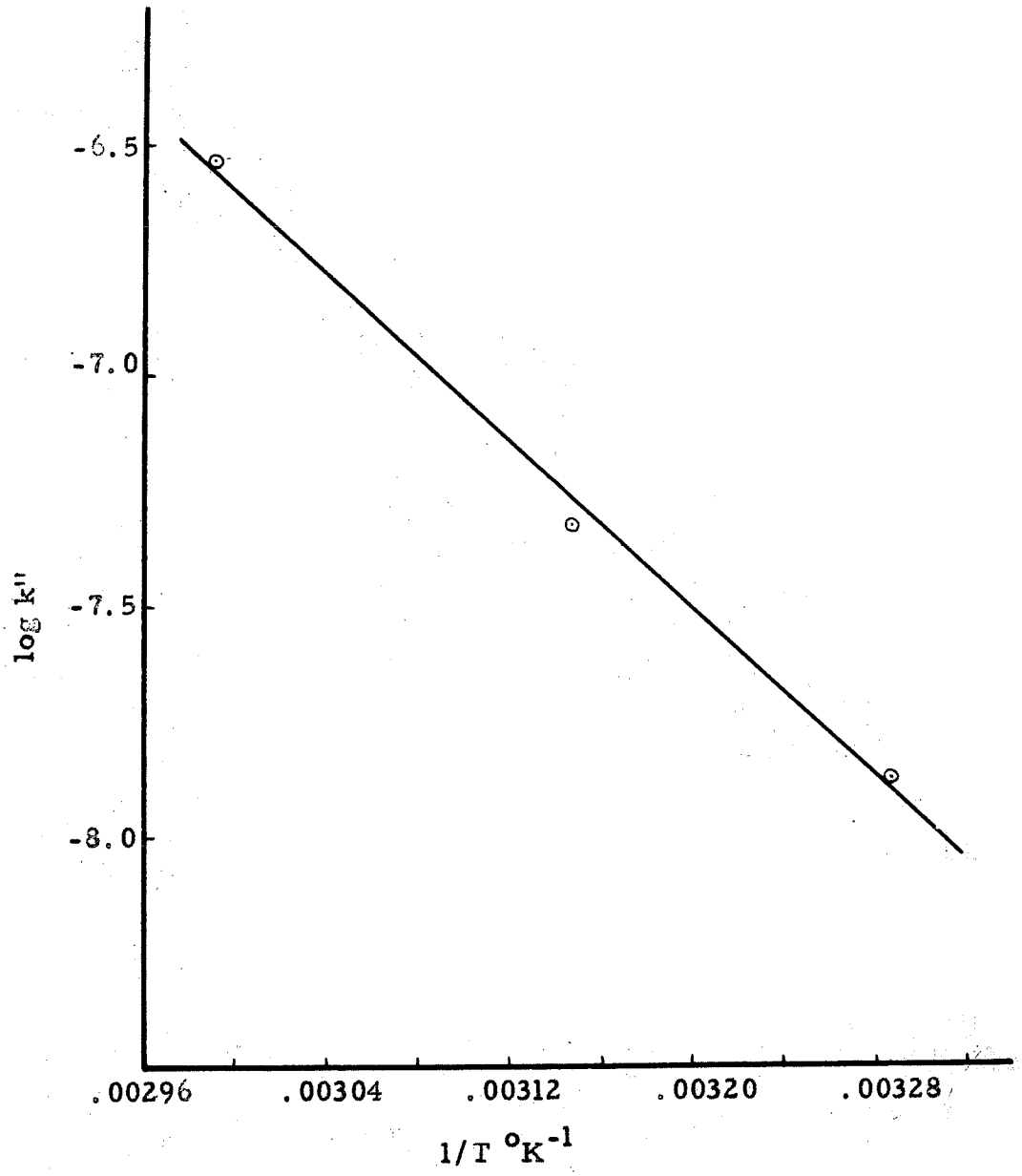

Figure 7. Rate of precipitation of silver sulfide as a function of temperature.

Overall Reaction:

Since the conditions in the reaction solutions are known only at the beginning of each run, for the purpose of comparison, the rate equation can best be expressed as an initial rate equation.

The initial rate equation appears to have the form

$$-\frac{d\left[Ag(I)\right]}{dt} = \frac{k''\left[Ag(I)\right]}{\left[H^+\right]^{1/2}\left[CH_3CSNH_2\right]^3} + 2k'\left[H^+\right]\left[CH_3CSNH_2\right]$$

where the best values for k' and k'' are 1.9×10^{-2} liter mole^{-1} minute^{-1} and 8.6×10^{-7} mole$^{3/2}$ liter$^{-3/2}$ minute^{-1}, respectively.

When comparing the rates of reaction of different metals with thioacetamide it must be remembered that the data are unique for the buffer conditions in which the individual determinations were made.

Analytical Considerations:

The results of this investigation point out more vividly than in any previous experiments the fallacy in assuming that thioacetamide can be used as a direct replacement for hydrogen sulfide.

With solutions at 90°C. and 0.1 VF in thioacetamide, the rate of the direct reaction of silver with thioacetamide is thirty times the rate of the direct reaction of lead with thioacetamide, in spite of the inhibiting effect of the thioacetamide; with 0.05 VF thioacetamide solutions, silver reacts 500 times faster than lead. This great difference in the rate of reaction could possibly be used in separations if no significant coprecipitation occurs.

The fast rate of direct reaction of silver with low concentrations of thioacetamide in acid solution should make the development of a method similar to the potentiometric titration of the thiosulfate complex of silver in alkaline solutions with thioacetamide developed by Bush et al. (4) possible under more varied conditions. The thioacetamide must be the reagent added in small quantities, for if silver nitrate were added to a thioacetamide solution the reaction would not be fast because of the stable complex formed.

Part II. The Effect of Chloride Ion on the Direct Reaction Between Lead and Thioacetamide

In an investigation of the reaction between lead and thioacetamide, Swift and Butler (1) found that lead sulfide was precipitated from acid solutions by two different reactions. In one the rate of precipitation of lead followed the acid catalysed hydrolysis of thioacetamide. The other was a direct reaction between the lead and thioacetamide. In an investigation of the reaction of arsenic(III) with thioacetamide, the same authors found no evidence for a direct reaction between the arsenic(III) and thioacetamide. Arsenic(III) exists as an anionic species under the conditions involved. This investigation was undertaken to determine the effect of changing the ionic species of the lead on the rate of precipitation of lead sulfide by thioacetamide by the direct mechanism.

Experimental

Reagents:

A standard 0.015 VF (volume formal) potassium dichromate solution was prepared by weight. A 0.1 VF sodium thiosulfate solution was standardized against the standard potassium dichromate.

Thioacetamide solutions, 1.0 VF, were prepared from Arapahoe reagent grade thioacetamide.

A lead nitrate solution, 0.5 VF, and a 1.0 VF sodium chloride solution were prepared by weight.

Sodium formate-formic acid buffer solutions, 0.081 M. in sodium

formate, were prepared from a 0.2 VF sodium hydroxide solution and 90% formic acid.

A 1.0 VF sodium perchlorate solution for the control of ionic strength was made by neutralizing standard perchloric acid with sodium hydroxide to a pH of 7, measured with a pH meter.

Reagent grade chemicals were used throughout the investigation.

Apparatus:

The reaction apparatus and sampling device were the same as those used by Swift and Butler (1).

Procedure:

The reaction solutions were prepared by mixing measured volumes of stock solutions of thioacetamide, buffer, sodium perchlorate, lead nitrate, and sodium chloride and diluting to 100 ml. with distilled water. The reaction solution was placed in a constant temperature bath at $90 \pm 1^{\circ}C$.

After the reaction solution had thermally equilibrated, approximately 10 ml. of the solution were forced through the sintered glass bubbler from the reaction tube into a sample tube at timed intervals. The sample tube was surrounded by an ice bath which quenched the reaction.

The sample was then centrifuged to remove any lead sulfide which passed into the sample tube. A 5.00 ml. sample was pipetted from the centrifugate and transferred to a test tube which contained 1.5 millimoles of sodium hydroxide. The precipitated lead sulfide was

removed by centrifugation and washed twice with two milliliter portions of hot water which contained 0.1 millimole of sodium hydrogen sulfide.

The lead sulfide was dissolved in 0.5 ml. of hot 12 VF hydrochloric acid, which was then evaporated to dryness under a heat lamp. The lead chloride was dissolved in hot acetic acid-sodium acetate solution, and an excess of potassium dichromate was added to precipitate lead chromate. This was removed by filtration and by washing with a hot dilute solution of sodium acetate. The lead chromate was dissolved in 15 ml. of 1 VF hydrochloric acid saturated with sodium chloride. The dichromate was determined iodometrically; a microburet was used for the titration with sodium thiosulfate.

Data and Discussion

Experimental runs were made at a pH of 4.0 to ensure that the direct mechanism for the reaction between lead and thioacetamide was the predominant one. The reaction solutions were initially 0.1 VF in thioacetamide, 0.01 VF in lead nitrate, and varied from 0 to 0.14 VF in sodium chloride. The ionic strength was adjusted with sodium perchlorate to 0.251 M. One experimental run was made which was 0.575 VF in sodium chloride, and was therefore of higher ionic strength. These reactions were run at 90°C. to give a conveniently measurable rate.

It was found that the presence of chloride ion decreased the rate of precipitation of lead sulfide by the direct reaction between lead(II) and thioacetamide in acid solution.

Plots were made of the lead(II) concentration vs time. From these plots, values of $-d\left[Pb(II)\right]/dt$ were determined at various lead(II) concentrations. Plots of $-d\left[Pb(II)\right]/dt$ vs lead(II) are shown in Figure 8. All of the plots are linear indicating that the overall rate of reaction is first order with respect to lead(II).

For use in the calculations which follow all of the lines have been extended to the initial lead concentration, 0.01 VF. Values for the constant k_3 calculated from the equation

$$-\frac{d\left[Pb(II)\right]}{dt} = k_3\left[Pb(II)\right]$$

at the beginning of each reaction are given in Table VIII and plotted vs chloride(I) in Figure 9.

Table VIII. The Effect of Chloride Ion on the Direct Reaction Between Lead(II) and Thioacetamide in Acid Solution

Initial CH_3CSNH_2 = 0.1 VF, $PbNO_3$ = 0.01 VF, pH = 4.0, μ = 0.251 M.

Cl (I) VF	$d\left[Pb(II)\right]/dt$ initial mole l^{-1} min^{-1}	k_3 [(a)] $minute^{-1}$
0	4.35×10^{-4}	4.35×10^{-2}
0.02	3.72×10^{-4}	3.72×10^{-2}
0.04	3.28×10^{-4}	3.28×10^{-2}
0.10	2.67×10^{-4}	2.67×10^{-2}
0.14	2.40×10^{-4}	2.40×10^{-2}
0.575 [(b)]	0.45×10^{-4}	0.45×10^{-2}

(a) calculated from $d\left[Pb(II)\right]/dt = k_3\left[Pb(II)\right]$.

(b) ionic strength greater than 0.251 M.

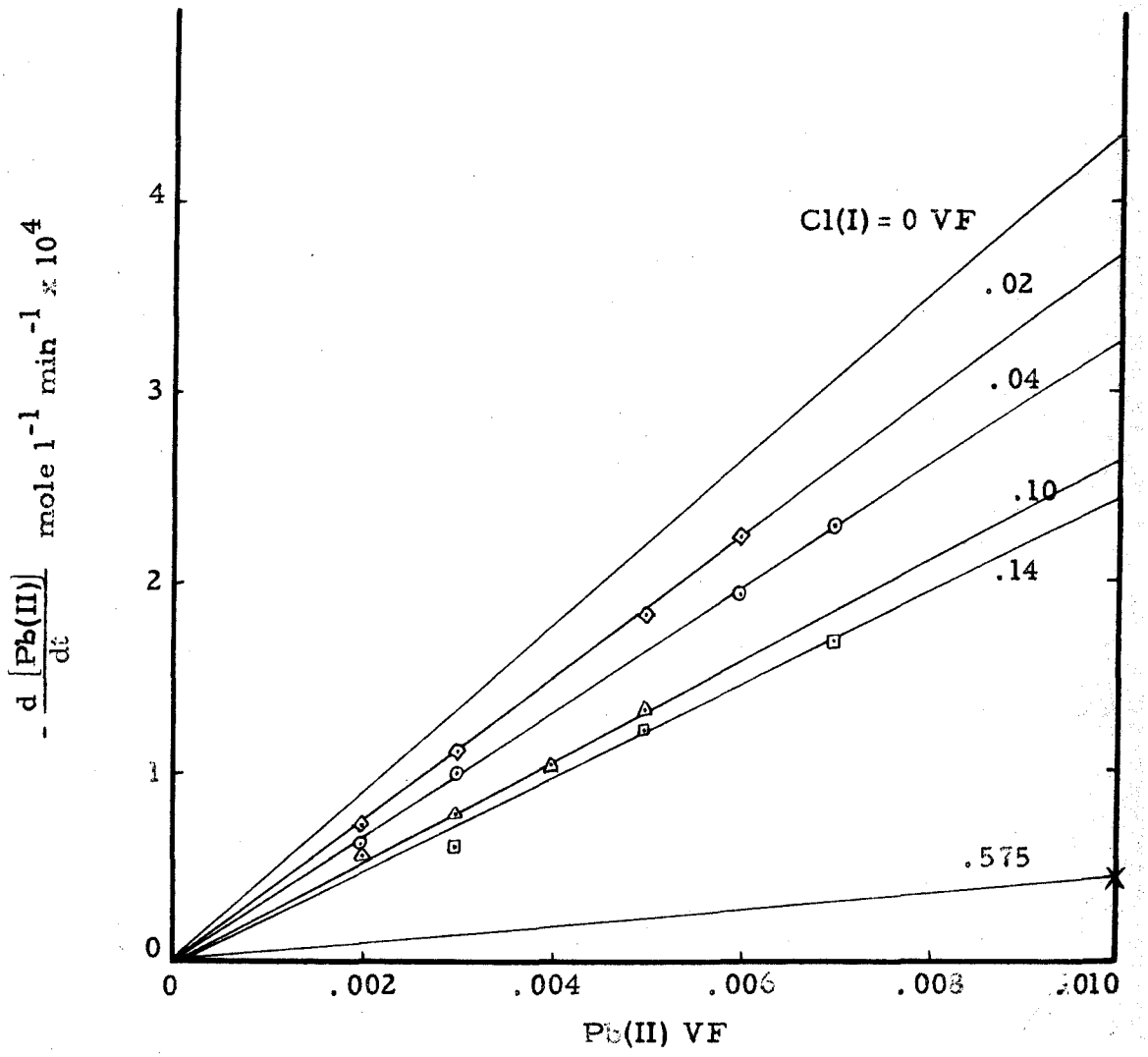

Figure 8. Rate of reaction of Pb(II) with thioacetamide vs tital lead concentration at various chloride concentrations.

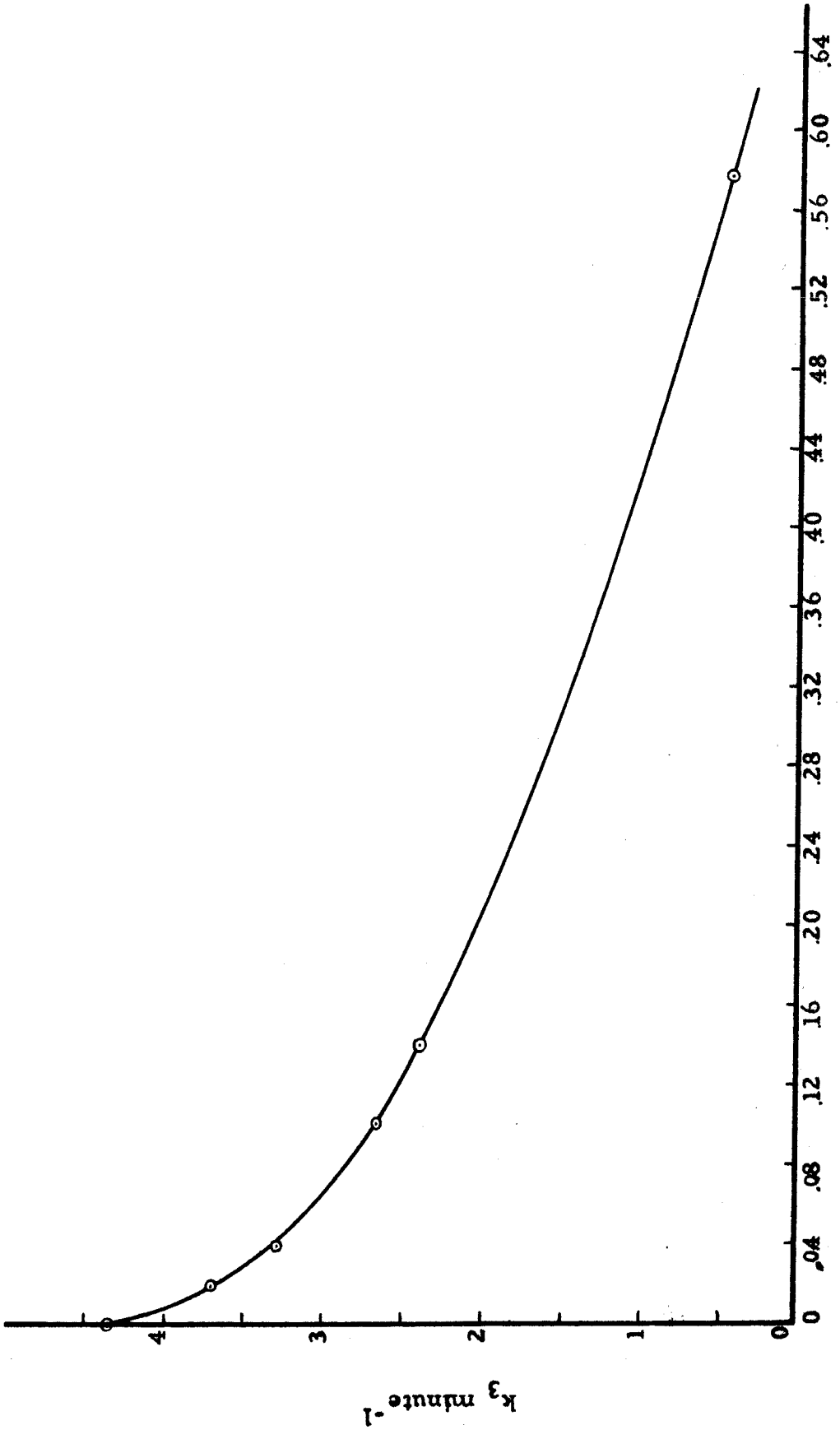

Figure 9. The effect of chloride on the direct rate of reaction.

If it is assumed that the lead monochloride and higher complexes of lead do not react at a significant rate with thioacetamide, then the concentration of uncomplexed lead can be calculated from the equation

$$k_3\left[\text{Pb(II)}\right] = 4.35 \times 10^{-2}\left[Pb^{++}\right] .$$

By making use of the values obtained, we can calculate the equilibrium constant for the reaction

$$PbCl^{+} = Pb^{++} + Cl^{-} .$$

The results of these calculations are shown in Table IX. From the values of the calculated equilibrium constants, it appears that this

Table IX. Calculated Equilibrium Constant for the Reaction $PbCl^{+} = Pb^{++} + Cl^{-}$, at 90°C.

Cl (I) VF	k_3 (a) minute^{-1}	K_1 (b) mole liter^{-1}
0.02	3.72×10^{-2}	0.109
0.04	3.33×10^{-2}	0.123
0.06	3.05×10^{-2}	0.134
0.08	2.84×10^{-2}	0.145
0.10	2.67×10^{-2}	0.153
0.14	2.40×10^{-2}	0.167

Initial Pb(II) 0.01 VF, thioacetamide 0.10 VF pH 4.0

(a) From Figure 9.

(b) Calculated assuming $\dfrac{k_3}{4.35 \times 10^{-2}} = \dfrac{\left[Pb^{++}\right]}{0.01}$

from $K_1 = \dfrac{\left[Pb^{++}\right]\left[Cl^{-}\right]}{\left[PbCl^{+}\right]}$.

assumption is false, and that the lead monochloride complex reacts at a significant rate.

Since the data indicate that the overall rate of reaction is first order with respect to lead(II) and that the chloride complex of lead reacts at a significant rate, the overall reaction rate equation can be written

$$\frac{d\left[Pb(II)\right]}{dt} = k_3\left[Pb(II)\right] = k_a\left[Pb^{++}\right] + k_b\left[PbCl^{+}\right] + k_c\left[PbCl_2\right] + \ldots.$$

Both the lead monochloride reaction rate constant and the dissociation constant of lead monochloride are unknown at 90°C. Values for these constants can be obtained by solving the equations

$$K_1 = \frac{\left[Pb^{++}\right]\left[Cl^{-}\right]}{\left[PbCl^{+}\right]}$$

$$\left[Pb(II)\right] k_3 = 4.35 \times 10^{-2}\left[Pb^{++}\right] + k_2\left[PbCl^{+}\right]$$

$$\left[Pb(II)\right] = \left[Pb^{++}\right] + \left[PbCl^{+}\right]$$

for two reaction runs. In Table X are the results of these calculations.

Table X. Determination of k_b and K_1 for the Equations

$$k_3\left[Pb(II)\right] = 4.35 \times 10^{-2}\left[Pb^{++}\right] + k_b\left[PbCl^{+}\right]$$

$$K_1 = \frac{\left[Pb^{++}\right]\left[Cl^{-}\right]}{\left[PbCl^{-}\right]}$$

Cl(I) experiment 1	Cl (I) experiment 2	k_b minute^{-1}	K_1
0.02 VF	0.04 VF	1.84×10^{-2}	0.053
0.02 VF	0.10 VF	1.61×10^{-2}	0.060
0.02 VF	0.14 VF	1.47×10^{-2}	0.064

The drift in the values of k_b and K_1 is probably caused by the formation of a significant amount of the next higher complex of lead, $PbCl_2$. If we extrapolate the data back to the lowest chloride (I) concentration used in the calculations, Cl (I) = 0.02 VF, as shown in Figure 10, we obtain a value for k_b of 1.96×10^{-2} minute^{-1} and for K_1 of 0.05 mole liter^{-1}.

These values are only semiquantitative at best, for the effect of the formate buffer on the rate of reaction is unknown. Swift and Butler (1) found that if the concentration of formate buffer is doubled, the rate of the reaction is about 50% less. This indicates the presence of formate complexes of lead under these conditions.

The data indicate that the rate of reaction is first order with respect to the ionic species Pb^{++}, $PbCl^+$ and $PbHCO_2^+$. The rate of reaction of the $PbCl^+$ with thioacetamide appears to be significant, but less than that of Pb^{++}.

No data have been obtained to describe the effect of hydrogen ion or thioacetamide on the direct rate of reaction of $PbCl^+$ with thioacetamide. The relative rates of the reactions of lead and lead monochloride with thioacetamide can therefore only be predicted to be about 2:1 at a pH of 4.0 and an initial thioacetamide concentration of 0.1 VF.

If the above method was applied to a system with no cation-buffer complex, or if the buffer was also used as the complexing agent, the equilibrium and reaction rate constants could be determined with greater validity not only for $PbCl^+$, but for the higher complexes of lead as well.

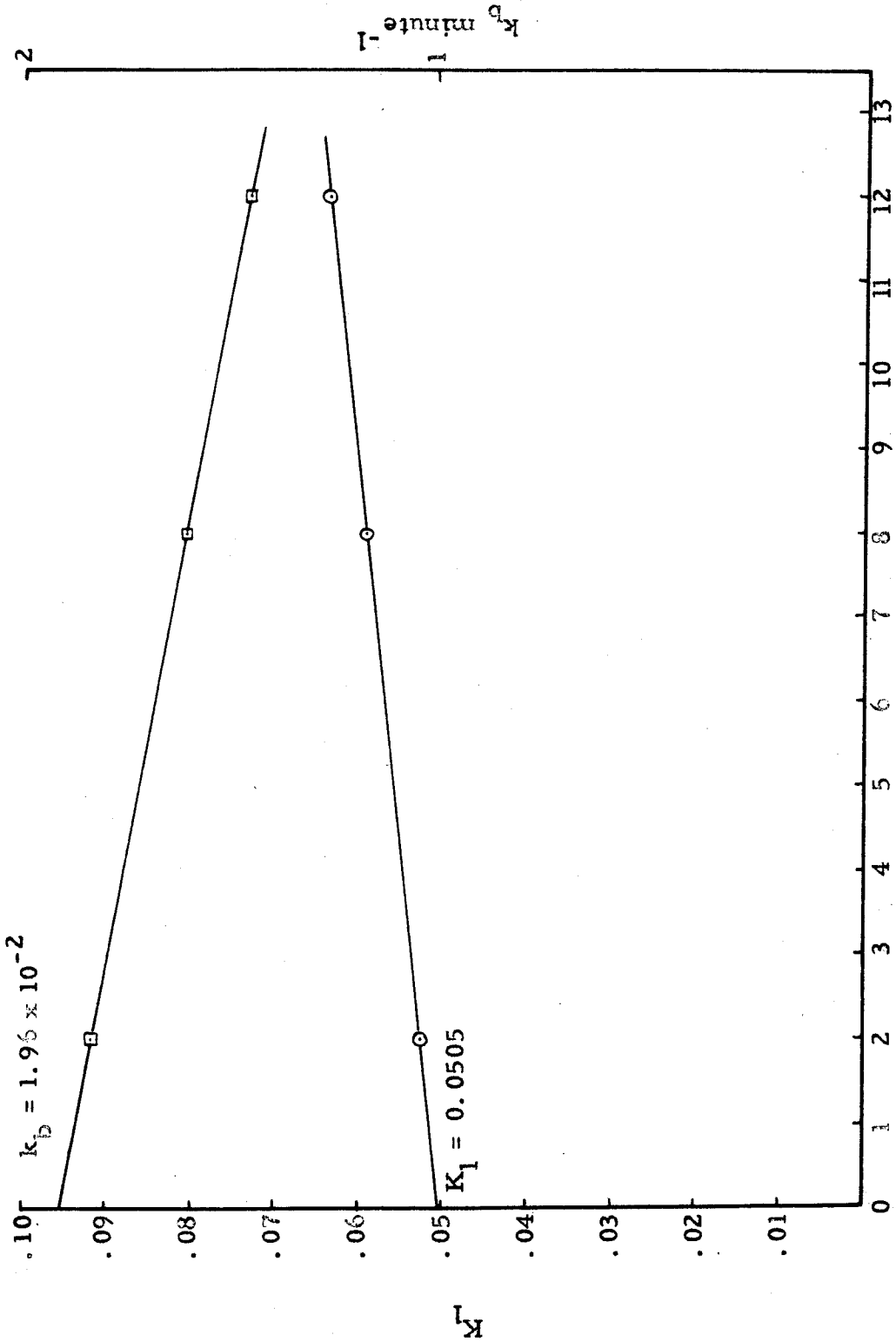

Figure 10. Determination of K_1 and k_b at 0.02 VF chloride.

Analytical Considerations

The data obtained in this investigation emphasize the importance of taking into consideration all the species present in a solution when planning sulfide precipitations with thioacetamide.

The comparisonsof direct reaction rates between thioacetamide and different metal ions are valid only if the data are obtained in a non-complexing media.

Part III. The Precipitation of Thallous Sulfide by Thioacetamide

An investigation of the mechanism of the precipitation of thallous sulfide was undertaken in order to provide a check on the reaction rate equation derived for silver. Thallium, like silver, can be kept in a unipositive state, but unlike silver has very little tendency to form complexes.

Experimental

Reagents:

Thioacetamide solutions, 1.0 VF were prepared by weight from Arapahoe reagent (lot 1402).

A solution of 0.005 VF potassium permanganate was prepared and standardized against sodium oxalate by the usual method.

A 0.08 VF thallous sulfate solution was prepared by weight.

A borate buffer solution was prepared by adding boric acid to 1 VF sodium hydroxide. The pH at 60°C. was 8.9.

Apparatus:

The same apparatus was used as in Part I.

Procedure:

The reaction solutions were prepared by mixing measured volumes of stock solutions of thioacetamide, buffer and thallous sulfate and diluting to 100 ml. with distilled water. The reaction solution was kept at 60°C. in the constant temperature bath.

At timed intervals approximately 10 ml. of solution were taken from the reaction solution and treated in the same way that the silver

solutions were in Part I.

The thallous sulfide was dissolved in 40 ml. of 1.2 VF hydrochloric acid. The solution was boiled, and evaporated down to 20 ml. in order to expel the hydrogen sulfide formed. It was then again diluted to 40 ml. with distilled water. Three grams of sodium fluoride were added, and the solution was titrated with 0.005 VF potassium permanganate to a faint pink color (5).

Data and Discussion

Qualitative investigations indicated that thallous sulfide could not be precipitated by thioacetamide at pH's of less than 4. In order to obtain rates of thallous sulfide precipitation that were conveniently measurable, the reactions had to be run at a pH of about 9. The most appropriate buffer to use in this range appeared to be a boric acid-buffer.

In their investigation on the reactions of thioacetamide in alkaline buffer systems, Peters and Swift (6) showed that the rate of formation of sulfide is greater in the presence of ammonia and carbonate buffer systems than that predicted from previous measurements in sodium hydroxide solutions. They showed that ammonia and carbonate catalysed and bicarbonate inhibited the alkaline hydrolysis of thioacetamide.

It seems that boric acid would have effects similar to those of the carbonate and ammonia buffer systems. The prediction of the rate of thioacetamide hydrolysis under the conditions used in these experiments does not appear possible without extensive investigations.

If both direct and hydrolysis mechanisms are significant for the precipitation of thallous sulfide by thioacetamide in these experiments, the reaction rate equation will have the form

$$-d\left[Tl(I)\right]/dt = k_4\left[Tl(I)\right]^n + \text{hydrolysis} \ .$$

We can determine the order of reaction, n, with respect to thallium by the following procedure. From a rectangular coordinate plot of thallium(I) vs time, determine the rate of reaction $d\left[Tl(I)\right]/dt$ at various thallium concentrations. If the reaction is first order with respect to thallium, a plot of $d\left[Tl\right]/dt$ vs $\left[Tl\right]$ will be a straight line. If it is second order a plot of $d\left[Tl\right]/dt$ vs $\left[Tl\right]^2$ will give a straight line. In Figure 11 both of these plots are shown for a typical experimental run. It can be seen that the plot $d\left[Tl\right]/dt$ vs $\left[Tl\right]^2$ is a straight line indicating that the reaction is second order with respect to thallium.

The intercept of $d\left[Tl\right]/dt$ at zero thallium concentration gives the contribution of the hydrolysis of thioacetamide to the overall reaction. A line through the origin parallel to the original curve gives the rate of the direct reaction at any thallium concentration. In Table XI are given the conditions and results of the experimental runs.

Effect of Thioacetamide Concentration:

The effect of the thioacetamide concentration upon the rate of the reaction was investigated over a range of thioacetamide concentrations from 0.1 to 0.3 VF. Rate constants calculated from the data are given in Table XII. The rate of precipitation is dependent upon the thioacetamide concentration to the first power.

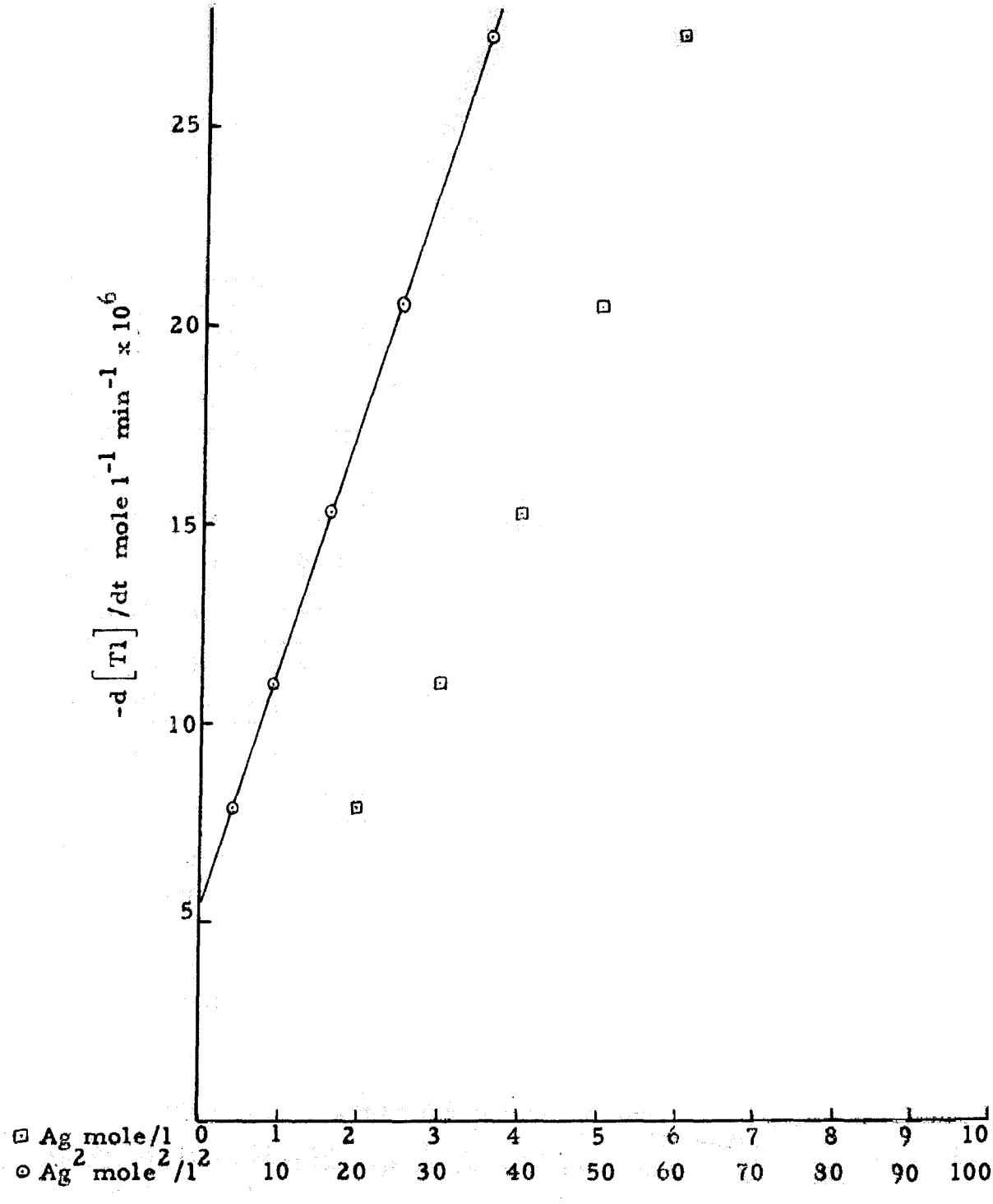

Figure 11. Effect of thallium (I) concentration on the rate of precipitation of thallous sulfide.

Table XI. Conditions and Results for the Precipitation of Thallous Sulfide by Thioacetamide with a Boric Acid Buffer at 60°C.

CH_3CSNH_2 VF	$H_2BO_3^-$ in buffer VF	dTl/dt direct Tl 0.01 VF mole l^{-1} min^{-1}	dTl/dt hydrolysis mole l^{-1} min^{-1}
0.1	0.1 pH 8.9	5.0×10^{-5}	4×10^{-6}
0.1	0.2 pH 8.9	2.5×10^{-5}	4×10^{-6}
0.2	0.2 pH 8.9	4.8×10^{-5}	6×10^{-6}
0.3	0.2 pH 8.9	8.8×10^{-5}	5×10^{-6}
0.1	0.2 pH 8.4	1×10^{-5}	2×10^{-6}

Table XII. The Effect of Thioacetamide Concentration on Rate of Thallous Sulfide Precipitation at 60°C.

Initial Tl(I) 0.01 VF; pH 8.9

CH_3CSNH_2 VF	d Tl/dt mole l^{-1} min^{-1}	k_d [(a)] mole^{-2} l^2 $minute^{-1}$
0.1	2.5×10^{-5}	2.5
0.2	4.8×10^{-5}	2.4
0.3	8.8×10^{-5}	2.9

(a) Calculated from $\frac{d[Tl(I)]}{dt} = k_d [Tl]^2 [CH_3CSNH_2]$

Effect of Hydrogen Ion Concentration:

The effect of hydrogen ion concentration was studied in only two solutions of different hydrogen ion concentrations. The data, given in Table XI, indicate that the hydrogen ion has an inhibiting effect on the rate of reaction. The effect from the two runs made was found to be -0.65 order. The slow rate of reaction at the lower pH made the

determination of the initial rate of reaction difficult, so that the error in the above value may be great. The inhibition order of hydrogen ion in this reaction is probably 0.5 order as in all the reactions previously investigated.

The direct reaction rate expression would then have the form

$$-\frac{d\,Tl(I)}{dt} = k_5 \frac{[Tl(I)]^2[CH_3CSNH_2]}{H^{+1/2}} .$$

The best value of k_5 is about 8×10^{-5} $mole^{3/2}$ $l^{3/2}$ $min.^{-1}$ under the conditions used in these experiments.

Buffer Effect:

The data in Table XI indicate that there is a significant buffer effect. If the concentration of buffer is doubled, the direct reaction rate of reaction is reduced by 50%.

Hydrolysis Reaction:

The data obtained in these experiments on the rate of thioacetamide hydrolysis are not sufficiently accurate to permit an analysis of the nature of hydrolysis to be made.

Analytical Considerations

This investigation shows that in alkaline solutions, as in acid solutions, the direct reaction between a metal ion and thioacetamide

contributes significantly to the rate of sulfide precipitation. If the correlation between the increase in solubility of a sulfide and the decrease in thioacetamide velocity constant proposed by Bowersox and Swift (7) holds, it appears that the effect of the alkaline hydrolysis of thioacetamide would be insignificant compared to the direct reaction for such very insoluble sulfides as those of silver, lead and cadmium. The direct reaction makes the precipitation of thallous sulfide feasible under conditions where the alkaline hydrolysis precipitation alone would take a prohibitive length of time.

Part IV. The Spectrographic Determination of Barium, Manganese and Titanium in Stony Meteorites

Recently attempts have been made to compile accurate data on the chemical composition of chondrites and other stony meteorites. From a collection of 286 chondrite analyses, Urey and Craig (8) were able to classify only 94 of them as superior analyses. Even in these superior analyses the concentrations of potassium, titanium, chromium, manganese, cobalt, nickel, and other elements of low concentration vary considerably and it is doubtful whether these values have high precision at all. Because of the great interest in the abundances of the elements, and the problem of the degree of uniformity of the composition of the universe, it is highly desirable that more accurate determinations of the elemental abundances in the solar system be secured. The desirability of determining the concentration of a minor element by the same method in the same laboratory for many meteorites is obvious if any rational comparison is to be made between the values obtained.

The three elements, barium, manganese, and titanium which have been determined in this study were selected both for their geochemical interest and the ease of determining their concentrations under identical conditions with an arc spectrograph.

Barium:

Most cosmic abundance values for barium are based on the determinations made by von Engelhardt in 1936 (9). Recently, Pinson, Ahrens and Franck (10) have determined the barium contents of 23 stony meteorites by spectrochemical methods, and Hamaguchi, Reed and Turkevich (11) have used neutron activation to determine the barium

content of five stony meteorites. Their values are given in Table XIII along with the values from this paper for comparison.

Table XIII. Barium in stony meteorites as determined by von Engelhardt, Pinson, Ahrens and Franck, and Hamaguchi, Reed and Turkevich.

Meteorite	Barium (ppm)			
	von E.	Pinson	Hamaguchi	this paper
Chondrites				
L'Aigle	3-10	--	--	--
Knyahinya	1-3	--	--	5
Holbrook	3-10	9	4.0	26*
Erxleben	1-3	--	--	--
Chantonnay	1-3	--	--	--
Barbotan	1-3	--	--	--
Avilez	$\lesssim 1$	--	--	--
Bjurbole	<1	8	--	5
Pultusk	--	7	--	3
Homestead	--	11	--	--
Rancome	--	7	--	28
Hayes Center	--	32	--	30
Waconda	--	7	--	--
Assun	--	8	--	--
Forest City	--	9	3.7	4
Hessle	--	7	--	--
Kernouve	--	6	--	--
Barratta	--	7	--	--
Mocs	--	6	--	5
Tennasilon	--	10	--	--
Monroe	--	5	--	--
Long Island	--	100	--	190
Beaver Creek	--	5	--	--
Lumpkin	--	6	--	--
Cangas de Onis	--	5	--	--
Estacado	--	6	--	--
Warrentown	--	5	--	--
Modoc	--	--	3.6	5
Richardton	--	--	3.2	4
Nuevo Larado	--	--	46	--

* Mean of eight samples, barium values were very erratic.

Table XIII Continued

Meteorite	Barium (ppm)			
	von E.	Pinson	Hamaguchi	this paper
Eucrites				
Stannern	48	--	--	--
Juvinas	10-30	--	--	--
Chladnites				
Johnstown	--	5	--	2.5
Chabonaceous Chondrites				
Orgueil	--	<1	--	--

Goldschmidt used von Englehardt's average (7 ppm) for all meteorites (eucrites and chondrites) as the cosmic abundance for barium. Abundance values given by Rankama and Sahama (12) and Brown (13) were based on Goldschmidt's value. Urey (14) omitted the eucrite values from the average and recalculated it to be 3 ppm. Pinson et al. in an attempt to show a high degree of uniformity in chondrites, discarded the high barium values they found for Hayes Center and Long Island and calculated an average concentration of barium in chondrites of 8 ppm. The concentrations found for barium by Hamaguchi et al. were about one half those found by Pinson. In the last two papers at least one meteorite of unusually high barium content was reported.

Manganese and Titanium:

Manganese and titanium are the most abundant of the trace elements found in stony meteorites. They have been determined many times in wet chemical analyses of meteorites, but seldom with any degree of accuracy. Average values for their abundances are usually taken from

the work of Goldschmidt (15). Table XIV gives the average concentrations of manganese and titanium in chondrites selected by previous workers.

Table XIV. The abundance of manganese and titanium in chondrites selected by previous workers.

	Goldschmidt (15)	Brown (3)	Urey (14)	Suess & Urey (13)
Titanium %	0.141	0.078	0.0735	0.0735
Manganese %	0.227	0.265	0.238	0.238

Recently Wahl and Wiik have determined the manganese and titanium contents of several chondrites by wet chemical methods. Their determinations and those obtained in this paper are given in Table XV.

Table XV. Manganese and titanium contents of chondrites as found by Wahl and Wiik (16)(17) and by Wiik (18).

Meteorite	Mn %	Ti %	reference	This paper	
				Mn %	Ti %
Dhurmsala	0.28	--	(16)	0.30	0.117
Felix	0.16	--	(16)	0.16	0.073
Knyahinya	0.19	--	(16)	0.27	0.066
McKinney	0.25	0.084	(17)	0.26	0.068
St. Michel	0.32	0.012	(18)	0.32	0.075

Analytical Technique

Sample Preparation:

Samples of meteorites ranging from 3 to 50 grams in weight, were crushed in a diamond mortar until they passed through 80 mesh bolting

cloth. Any metallic particles that could not be finely crushed were added as they were to the sieved portion. Care was taken to exclude oxide crust from the samples wherever possible. Fifty milligram portions were split from the larger samples and mixed with 200 milligrams of spectrographically pure carbon. All splitting of samples was done with a high purity aluminum microsplitter. A sample of quartz crushed under the same conditions as the meteorites showed no evidence of barium, manganese or titanium contamination.

Standard Preparation:

All compounds used in this work were "Specpure" grade obtained from Johnson Matthey and Co. Ltd.

A standard base approximating the composition of stony meteorites was prepared by mixing magnesium oxide, ferric oxide and silica in the proportions 1:1.5:1.6 by weight. Barium carbonate, titanium dioxide and Mn_3O_4 were added to the base to give a primary standard. Concentration steps of 10,000, 4,640, 2,154, and so on down to 1 ppm were prepared by diluting the primary standard with the base.

Spectrographic Methods:

The standards and samples were exposed using the following equipment and methods:

Spectrograph: Jarrel-Ash 3.4 m grating instrument, Wadsworth mount, dispersion 5.2A/mm in the first order.

Excitation: 13 ampere D.C. arc (short circuit) from a Jarrel-Ash Unisource. Sample as anode. Analytical gap, 4mm magnified 5X and focused on the slit. Central 2mm used with a slit width of 10 microns; 20 mg

samples were burned to completion (100-400 seconds). Total energy method with no internal standardization.

Electrodes: High purity 1/4 inch graphite rods as anode. Shape of anode described by Myers (1951). Pointed 1/8 inch cathode.

Wave-length Range: 2300-4800 A in the first order.

Plates: Eastman Kodak III-0.

Processing: 4 minutes in DK-50 developer at 20°C, 20 second short stop, 10 minute in acid fix, 20 minute wash.

Plate Calibration: Selected iron lines after method of Dieke and Crosswhite (1943). Each plate is calibrated.

Densitometer: Jarrel-Ash model No. 2100.

Precision:

The concentrations of barium, manganese and titanium in the stony meteorites were within the sensitivity limits for these elements under the conditions used. Each sample was exposed at least twice; the average was regarded as one analysis.

The analytical lines used were barium 4554.0Å, manganese 2949.2Å, and titanium 3261.6Å.

The percent standard deviation from the mean, including both analytical and sampling errors, is estimated to be 12% for titanium, 7% for manganese, and 20% for barium. The major source of error for the barium is in the sampling, and will be discussed later in the paper.

Results and Correlations

The concentrations of barium, manganese and titanium in 94 stony meteorites are shown in Table XVI.

Table XVI. Barium Manganese and Titanium Contents of Stony Meteorites

Meteorite	Barium ppm.	Manganese %	Titanium %
FALLS			
Alexandrovsky	10	0.284	0.063
Alfianello	3	0.280	0.060
Allegan	4	0.222	0.055
Beardsley	5	0.270	0.078
Bjurbole	5	0.224	0.055
Chateau Renard	6	0.256	0.061
Colby, Wisconsin	4.5	0.201	0.046
Dhurmsala	6	0.298	0.117
Elenovka	5	0.312	0.076
Forest City	4	0.225	0.066
Holbrook	26*	0.248	0.066
Ichkala	4	0.224	0.050
Kesen	4	0.244	0.072
Knyahinya	5	0.268	0.066
Krasnoi-Ugol	5	0.270	0.074
Kuleschovka	3.5	0.275	0.081
Kunashak	4	0.275	0.059
Marion	3	0.250	0.056
Maziba	4	0.315	0.071
Mocs	6	0.270	0.072
Modoc	9	0.270	0.067
Mordvinovka	6.5	0.258	0.060
Mount Browne	4	0.260	0.058
Nanjemoy	13	0.229	0.065
New Concord	4	0.257	0.064
Nikolskoie	2	0.238	0.058
Ochansk (1)	5	0.278	0.068
Ochansk (2)	4	0.246	0.053
Olivenza	6	0.295	0.074
Olmedilla de Alarcon	5	0.231	0.062
Pantar	5	0.233	0.057
Parmallee	3.5	0.310	0.073
Pervomaisky	5	0.263	0.071
Pultusk	3	0.225	0.051

* Erratic results from different samples, mean of 8 samples.

Table XVI Continued

Meteorite	Barium ppm.	Manganese %	Titanium %
Richardton	4	0.265	0.062
Saint Michel	4	0.322	0.075
Saratov	22	0.244	0.068
Sautschenskoje	4	0.294	0.068
Stavropol	2.5	0.255	0.076
Tane	5	0.268	0.064
Uberaba	4	0.245	0.059
Weston	6	0.245	0.060
Yatoor	6	0.250	0.058
Zhovtnevyi	6	0.298	0.071
FINDS CHONDRITES			
Acme	120	0.204	0.058
Alamagordo	26	0.240	0.059
Arriba	53	0.248	0.073
Aurora	20	0.215	0.050
Beenham	34	0.242	0.051
Berdyansk	7	0.231	0.068
Brisco County	150	0.268	0.060
Cavour	4	0.228	0.054
Chuvashskie-Kissy	5	0.199	0.050
Colby, Kansas	170	0.225	0.055
Coldwater	10	0.222	0.056
Coolidge	32	0.130	0.095
Covert	115	0.215	0.061
DeNova	115	0.256	0.065
Farley	290	0.170	0.042
Fayette County(Bluff)	3	0.255	0.061
Gladstone	17	0.266	0.066
Goodland	10	0.250	0.063
Harrisonville	7	0.243	0.061
Hayes Center	30	0.290	0.075
Hugoton	200	0.200	0.048
Kansas City	4	0.183	0.076
Kelly	165	0.245	0.049
Kingfisher	5	0.266	0.064
Ladder Creek	94	0.247	0.063
LaLande	210	0.225	0.052
Long Island	190	0.248	0.055
Marsland	3	0.218	0.053
McKinney	6	0.257	0.068
Melrose	155	0.221	0.057
Morland	5	0.258	0.055
Ness County (1894)	20	0.215	0.056
Orlovka	18	0.240	0.059
Otis	7	0.249	0.066

Table XVI Continued

Meteorite	Barium ppm.	Manganese %	Titanium %
Petropavlovka	4	0.231	0.064
Plainview	10	0.211	0.058
Potter	155	0.263	0.051
Ransom	28	0.233	0.068
Roy	72	0.243	0.054
Rush Creek	5	0.240	0.052
Seibert	125	0.255	0.067
Texline	13	0.245	0.061
Tryon	190	0.230	0.059
Tulia	120	0.231	0.060
Wilmot	82	0.173	0.051
CARBONACEOUS CHONDRITES			
Felix	4	0.160	0.073
Murray County	4	0.257	0.054
ACHONDRITES			
Cumberland Falls	14	0.245	0.040
Johnstown	2.5	0.352	0.081
Norton County	2	0.115	0.030
Shalka	4	0.459	0.036
Shaw	26	0.248	0.059

Barium:

A survey of the barium contents of the chondrites indicated that many of them were high. Most of the high barium chondrites were finds; i.e., they were not seen to fall. In analysing the data, it was found to be of value to consider the meteorite which were seen to fall separately from those which were found and are of uncertain terrestrial age.

In Figure 12 a histogram shows the frequency of occurrence vs the logarithm of the barium concentration for 44 observed chondrite falls. The distribution appears to be log-normal in shape. The median

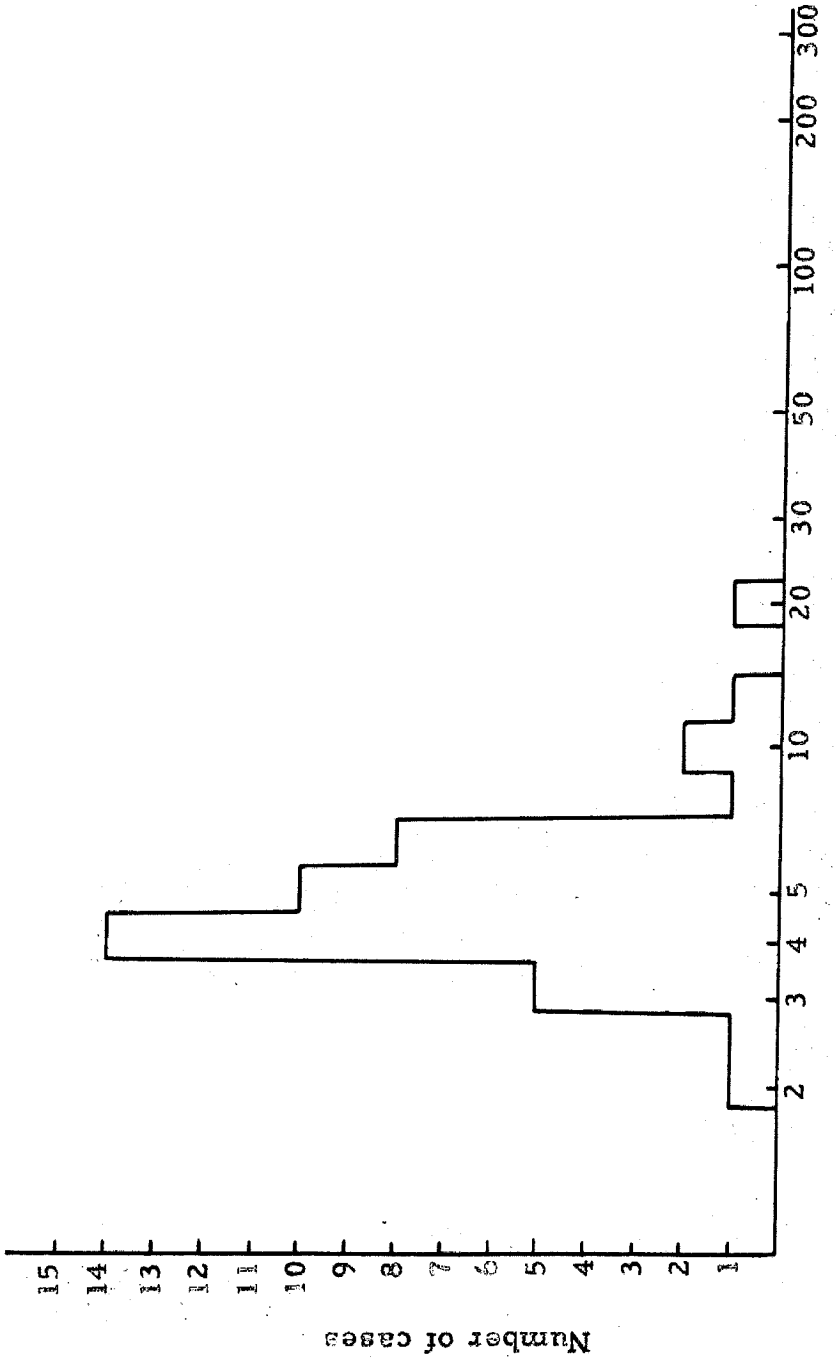

Figure 12. Distribution of barium in chondrite falls.

is 4.5 ppm and the mode is 4 ppm.

Shown in Figure 13 is a histogram with the frequency of occurrence vs the logarithm of the barium concentration for 44 chondrite finds. The distribution appears to be tetramodal, with peaks at 5, 10, 25, and 150 ppm barium, and is therefore quite different than that for falls.

This appearance of grouping is not unique for barium. Lovering et al (19) have shown that iron meteorites can be divided into four groups on the basis of their gallium and germanium contents. Yavnell (20) has grouped iron meteorites into six subclasses, stony-iron meteorites into three subclasses, and chondrites into four subclasses on the basis of differences in their major chemical composition.

If we compare the histograms of the falls and finds, it appears that several of the falls can be placed in one of the higher barium groups indicated by the find data.

Analysis of the Holbrook Chondrite:

The Holbrook chondrite fall consisted of many individual stones ranging in size from a 6.6 kg mass to minute grains. The specimen used in this study consisted of pea sized fragments and complete stones. The barium contents of eight different samples varied greatly. A description of the samples and their barium, manganese, and titanium contents are given in Table XVII.

The manganese and titanium seem to be distributed fairly uniformly throughout the meteorite. The localized concentration of barium suggests that it is concentrated in a mineral phase that is not uniformly distributed in the meteorite. Geochemically, barium is concentrated in

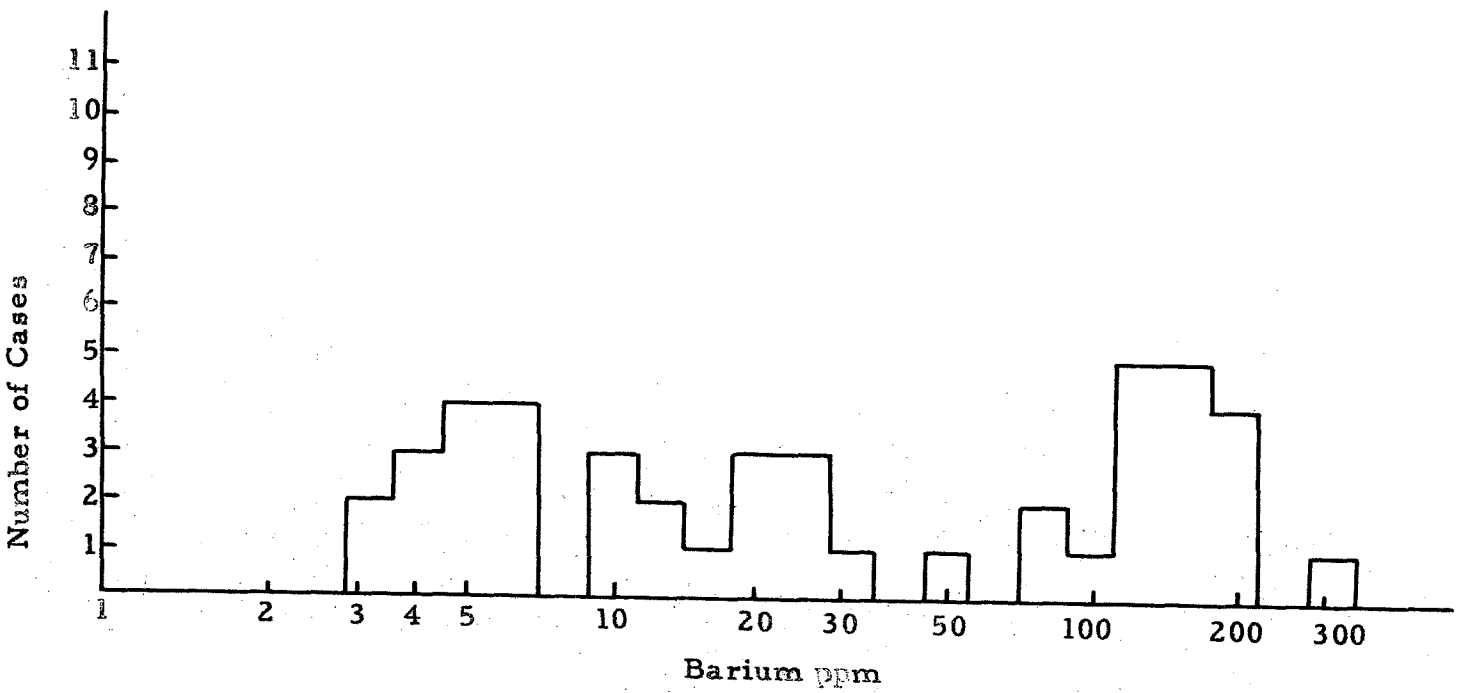

Figure 13. Distribution of barium in chondrite finds.

Table XVII. Concentrations of Barium, Manganese and Titanium in the Holbrook Chondrite

Sample	Ba ppm		Mn %	Ti %
A. several pea sized fragments 5 g.	28		0.258	0.068
B. single fragment 1 g.	9		0.255	0.066
C. mainly black fusion crust 1 g.	8		0.265	0.057
D. single complete stone 1 g.	74		0.258	0.068
E. fine dust from complete sample 2 g.	29		0.246	0.061
F. non-magnetic phase 0.5 g.	24		0.251	0.070
G. black crust 0.5 g.	110		0.243	0.076
H. small chips from all fragments 3 g.	27		0.228	0.062
median	26	avg	0.248 ±0.018	0.066 ±0.008

relatively few mineral phases. In igneous rocks it is usually trapped by potassium minerals. No feldspars were reported by Foote in his preliminary petrographic analysis of the meteorite, but a glassy phase was reported to be present (21). This glass could, and in several other meteorites does, have a feldspathic composition. If barium is present in the silicate phase, it will most likely be found in this glass. It is also possible that the barium is present in one of the minor meteoric minerals such as oldhamite (CaS). The latter choice seems more likely to explain a localized distribution of barium since its distribution would tend to be more erratic than that of the glassy phase.

The rationalization for dividing stony meteorites into groups on the basis of their trace element concentrations is more difficult than for

grouping iron meteorites. If meteorites are even partially the products of a magmatic type differentiation, the barium content could be changed appreciably by the appearance of even a small amount of a new mineral phase. For this reason it is important to try and locate the host mineral for barium in the chondrites.

It is also important to remember that in the case of meteorites that have been on the ground for an undetermined length of time before they were found, weathering and other alteration processes could have taken place to a greater or lesser extent. A too rigorous analysis of these meteorites on the basis of their trace element contents should not be attempted due to this unknown parameter.

Several factors indicate that the high barium concentrations are original and not the products of contamination. Two of the meteorites that were picked up immediately after they fell have barium concentrations greater than 20 ppm. The contamination of the chondrites to give barium contents greater than 150 ppm seems unlikely to have been caused naturally on such a widespread scale. Experiments described later in the paper indicate that some of the barium is present in acid insoluble silicates.

In order to obtain some idea concerning the form in which barium occurs in the chondrites, samples of Beenham, Kansas City and Wilmot were boiled for about three minutes in 10 ml of 0.1 VF nitric acid. Comparison of the barium contents in the unleached and leached meteorites are shown in Table XVIII.

Table VIII. The Effect of Boiling Chondrite Samples in 0.1 VF Nitric Acid

Meteorite	Barium ppm	
	Unleached sample	Leached sample
Beenham	34	19
Kansas City	4	4
Wilmot	82	90

The data indicate that in the Beenham chondrite barium is present in an easily dissolved phase. Under the conditions used, the concentration leached out exceeds the solubility of silicate-bound barium or barium sulfate.

A qualitative analysis of the solvent gave the following results.

Table XIX. Qualitative Analysis of Nitric Acid Leach Solution

Meteorite	Ca	Cr	Ba	Mn	Ni	Ti	Mg
Beenham	high	low	high	high	high	no	high
Kansas City	high	low+	low	high	med.	no	high
Wilmot	low	low	low	low	low	no	low

Undissolved residues of chondrites that had been treated with hot 1 VF HCl in the process of an analysis scheme for sulfur were qualitatively checked for barium in the arc spectrograph. The results are shown in Table XX. Even under these conditions some of the barium was not dissolved. This indicates that it is probably tied up in a silicate mineral that is not readily attacked by the acid.

Table XX. Barium Contents of Residues Left from Strong Acid Leaching of Chondrites

Meteorite	Barium ppm	
	Unleached meteorite	Leached meteorite
Beenham	34	6
Coolidge	32	20
Covert	115	60
De Nova	115	60
Hayes Center	30	30
Ladder Creek	94	40
LaLande∂	210	60
Long Island	190	50
Melrose	155	20
Ness County (1894)	20	10
Plainview	10	10
Roy	72	20
Tulia	120	30
Wilmot	82	20

If oldhamite is the host mineral for a significant portion of the barium found in chondrites, there might be a positive correlation between barium and sulfur content. Table XXI gives the stony meteorites for which both barium and sulfur determinations are available. The sulfur concentrations are taken from unpublished data of Pollack and Brown (22), and the compilation of meteorite analyses by Urey and Craig (8).

Figure 14 is a plot of sulfur content vs the logarithm of the barium content for the meteorites listed in Table XXI. At first there does not appear to be a general correlation between barium and sulfur. However, if only the falls are considered, a positive correlation is apparent. Further investigation reveals three additional possible groupings showing the same barium sulfur trends as that observed for the falls. The four groups are shown on the figure.

Table XXI. Barium and Sulfur Contents of Stony Meteorites

Meteorite	Ba ppm	S %	Reference
Falls			
Allegan	4	1.84	Urey and Craig
Beardsley	5	1.90	Pollack and Brown
Bjurbole	5	1.99	Urey and Craig
Forest City	4	1.54	Pollack and Brown
Knyahinya	5	2.11	Urey and Craig
Mocs	6	2.13	Pollack and Brown
Modoc	9	2.39	Pollack and Brown
Mount Browne	4	2.02	Urey and Craig
Olivinza	6	2.19	Urey and Craig
Olmedilla de Alarcon	5	1.69	Urey and Craig
Pantar	5	1.92	Pollack and Brown
Richardton	4	1.74	Pollack and Brown
Saint Michel	4	2.22	Urey and Craig
Saratov	22	2.30	Urey and Craig
Finds			
Acme	120	0.44	Pollack and Brown
Aurora	20	1.54	Pollack and Brown
Beenham	34	2.30	Pollack and Brown
Brisco County	150	2.29	Pollack and Brown
Colby, Kansas	170	0.88	Pollack and Brown
Coolidge	32	0.48	Pollack and Brown
Covert	115	0.57	Pollack and Brown
DeNova	115	2.24	Pollack and Brown
Farley	290	0.38	Pollack and Brown
Fayette County	3	2.25	Pollack and Brown
Gilgoin Station	13	1.45	Pollack and Brown
Goodland	10	2.09	Pollack and Brown
Harrisonville	7	1.36	Pollack and Brown
Hayes Center	30	1.99	Pollack and Brown
Hugoton	200	0.65	Pollack and Brown
Kansas City	4	0.88	Pollack and Brown
Kelly	165	0.67	Pollack and Brown
Kingfisher	5	1.61	Pollack and Brown
Ladder Creek	94	1.67	Pollack and Brown
LaLande	210	0.71	Pollack and Brown
Long Island	190	1.47	Pollack and Brown
Marsland	3	1.45	Pollack and Brown
McKinney	6	2.36	Urey and Craig
Melrose	155	1.60	Pollack and Brown
Ness County (1894)	20	1.68	Pollack and Brown
Otis	7	0.80	Pollack and Brown
Plainview	10	1.49	Pollack and Brown

Table XXI Continued

Meteorite	Ba ppm	S %	Reference
Roy	72	1.03	Pollack and Brown
Rush Creek	5	2.25	Pollack and Brown
Texline	13	1.58	Pollack and Brown
Tryon	190	0.76	Pollack and Brown
Tulia	120	0.26	Pollack and Brown
Wilmot	82	0.05	Pollack and Brown
Carbonaceous Chondrites			
Felix	4	2.01	Pollack and Brown
Murray County	4	0.39	Pollack and Brown
Achondrites			
Johnstown	2.5	0.35	Pollack and Brown
Norton County	2	0.48	Pollack and Brown
Shalka	4	0.14	Urey and Craig
Shaw	26	1.27	Pollack and Brown

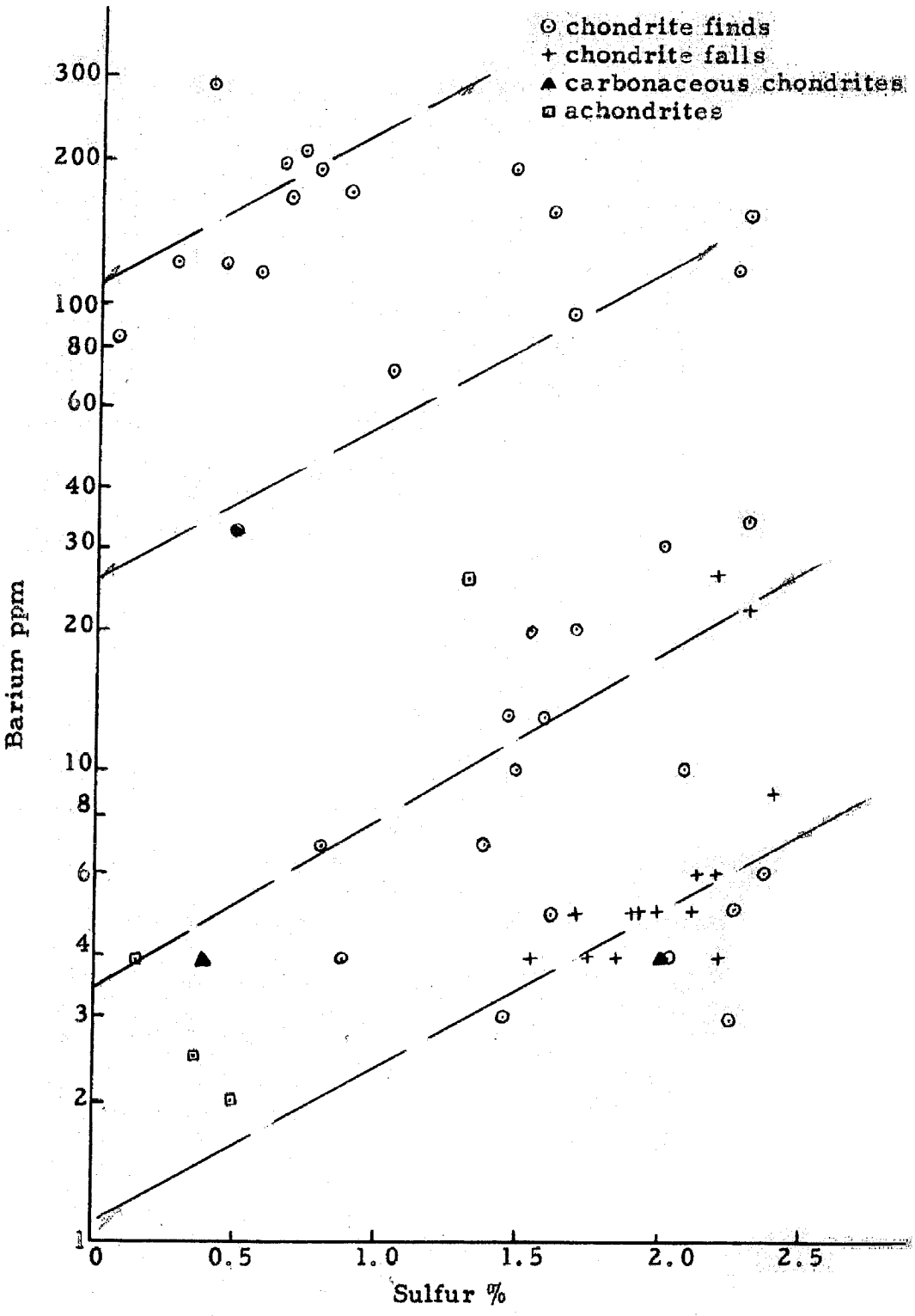

Figure 14. Relation between barium and sulfur in stony meteorites.

The extrapolation of the trend in each group to zero sulfur concentration indicates that the barium content of the silicate phase is different for each. This was also indicated in the leaching experiments described earlier.

It appears that the barium is distributed between the silicate and alkaline earth sulfide phases of a chondrite. The presence of oldhamite in a chondrite does not necessarily mean that it will have a high barium content, for the Allegan chondrite has been reported to have a relatively high oldhamite content but it is low in barium.

Manganese and Titanium:

Figure 15 is a plot of manganese vs titanium for the stony meteorites listed in Table XVI. A direct correlation is apparent. The best straight line through the origin and the plotted concentration values has the form Ti = 0.249 Mn. Three meteorites, Dhurmsala, Coolidge and Kansas City have been excluded from the calculation because of their large divergence from the direct correlation. The manganese and titanium values for carbonaceous chondrites and achondrites are also shown in the figure.

The manganese and titanium contents of both falls and finds appear to have normal distributions. For the falls the average concentrations are manganese 0.260 ± 0.028%, and titanium 0.064 ± 0.008%. The average concentrations in the finds are manganese 0.235 ± 0.023% and titanium 0.059 ± 0.007%.

The ratios of titanium to manganese in the falls and finds are 0.246 and 0.251 respectively. The reason for the difference in absolute

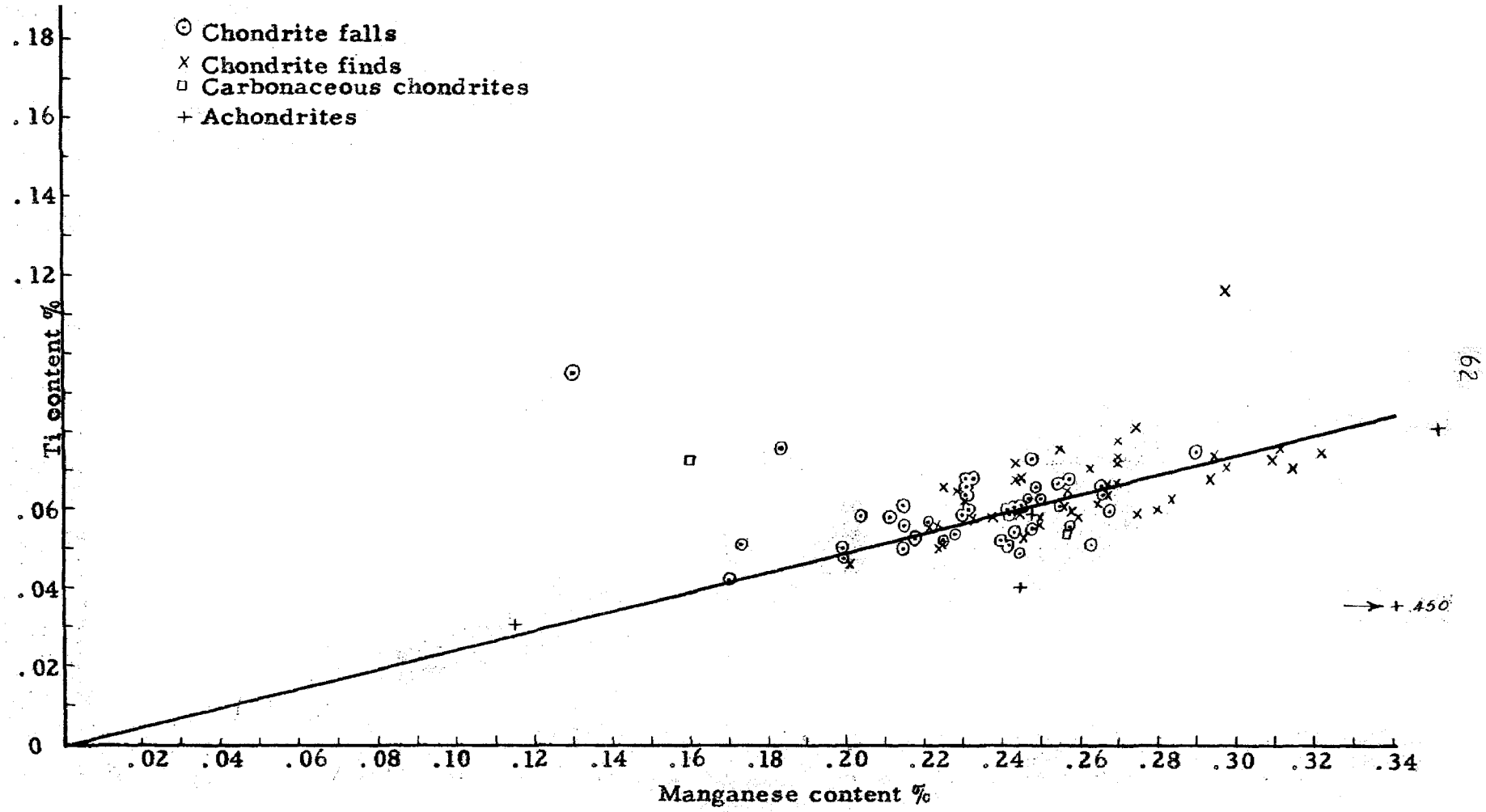

Figure 15. Variation of titanium content of stony meteorites with manganese content.

concentrations and the similarity in ratios appears to be related to the physical properties of the meteorite. The finds contain more iron-nickel and sulfide phase than the falls. Since both manganese and titanium always occur predominantly in the silicate phase and their ratio is constant, their concentrations decrease when the amount of silicate phase is smaller. The greater metal content of the falls was very noticeable when the meteorite samples were crushed.

Falls vs Finds:

It has already been noted that the finds generally contain more metal than the falls. The finds are usually hard dense meteorites while the falls are in several cases so friable that they can be crumbled between the fingers.

It is suggested that finds are a biased sample for stony meteorites, since the more friable meteorites can easily be weathered away. A good example of the rapid rate at which this can take place is given by Wahl and Wiik in their paper on the Varpaisjarvi chondrite (17).

To determine the average composition of an element in stony meteorites, a random sample must be used; only meteorites which have been seen to fall provide this random sample.

If we take the average concentrations of manganese and titanium in falls only, adjustments must be made for both in the data of Suess and Urey (23). The values determined here are 0.260 ± 0.028% of manganese and 0.064 ± 0.008% titanium. The average barium concentration in chondrite falls is 5.8 ± 5.2 ppm.

Part V. The Determination of Manganese, Chromium, Iron, Nickel and Cobalt in Chondrites by X-ray Fluorescence Spectroscopy

There are indications that chondrites, like iron meteorites can be divided into groups on the basis of their chemical composition. In order to investigate the possibility of such groups, a large number of reliable chemical analyses are needed. A rapid method is desired that offers reasonable reliability without involving the time or expense of complete chemical analysis. In an effort to meet this need, the possibilities of using X-ray fluorescence spectroscopy have been investigated.

X-ray fluorescence spectroscopic methods have recently been developed for the major element analysis of rock samples. This method would be particularly attractive for the analysis of stony meteorites because it is non-destructive and would not require the loss of valuable meteorite specimens.

Instrumentation:

A Norelco X-ray spectrograph was used with the tungsten target X-ray tube operated at 40 KVP and 25 ma. A lithium fluoride crystal in an air path was used in conjunction with a 0.020" x 3" parallel plate collimator. The detector was an argon-methane filled flow proportional counter.

Samples were placed in Zytel boat holders.

Analytical Techniques:

The analytical lines chosen (Table XXII) are such that they can be resolved from nearby interferences. The peaks were located by counting over the required angle positions and the same peak position was

Table XXII. Analytical Lines for X-ray Fourescence Spectroscopy

Element	Peak Used
Cobalt	$K\alpha 2^{o}$
Iron	$K\beta 2^{o}$
Nickel	$K\alpha 2^{o}$
Chromium	$K\alpha$
Manganese	$K\alpha$

used for all analyses. Counting rates were determined for each peak and its background with a minimum of 5,000 counts being taken for the peaks. Background counts were taken about 1.5^{o} 2 θ on both sides of each peak; 2000 total counts were sufficient.

Preparation of Samples and Standards

The same samples were used as for the emission spectrographic technique described in Part IV. These crushed, untreated samples were placed directly in the Zytel holders. Magnetic and non-magnetic splits of the crushed meteorite samples were obtained by removing magnetic material manually with a permanent alnico magnet. Slabs of whole meteorites were cut to the proper size to fit the sample holders with a diamond saw. Several meteorites were converted to an oxide form by treating them with aqua-regia. The aqua-regia dissolves both the troilite (FeS) and iron-nickel phases, and probably a good part of the basic silicate minerals such as olivine. The resulting solutions were evaporated and heated to 500^{o}C in a muffle furnace. The residues were removed as completely as possible with a spatula and ground in an agate mortar. Standards were used that were already available in this laboratory. They were prepared by mixing aliquot portions of

solutions of iron, nickel, cobalt, manganese and chromium, evaporating the resulting solutions to dryness and igniting the residues to oxides.

A check standard was made by mechanically mixing oxides of silicon, magnesium, iron, manganese, nickel, cobalt, and chromium in the proportions of an average chondrite.

The standards made up for the emission spectrographic study of chondrites were also run in the X-ray fluorescence spectrograph.

Data on the composition and counting rates for the standards are given in Table XXIII. In Figure 16 the concentration ratios vs peak intensity ratios are plotted for Mn/Fe.

Data and Correlations:

Figure 17 shows the X-ray fluorescence Mn/Fe intensity ratios for five chondrites plotted against the Mn/Fe concentration ratios. The manganese concentrations were taken from the emission spectrographic data given in Part IV, and the iron concentrations were determined in the same samples used in this investigation by wet chemical analysis (24). It is apparent that the plotted points neither fall on the standard curve nor indicate a revised standard curve.

These same samples were then treated with aqua-regia, evaporated to dryness and ignited at 500°C. This treatment oxidized both the iron-nickel and troilite phases. Part of the basic minerals such as olivine would probably also be decomposed and converted to oxide form. The X-ray fluorescence intensity ratios obtained are plotted vs the concentration ratios along with the untreated chondrite ratios in Figure 17.

Table XXIII. Concentrations and X-ray Fluorescence Peak Intensities for Standards

Standard	Cr	Mn	Fe	Co	Ni	Cr/Fe	Mn/Fe	Co/Fe	Ni/Fe	Ni/Co	Cr/Mn
No. 1 Conc.	1	0.336	212	0.5	10	0.00472	0.00158	0.00236	0.0472	20	2.98
X-ray	476.8	160.0	4084	89.02	804.4	0.117	0.0392	0.0218	0.197	9.01	2.98
No. 2 Conc.	1	0.672	212	0.5	10	0.00472	0.00317	0.00236	0.0472	20	1.49
X-ray	455.7	295.4	3937	87.95	766.4	0.116	0.0750	0.0223	0.195	8.73	1.55
No. 4 Conc.	1	3.36	212	0.5	10	0.00472	0.0158	0.00236	0.0472	20	0.298
X-ray	443.3	1427	3894	83.33	797.7	0.114	0.367	0.0214	0.205	9.59	0.311
No. 7 Conc.	2	1.008	212	1.0	20	0.00943	0.00475	0.00472	0.0943	20	1.986
X-ray	689.9	396.5	3691	160.2	1495	0.1869	0.1074	0.0534	0.405	9.34	1.74
No. 8 Conc.	3	1.008	212	1.5	30	0.01415	0.00475	0.00708	0.1415	20	2.98
X-ray	894.0	369.0	3404	216.9	2130	0.263	0.108	0.0637	0.626	9.82	2.42
No. 9 Conc.	1	--	212	0.5	10	0.00472	--	0.00236	0.0472	20	--
X-ray	457.9	--	4105	84.74	734.1	0.112	--	0.0206	0.179	8.66	--
No. 10 Conc.	1	1.68	212	--	10	0.00472	0.00792	--	0.0472	0	0.595
X-ray	460.7	721.6	4054	--	746.5	0.114	0.178	--	0.184	0	0.640
Artificial Chondrite											
Conc.	1.05	1.12	252	0.65	10.69	0.00417	0.00444	0.00258	0.0424	16.4	0.937
X-ray	390.6	372.0	3978	79.89	618.3	0.0982	0.0935	0.0201	0.155	7.74	1.05

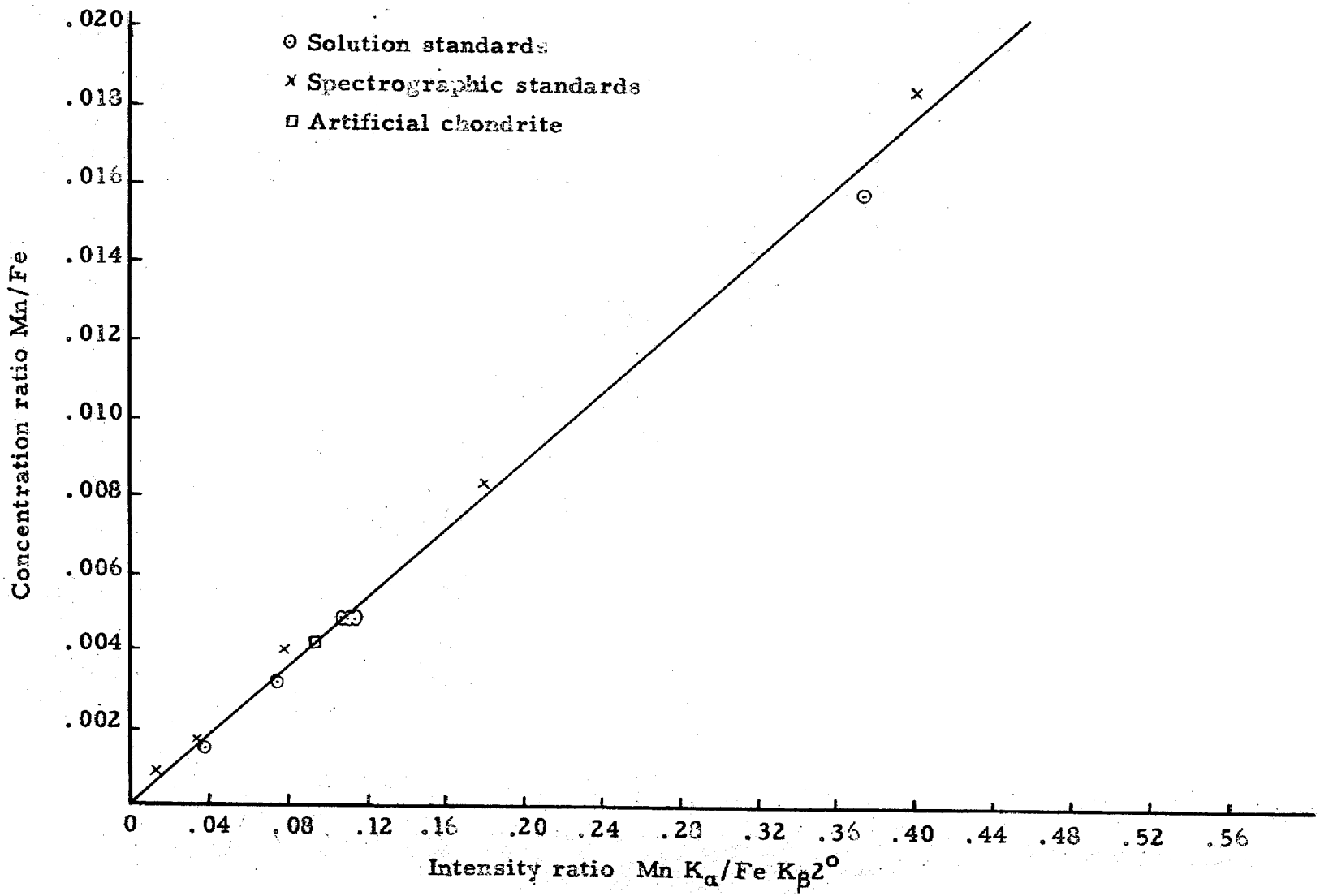

Figure 16. Standard manganese-iron curve.

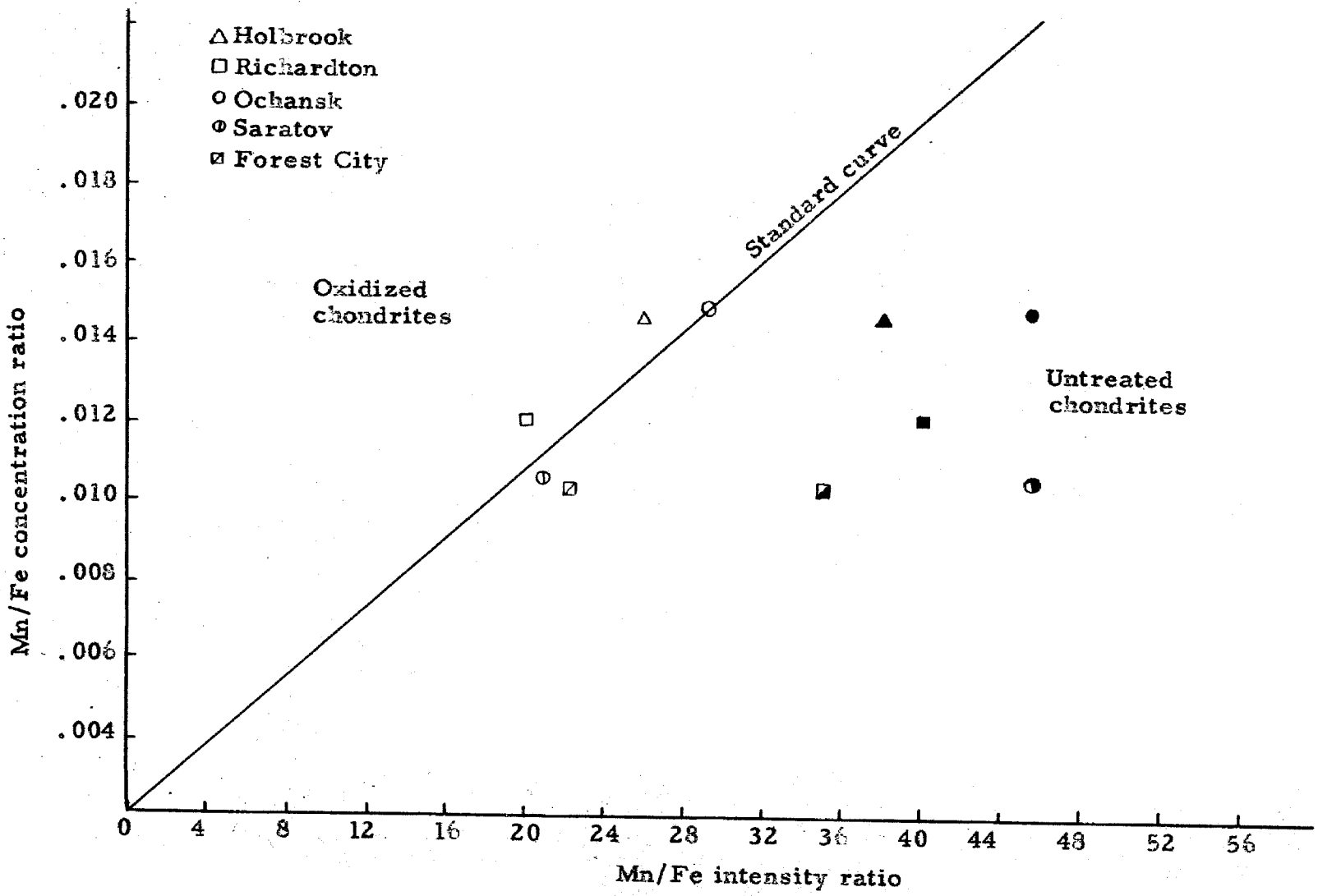

Figure 17. Mn/Fe intensity ratios for untreated and oxidized chondrites.

The points plotted for the treated samples fall on the oxide standard curve.

In order to investigate possible interelement effects, ferric oxide, iron metal, nickel metal, and chromic sesquioxide were mixed with separate untreated splits of the Forest City chondrite. The elements were added in concentrations that would approximately double their concentration in the natural meteorite. The mixtures, peak intensities and peak intensity ratios are shown in Table XXIV.

From the data in Tables XXIII and XXIV it is apparent that only iron causes a significant interelement effect when its concentration is doubled. This effect appears to be greater when iron is added as ferric oxide rather than iron metal. In Table XXV are given the peak intensities and intensity ratios for seven chondrites in both the untreated and oxidized states. The interelement effect from adding ferric oxide is small compared to the intensity ratio changes caused by oxidizing the sample. The greatest changes took place in the Co/Fe, Ni/Fe, Co/Mn, and Ni/Mn intensity ratios. In all cases the ratio increased when the sample was oxidized. This is caused mainly by a large peak intensity increase for nickel and cobalt. Iron also shows a peak intensity increase but to a lesser extent.

The data indicate that the differences in the intensity ratios given in Table XXV and shown in Figure 17 are primarily due not to differences in the chemical composition, but rather to physical inhomogeneities in the chondrites. Although the chondrites are macroscopically homogeneous, atomistically they are not. Cobalt and nickel are always found

Table XXIV. Interelement Effects on X-ray Fluorescence Data

	Co	Fe	Ni	Cr	Mn	$\frac{Ni}{Co}$	$\frac{Cr}{Mn}$	$\frac{Fe}{Mn}$	$\frac{Co}{Mn}$	$\frac{Ni}{Mn}$	$\frac{Co}{Fe}$	$\frac{Ni}{Fe}$
No. 69												
Forest City	38.0	2250.4	343.8	866.0	840.3	8.77	1.03	2.68	0.045	0.409	0.017	0.153
	41.62	2501.9	391.8	913.1	889.1	9.41	1.03	2.67	0.047	0.441	0.017	0.156
	42.46	2690.8	410.3	996.9	936.6	9.67	1.07	2.87	0.045	0.458	0.016	0.152
	41.46	2591.6	408.0	920.7	901.1	9.85	1.02	2.88	0.046	0.453	0.016	0.158
0.500g Forest City	33.95	4366.6	224.9	809.3	669.1	6.63	1.21	x	0.051	0.336	x	x
+0.125g Fe_2O_3	27.01	4489.1	212.3	856.5	659.5	7.86	1.30	x	0.041	0.332	x	x
0.500g Forest City	30.94	3779.0	286.1	831.3	722.1	9.25	1.15	x	0.043	0.396	x	x
+0.0875g Fe												
0.500g Forest City	37.86	2480.2	1786	944.4	929.2	x	1.02	2.67	0.041	x	0.015	x
0.010g Ni												

Table XXV. Comparison of Data for Untreated and Oxidized Chondrites

	Co	Fe	Ni	Cr	Mn	$\frac{Ni}{Co}$	$\frac{Cr}{Mn}$	$\frac{Co}{Fe}$	$\frac{Ni}{Fe}$	$\frac{Cr}{Fe}$	$\frac{Ni}{Mn}$	$\frac{Co}{Mn}$	$\frac{Fe}{Mn}$
M-72-U	21.2	2282	167.2	839.3	867.7	7.88	0.967	0.00928	0.0732	0.368	0.193	0.0244	2.63
M-72-O	68.43	3246	824.9	772.8	845.4	12.0	0.914	0.0210	0.254	0.238	0.976	0.0809	3.84
M-212-U	36.90	2668	309.8	977.4	949.5	8.41	1.02	0.0138	0.116	0.366	0.326	0.0389	2.81
M-212-O	76.23	3210	851.6	710.9	760.9	11.1	0.93	0.0237	0.265	0.221	1.11	0.100	4.22
M-50-U	32.24	2458	328.2	1022.	988.2	10.5	1.03	0.0131	0.133	0.416	0.332	0.0326	2.49
M-50-O	81.81	3578	1084.	785.4	716.1	13.2	.09	0.0228	0.303	0.220	1.515	0.114	5.00
M-215-U-A	16.10	2340	199.6	1119.	1075.	12.4	1.04	0.00687	0.0853	0.478	0.186	0.0150	2.18
M-215-B-O	106.6	3630	1060.	715.4	618.3	9.96	1.15	0.0293	0.292	0.197	1.71	0.172	3.42
M-13-U	15.59	2257	159.4	1279.	1303.	10.2	0.982	0.00690	0.0706	0.567	0.122	0.0120	1.73
M-13-U	13.94	2273	150.8	1052.	1042.	10.8	1.00	0.00613	0.0664	0.463	0.145	0.0133	2.18
M-13-O	114.2	3970	1132.	784.4	685.0	9.91	1.14	0.0287	0.285	0.198	1.65	0.166	5.80
M-120-U	16.69	2556	210.7	1072.	1061.	13.0	1.01	0.00653	0.0825	0.420	0.199	0.0157	2.41
M-208-O	104.1	3713	1089.	811.7	774.5	10.4	1.04	0.0280	0.293	0.219	1.407	0.134	4.79
M-69-U	42.46	2690	410.3	996.9	936.6	9.69	1.06	0.0157	0.152	0.370	0.438	0.0453	2.87
M-69-O	95.41	4119	963.0	1092.	913.7	10.0	1.19	0.0231	0.233	0.265	1.05	0.104	4.51

in the iron phase of the meteorites. They are therefore always bound together with iron in the untreated meteorites and have inter-atomic influences upon each other that are not present to such a great extent when they are evenly distributed in the sample as in the artificial standards or oxidized samples.

Standard concentration-peak intensity ratio curves, similar to the curve in figure 16, have been constructed for chromium, nickel and cobalt. From these curves, concentrations of manganese, cobalt, chromium, and nickel in the chondrites listed in Table XXV have been determined. Iron was used as the basis of calculation rather than manganese because of the greater precision with which it has been determined in these samples. The results of these determinations are listed in Table XXVI. Unfortunately complete analyses of these samples by other methods have not yet been completed in order to check these data. Included in Table XXVI are the emission spectrographic manganese values and concentrations for the other elements from previous analyses of these chondrites.

In order to evaluate the usefulness of data obtained for the peak intensities of untreated chondrites, 37 chondrite falls and 46 chondrite finds were run in the X-ray fluorescence spectrograph. Many of the finds were run both as solid slabs (M-No.-S) and powdered samples (M-No.-U). The data obtained are shown in Table XXVII. The data for the slabs are the average of at least two samples.

It can be seen in Table XXVII that the peak intensity ratios for the slab and powdered samples of the same chondrite are different in

Table XXVI. X-ray Fluorescent Spectroscopic and Previous Determinations of Manganese, Chromium, Cobalt and Nickel in Chondrites

Chondrite and method	Fe%	Mn%	Cr%	Co%	Ni%
Holbrook, wet, Pollack (24)	19.5	--	--	--	--
Holbrook, M-72-O, X-ray	19.5	0.224	0.254	0.045	1.15
Holbrook, M-72-U, spec.	--	0.248	--	--	--
Holbrook, wet, Nichiporuk	--	--	--	--	0.95
Richardton, wet, Pollack (24)	26.2	--	--	--	--
Richardton, M-72-O, X-ray	26.2	0.234	0.317	0.066	1.83
Richardton, M-72-U, spec.	--	0.265	--	--	--
Ochansk, wet, Wiik (18)	19.14	0.20	0.10	0.10	1.58
Ochansk, M-215-O, X-ray	19.14	0.247	0.203	0.062	1.29
Ochansk, M-215-U, spec.	--	0.246	--	--	--
Saratov, wet, Wiik (18)	28.50	0.28	0.45	0.05	0.99
Saratov, M-208-O, X-ray	28.50	0.272	0.342	0.089	1.93
Saratov, M-208-U, spec.	--	0.244	--	--	--
Forest City, wet, Pollack (24)	26.6	--	--	--	--
Forest City, M-69-O, X-ray	26.6	0.261	0.40	0.068	1.45
Forest City, M-69-U, spec.	--	0.225	--	--	--
Forest City, wet, Blake	24.97	0.27	0.32	--	1.73

Table XXVII. Data for X-Ray Fluorescence Spectroscopic Analyses

Number	Meteorite	Peak Intensities					Peak Intensity Ratios			
	CHONDRITE FALLS	Co	Fe	Ni	Cr	Mn	$\frac{Co}{Mn}$	$\frac{Fe}{Mn}$	$\frac{Ni}{Mn}$	$\frac{Cr}{Mn}$
M-213-U	Alexandrovsky	20.78	2280	212.9	1057	1058.	0.0196	2.15	0.201	0.999
M-183-U	Alfianello	11.90	2172	113.5	708.1	899.6	0.0132	2.41	0.126	0.787
		11.07	2225	92.5	743.1	921.2	0.0120	2.41	0.100	0.806
M-179-U	Allegan	11.31	1942	114.3	891.9	964.1	0.0117	2.02	0.116	0.925
		10.79	2001	112.9	917.7	989.4	0.0109	2.02	0.114	0.927
M-67-U	Beardsley	18.58	2175	180.9	967.9	991.6	0.0187	2.19	0.182	0.976
M-181-U	Bjurbole	18.77	2537	132.1	968.7	1028.	0.0182	2.46	0.128	0.941
		20.90	2522	149.2	963.4	1008.	0.0207	2.50	0.148	0.955
M-192-U	Chateau Renard	14.84	2654	124.1	988.5	984.2	0.0150	2.69	0.126	1.00
		10.75	2213	97.38	881.2	853.8	0.0125	2.59	0.114	1.03
M-184-U	Colby, Wisc.	41.68	2497	139.1	884.9	955.4	0.0153	2.61	0.145	0.884
		9.31	2304	112.1	825.2	919.4	0.0101	2.50	0.121	0.897
M-180-U	Dhurmsala	11.78	2274	59.31	1091.	959.6	0.0122	2.37	0.061	1.13
		9.80	2257	60.38	1095.	952.6	0.0102	2.37	0.063	1.14
M-210-U	Elenovka	7.94	2336	100.6	893.5	929.6	0.0085	2.51	0.108	0.961
M-69-U	Forest City	41.62	2501	391.8	913.0	889.0	0.0468	2.81	0.440	1.02
M-72-U	Holbrook	21.2	2282	167.2	839.3	867.7	0.0244	2.63	0.193	0.967
M-214-U	Ichkala	22.57	2377	213.2	968.2	1018.	0.0221	2.33	0.209	0.951
M-178-U	Kesen	26.86	2293	266.5	995.8	968.9	0.0277	2.36	0.275	1.02
		24.37	2200	260.0	950.0	914.5	0.0266	2.40	0.284	1.03

Table XXVII (continued)

Number	Meteorite	Peak Intensities					Peak Intensity Ratios			
		Co	Fe	Ni	Cr	Mn	$\frac{Co}{Mn}$	$\frac{Fe}{Mn}$	$\frac{Ni}{Mn}$	$\frac{Cr}{Mn}$
M-193-U	Knyahinya	18.87	2471	176.3	927.4	989.4	0.0190	2.49	0.178	0.937
		21.41	2432	160.1	922.7	977.8	0.0219	2.48	0.163	0.943
M-218-U	Krasnyi-Ugol	12.89	2571	124.2	1033.9	1026.	0.0125	2.50	0.121	1.00
M-219-U	Kuleshovka	13.88	2584	127.8	935.4	1050.	0.0132	2.46	0.121	0.890
M-209-U	Kunashak	12.26	2620	137.1	966.9	990.1	0.0123	2.64	0.138	0.976
M-185-U	Marion	21.56	2556	180.1	984.6	997.2	0.0216	2.56	0.180	0.987
		21.01	2480	192.6	924.1	927.1	0.0226	2.67	0.207	0.997
M-189-U	Maziba	12.65	2514	118.2	935.2	1025.	0.0123	2.45	0.115	0.972
		9.48	2177	80.7	856.8	914.8	0.0103	2.38	0.088	0.936
M-73-U	Mocs	15.62	2386	128.7	881.9	984.1	0.0158	2.42	0.130	0.896
M-188-U	Modoc	38.06	2545	309.2	743.4	876.6	0.0434	2.90	0.352	0.848
		39.24	2644	309.3	794.2	918.7	0.0427	2.87	0.336	0.864
M-212-U	Mordvinokva	20.43	2471	129.6	888.6	936.7	0.0218	2.63	0.138	0.948
M-190-U	Mount Browne	12.93	2070	126.3	1020.	1017.	0.0181	2.03	0.124	1.02
		13.41	2051	133.3	1011.	1015.	0.0132	2.02	0.131	0.99
M-198-U	Nanjemoy	11.86	1973	117.9	1040.	951.1	0.0124	2.07	0.124	1.07
		12.59	2118	128.9	997.7	1029.	0.0122	2.05	0.125	0.969
M-182-U	New Concord	14.39	2370	106.3	911.9	1016.	0.0142	2.34	0.105	0.901
		14.67	2335	129.7	891.0	977.5	0.0150	2.38	0.132	0.911
M-225-U	Nikolskoie	13.48	2579	104.6	903.3	945.2	0.0142	2.62	0.110	0.955

Table XXVII (continued)

Number	Meteorite	Peak Intensities					Peak Intensity Ratios			
		Co	Fe	Ni	Cr	Mn	$\frac{Co}{Mn}$	$\frac{Fe}{Mn}$	$\frac{Ni}{Mn}$	$\frac{Cr}{Mn}$
M-194-U	Ochansk (1)	15.06	2190	148.3	1009.	954.4	0.0157	2.29	0.155	1.05
		11.15	2192	126.8	1051.	1010.	0.0110	2.17	0.125	1.04
M-215A-U	Ochansk (2)	16.10	2340	199.6	1119.	1075.	0.0149	2.18	0.186	1.04
M-200-U	Olivenza	19.15	2975	81.3	985.0	988.7	0.0193	3.01	0.082	0.996
		16.87	2694	99.78	866.8	864.9	0.0195	3.11	0.115	1.00
M-201-U	Olmedilla de Alarcon	12.76	2321	123.4	855.3	1067.	0.0119	2.17	0.115	0.800
		6.34	2120	97.73	1046.	1024.	0.0061	2.06	0.095	1.02
M-13-U	Pantar	32.24	2458	328.2	1022.	988.2	0.0326	2.48	0.332	1.03
M-191-U	Parnallee	21.99	2529	245.5	1052.	1068.	0.0205	2.36	0.229	0.984
		15.97	2055	189.1	914.9	877.7	0.0181	2.34	0.215	0.936
M-211-U	Pervomarsky	20.43	2471	129.6	888.6	936.7	0.0218	2.63	0.138	0.948
M-204-U	Pultusk	11.36	1725	132.7	847.3	834.4	0.0136	2.07	0.159	1.02
M-50-U	Richardton	32.24	2458	328.2	1022.	988.2	0.0326	2.48	0.332	1.03
M-177-U	St. Michel	19.91	2370	164.3	924.7	937.2	0.0212	2.52	0.175	0.986
		20.75	2428	170.6	959.5	934.8	0.0222	2.59	0.182	1.02
M-208-U	Saratov	16.69	2555	210.7	1072.	1061.	0.0157	2.40	0.198	1.01
		12.18	2203	187.8	891.1	846.8	0.0143	2.60	0.221	1.05
M-216-U	Sawtschenskoje	13.21	2777	97.59	1041.	1029.	0.0128	2.69	0.095	1.01
M-217-U	Stavropol	20.29	2608	140.8	985.7	1002.	0.0202	2.60	0.140	0.983
M-196-U	Tane	17.59	2561	169.1	920.2	985.2	0.0178	2.60	0.171	0.936
		18.48	2405	144.4	872.1	936.9	0.0197	2.56	0.154	0.930

Table XXVII (continued)

Number	Meteorite	Peak Intensities					Peak Intensity Ratios			
		Co	Fe	Ni	Cr	Mn	$\frac{Co}{Mn}$	$\frac{Fe}{Mn}$	$\frac{Ni}{Mn}$	$\frac{Cr}{Mn}$
M-197-U	Uberaba	20.14	2291	170.9	1027.	1036.	0.0104	2.21	0.164	0.991
		15.16	2188	148.8	1018.	1019.	0.0148	2.14	0.145	0.998
M-199-U	Weston	17.20	2262	177.7	971.0	924.5	0.0186	2.44	0.192	1.05
		22.14	2345	193.2	1037.	969.8	0.0228	2.41	0.199	1.07
		22.36	2246	197.0	988.4	917.1	0.0243	2.44	0.214	1.07
M-203-U	Yatoor	25.62	2371	258.9	1003.	993.8	0.0257	2.38	0.260	1.01
		21.92	2171	244.4	937.2	939.7	0.0233	2.31	0.260	0.997
M-202-U	Zhovtnevyi	10.30	2272	117.9	984.0	1126.	0.0091	2.01	0.104	0.873
		14.36	2212	129.1	942.0	1032.	0.0139	2.14	0.125	0.912
	CHONDRITE FINDS									
M-26-S*	Acme	73.2	3145	630.0	821.8	838.0	0.0873	3.75	0.751	0.980
M-26-U*		56.4	2984	552.6	668.3	664.1	0.0849	4.49	0.832	1.00
M-1-S	Alamogordo	50.1	2617	365.0	911.3	919.6	0.0545	2.84	0.396	0.991
M-32-S	Arriba	58.6	2907	534.9	834.1	935.1	0.0627	3.10	0.572	0.892
M-66-U	Aurora	11.0	2187	391.3	904.3	845.7	0.0130	2.58	0.462	1.06
M-9-S	Beenham	25.8	2572	250.7	935.2	1048.	0.0246	2.45	0.239	0.892
		10.2	2090	107.7	871.4	895.5	0.0114	2.33	0.120	0.973
M-221-U	Berdiansk	61.09	2955	576.5	802.0	828.6	0.0737	3.56	0.695	0.968
M-42-S	Brisco County	50.7	2565	388.9	749.6	900.2	0.0563	2.84	0.432	0.832
M-42-U		124.1	3646	762.8	1342.	1420.	0.0874	2.56	0.537	0.945

* S = slab
U = powder

Table XXVII (continued)

Number	Meteorite	Peak Intensities					Peak Intensity Ratios			
		Co	Fe	Ni	Cr	Mn	$\frac{Co}{Mn}$	$\frac{Fe}{Mn}$	$\frac{Ni}{Mn}$	$\frac{Cr}{Mn}$
M-3-S	Cavour	61.5	2926	434.6	886.8	958.7	0.0641	3.05	0.453	0.925
M-223-U	Chuvashskie	111.8	3843	1093.	849.1	739.5	0.151	5.19	1.47	1.14
M-45-S	Colby, Kansas	85.8	3339	691.3	892.3	819.7	0.104	4.07	0.843	1.08
M-45-U		130.1	3927	958.6	1342.	1188.	0.109	3.30	0.806	1.13
M-4-S	Coldwater	75.9	3059	657.7	918.7	889.3	0.0853	3.44	0.739	1.03
M-41-S	Coolidge	68.0	2958	594.8	1028.	495.7	0.137	5.96	1.19	2.07
M-41-U		132.4	3535	904.9	1516.	750.9	0.176	4.70	1.20	2.01
M-68-S	Covert	90.6	3528	768.1	798.3	791.0	0.114	4.46	0.971	1.009
M-68-U		70.0	3085	606.0	771.9	706.2	0.099	4.36	0.858	1.09
M-38-S	DeNova	46.2	2727	381.1	753.6	984.3	0.0469	2.77	0.387	0.765
M-38-U		33.2	2227	220.2	772.0	858.5	0.0387	2.59	0.256	0.899
M-39-S	Farley	91.4	3626	762.7	884.6	839.9	0.108	4.31	0.908	1.05
M-39-U		134.3	4108	766.8	1072.	955.8	0.140	4.29	0.802	1.12
M-44-S	Fayette County	37.3	2670	261.1	856.6	997.0	0.0374	2.67	0.261	0.859
M-44-U		90.1	3312	471.8	1253.	1304.	0.0691	2.53	0.361	0.960
M-76-S	Gilgoin Station	48.1	2841	383.7	1041.	1043.	0.0467	2.72	0.367	0.998
M-76-U		30.8	2281	288.2	917.1	868.1	0.0355	2.62	0.332	1.056
M-2-S	Gladstone	57.8	2932	476.0	952.9	943.0	0.0613	3.10	0.504	1.01
M-34-S	Goodland	42.1	2663	311.9	949.2	944.6	0.0446	2.81	0.330	1.00
M-34-U		20.6	2219	239.3	854.8	826.0	0.0249	2.68	0.289	1.03
M-12-S	Harrisonville	44.3	2795	373.4	814.2	931.6	0.0475	3.00	0.400	0.874
M-12-U		51.6	2475	485.3	733.0	807.8	0.0639	3.06	0.600	0.908

Table XXVII (continued)

Number	Meteorite	Peak Intensities					Peak Intensity Ratios			
		Co	Fe	Ni	Cr	Mn	$\frac{Co}{Mn}$	$\frac{Fe}{Mn}$	$\frac{Ni}{Mn}$	$\frac{Cr}{Mn}$
M-40-S	Hayes Center	37.8	2723	301.5	974.2	1003.	0.0377	2.71	0.300	0.970
M-40-U		71.9	3878	388.3	1403.	1361.	0.0528	2.84	0.285	1.03
M-35-U	Hugoton	74.0	3011	576.4	759.3	665.7	0.111	4.52	0.865	1.15
M-11-U	Kansas City	32.4	2685	700.0	685.1	678.4	0.0477	3.95	1.03	1.00
M-47-S	Kelly	62.9	2812	626.4	836.3	932.6	0.0674	3.01	0.671	0.896
M-47-U		150.3	3529	1057.	1212.	1221.	0.123	2.89	0.866	0.993
M-46-S	Kingfisher	85.6	3221	763.8	881.7	965.0	0.0887	3.33	0.791	0.913
M-46-U		149.4	3795	1056.	1471.	1405.	0.106	2.70	0.749	1.04
M-6-S	Ladder Creek	64.8	2882	570.3	829.9	915.6	0.0708	3.14	0.622	0.906
M-6-U		58.2	2190	515.5	705.8	742.5	0.0783	2.95	0.694	0.950
M-7-S	LaLande	57.9	2954	611.0	882.2	952.1	0.0608	3.02	0.641	0.926
M-7-U		59.4	2582	559.3	729.7	779.7	0.0762	3.31	0.717	0.935
M-10-S	Long Island	59.1	2876	553.2	857.6	1016.	0.0581	2.83	0.554	0.843
M-10-U		45.6	2458	422.2	735.3	780.7	0.0584	3.14	0.540	0.941
M-33-S	Marsland	52.0	2703	448.9	961.6	937.8	0.0554	2.88	0.478	1.02
M-33-U		33.7	2125	312.9	859.6	817.6	0.0412	3.19	0.382	1.05
M-5-S	McKinney	38.6	2847	381.2	1034.	1007.	0.0383	2.82	0.378	1.02
M-16-S	Melrose	70.3	2901	532.4	868.1	933.5	0.0743	3.10	0.570	0.929
M-16-U		52.0	2547	365.5	695.5	755.6	0.0688	3.37	0.483	0.920
M-18-S	Marland	57.7	2870	449.5	807.3	924.2	0.0624	3.10	0.486	0.873
M-15-S	Ness County	68.5	2974	637.5	820.6	964.2	0.0710	3.08	0.661	0.851
M-15-U		53.5	2284	476.4	655.1	722.6	0.0740	3.16	0.659	0.906

Table XXVII (continued)

Number	Meteorite	Peak Intensities					Peak Intensity Ratios			
		Co	Fe	Ni	Cr	Mn	$\frac{Co}{Mn}$	$\frac{Fe}{Mn}$	$\frac{Ni}{Mn}$	$\frac{Cr}{Mn}$
M-220-U	Orlovka	57.29	3126	603.8	933.0	890.4	0.0643	3.51	0.678	1.04
M-17-S	Otis	68.2	2968	593.1	794.0	1043.	0.0654	2.84	0.568	0.761
M-17-U		55.0	2490	499.5	631.0	716.1	0.0768	3.47	0.697	0.881
M-224-U	Petropavlovka	19.65	2174	236.4	1019.	997.2	0.0197	2.18	0.237	1.02
M-14-S	Plainview	51.4	2795	436.1	915.7	949.7	0.0541	2.94	0.459	0.964
M-14-U		33.4	1980	309.5	741.9	749.6	0.0446	2.64	0.412	0.989
M-48-S	Potter	76.5	2848	651.6	796.7	881.5	0.0868	3.23	0.739	0.903
M-23-S	Ransom	53.6	2802	428.2	842.5	886.3	0.0605	3.16	0.483	0.950
M-36-U	Roy	70.2	2873	710.3	791.4	780.5	0.0899	3.68	0.910	1.01
M-51-S	Rush Creek	44.8	2621	371.7	802.0	911.2	0.0492	2.87	0.407	0.980
M-51-U		34.5	2291	331.4	746.6	802.4	0.0430	2.85	0.413	0.930
M-31-S	Seibert	76.3	3208	675.4	914.3	919.9	0.0829	3.48	0.734	0.993
M-20-S	Texline	49.2	2768	399.9	912.8	945.0	0.0521	2.92	0.423	0.965
M-20-U		28.2	2013	270.2	797.5	815.1	0.0346	2.47	0.331	0.977
M-22-S	Tryon	77.3	3194	610.0	794.0	906.0	0.0853	3.52	0.673	0.876
M-22-U		65.5	2828	516.9	742.2	758.2	0.0864	3.73	0.681	0.978
M-19-S	Tulia	80.3	3216	687.0	888.1	817.5	0.0982	3.93	0.840	1.08
M-19-U		48.3	2655	492.2	746.6	665.3	0.0726	3.99	0.735	1.12
M-21-S	Wilmot	70.7	3706	570.4	887.5	763.9	0.0925	4.85	0.746	1.16
M-21-U		67.8	3145	425.6	727.7	630.3	0.107	4.99	0.675	1.15

several cases. In the analysis of the data which follows, the data from the slabs were used, where possible, because there was less chance for sampling errors and it gave better results than did the powder data.

Six slabs cut from the Covert chondrite were analyzed on both sides. The peak intensity ratios were Co/Mn - 0.114 $\pm$ 0.014, Fe/Mn - 4.45 $\pm$ 0.28, and Ni/Mn - 0.954 $\pm$ 0.095. The relatively low standard deviations from the mean show that the slabs represent a homogeneous sample.

The peak intensities for chromium and manganese and the Cr/Mn peak intensity ratio are relatively constant for most of the chondrites in Table XXVII. Both chromium and manganese are found in the non-metallic portion of chondrites and showed no constant difference between their ratios in the untreated and oxidized samples in Table XXV. The manganese and chromium concentrations given in the compilation of meteorite analyses by Urey and Craig fluctuated greatly. This investigation indicates that in most cases their reported values are probably in error. Chromium has been reported as occurring in both the silicate and sulfide phases of chondrites while manganese always appears to be concentrated in the silicate phase alone. For this reason the peak intensity ratios have been taken relative to manganese.

Plots of Ni/Mn vs Fe/MN, Co/Mn vs Fe/Mn, and Co/Mn vs Ni/Mn for the untreated chondrites are shown in figures 18, 19 and 20, respectively. Clearly indicated on these plots is the fact that the chondrite falls generally have a much lower metal content than the finds. This conclusion is in agreement with the data in Part IV of this thesis and

with observations made when the chondrites were crushed.

Indications of grouping of the chondrites are present, but not clearly definable. The evidence for grouping is more evident for the falls than the finds. In Figures 21, 22, and 23 plots with the same coordinates as above are given on a larger scale for the falls only. Suggested trends and groups are indicated on the figures.

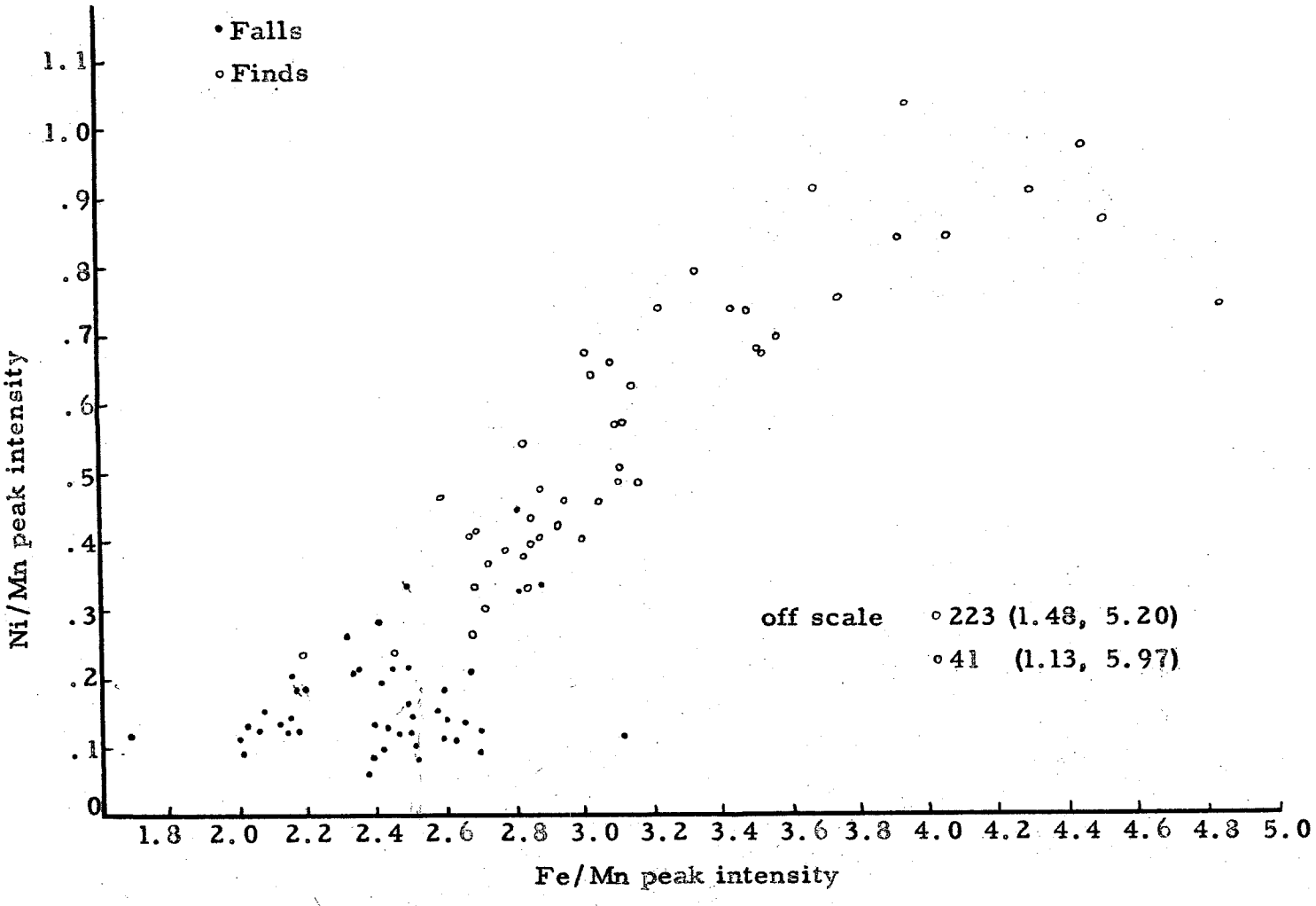

Figure 18. Relation between Ni/Mn and Fe/Mn peak intensity ratios for chondrites.

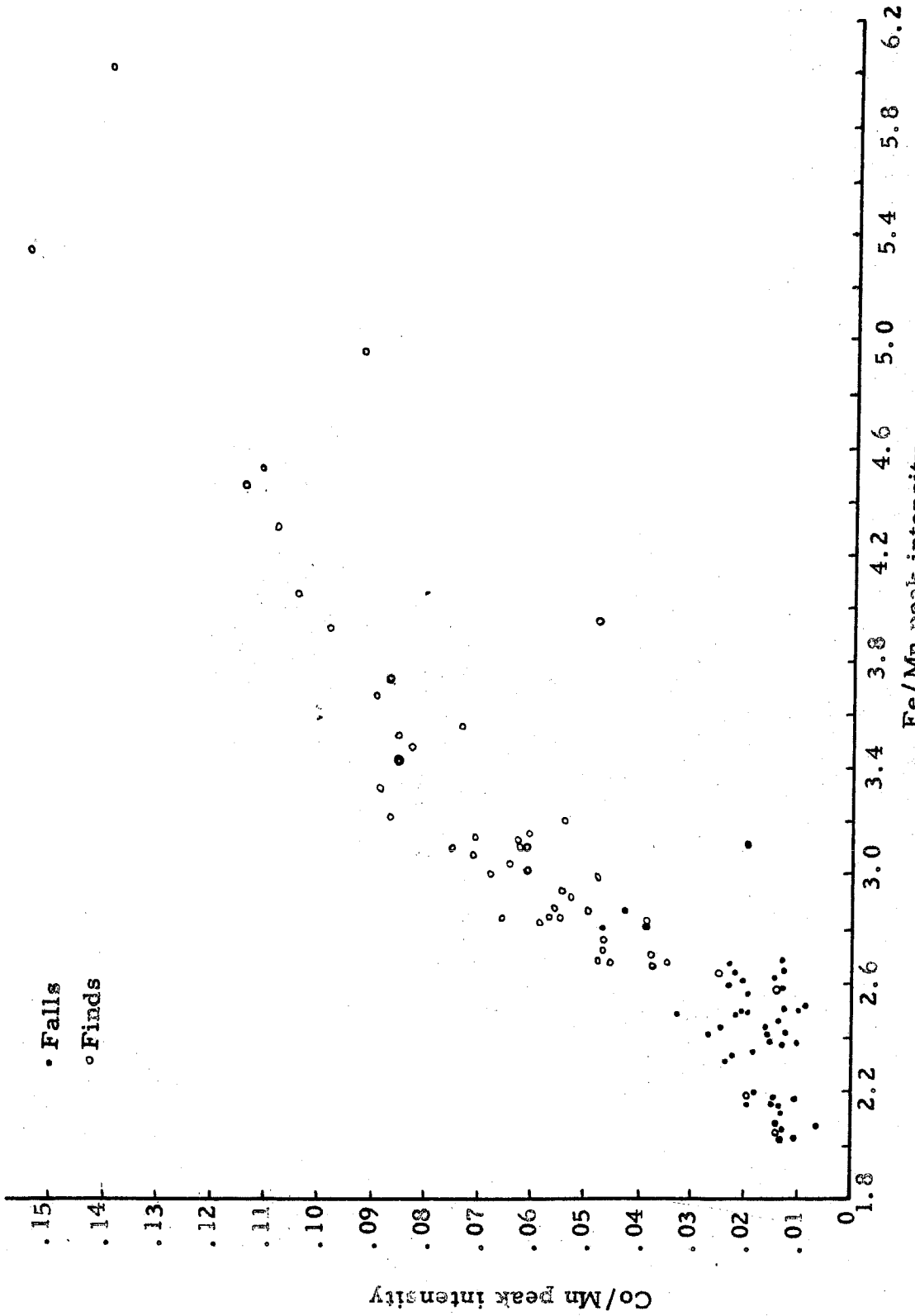

Fig. 19. Relation between Co/Mn and Fe/Mn peak intensity ratios for chondrites.

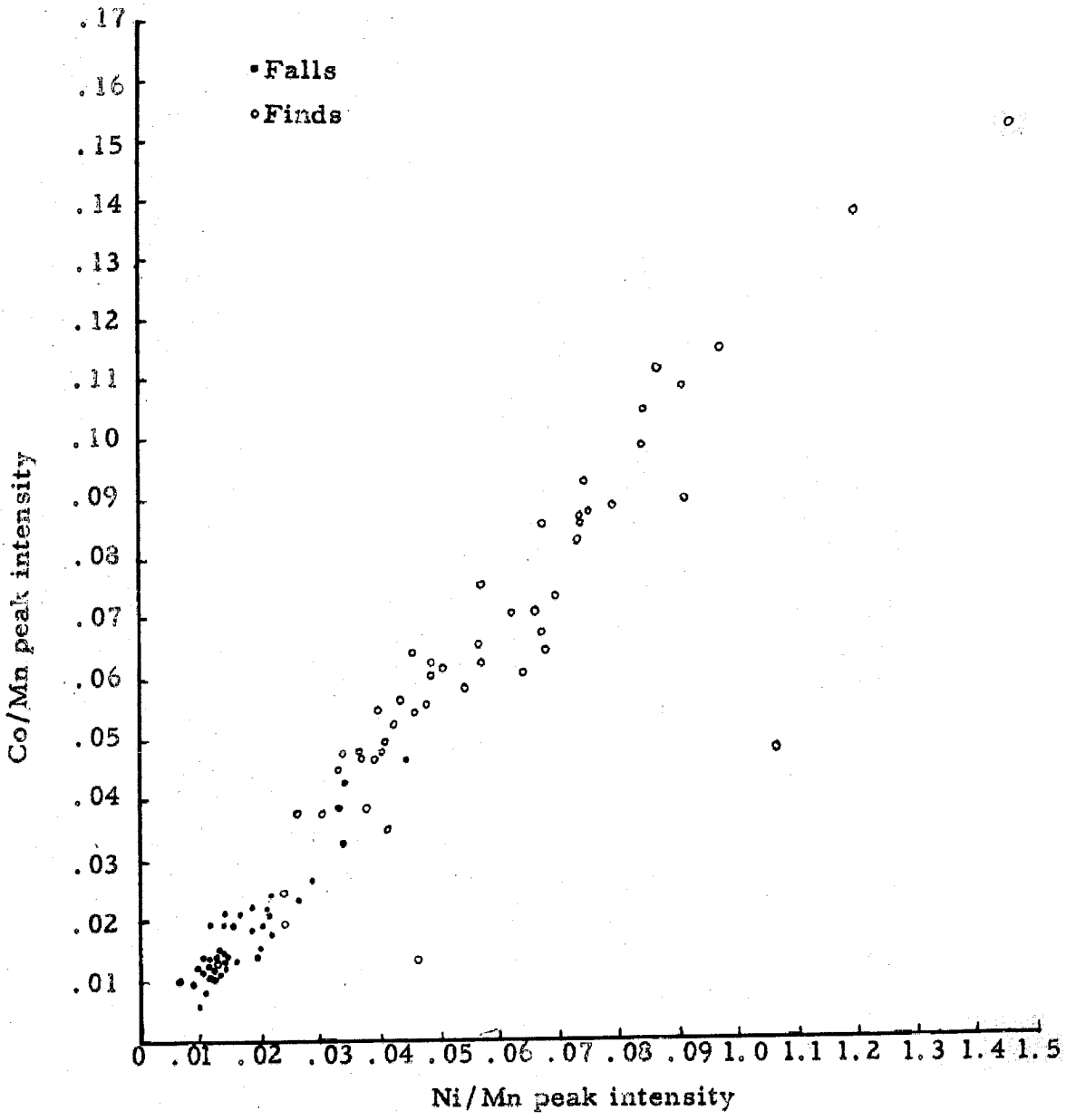

Figure 20. Relation between Co/Mn and Ni/Mn peak intensity ratios for chondrites.

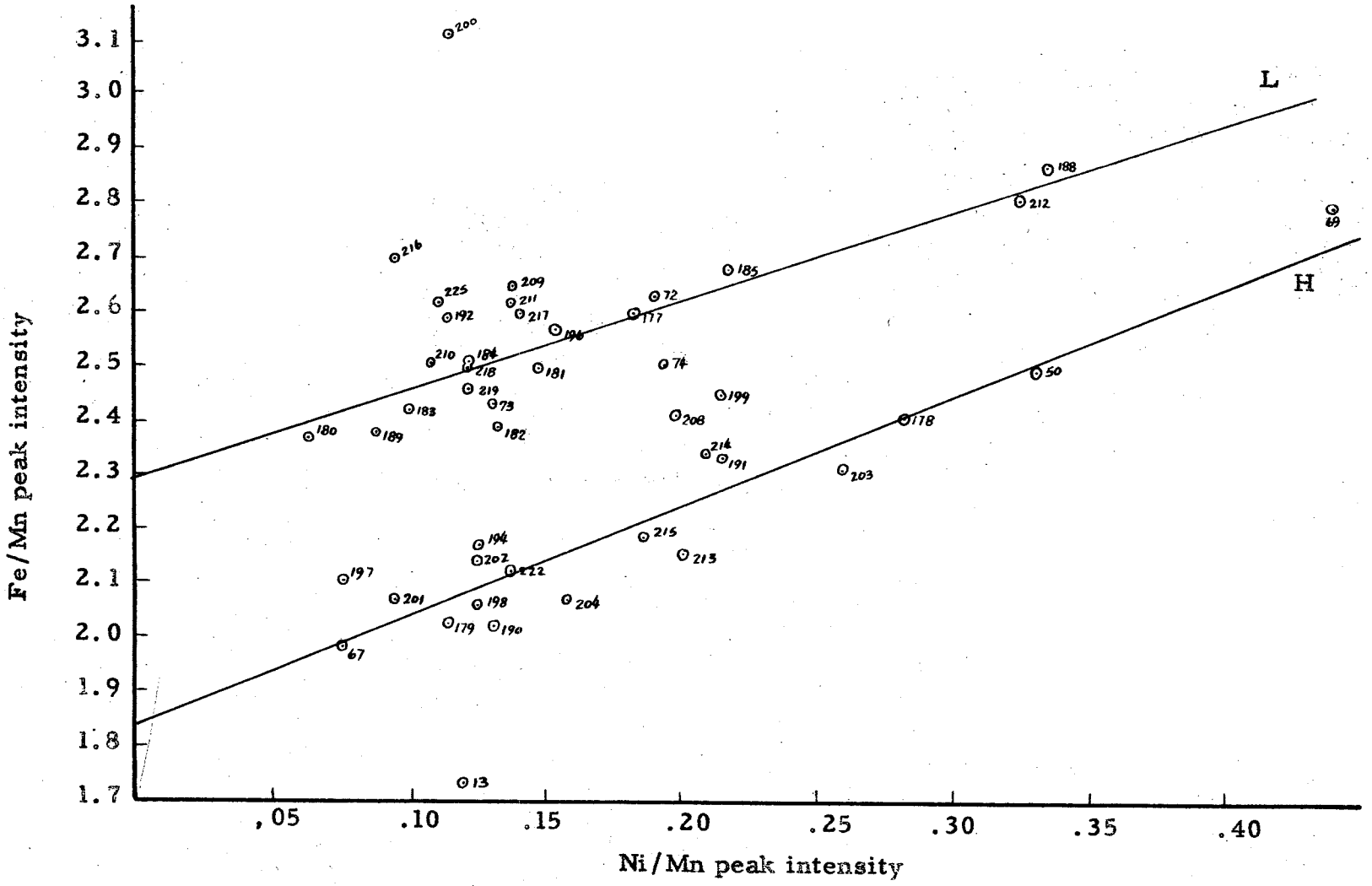

Figure 21. Relation between Fe/Mn and Ni/Mn peak intensity ratios for chondrite falls.

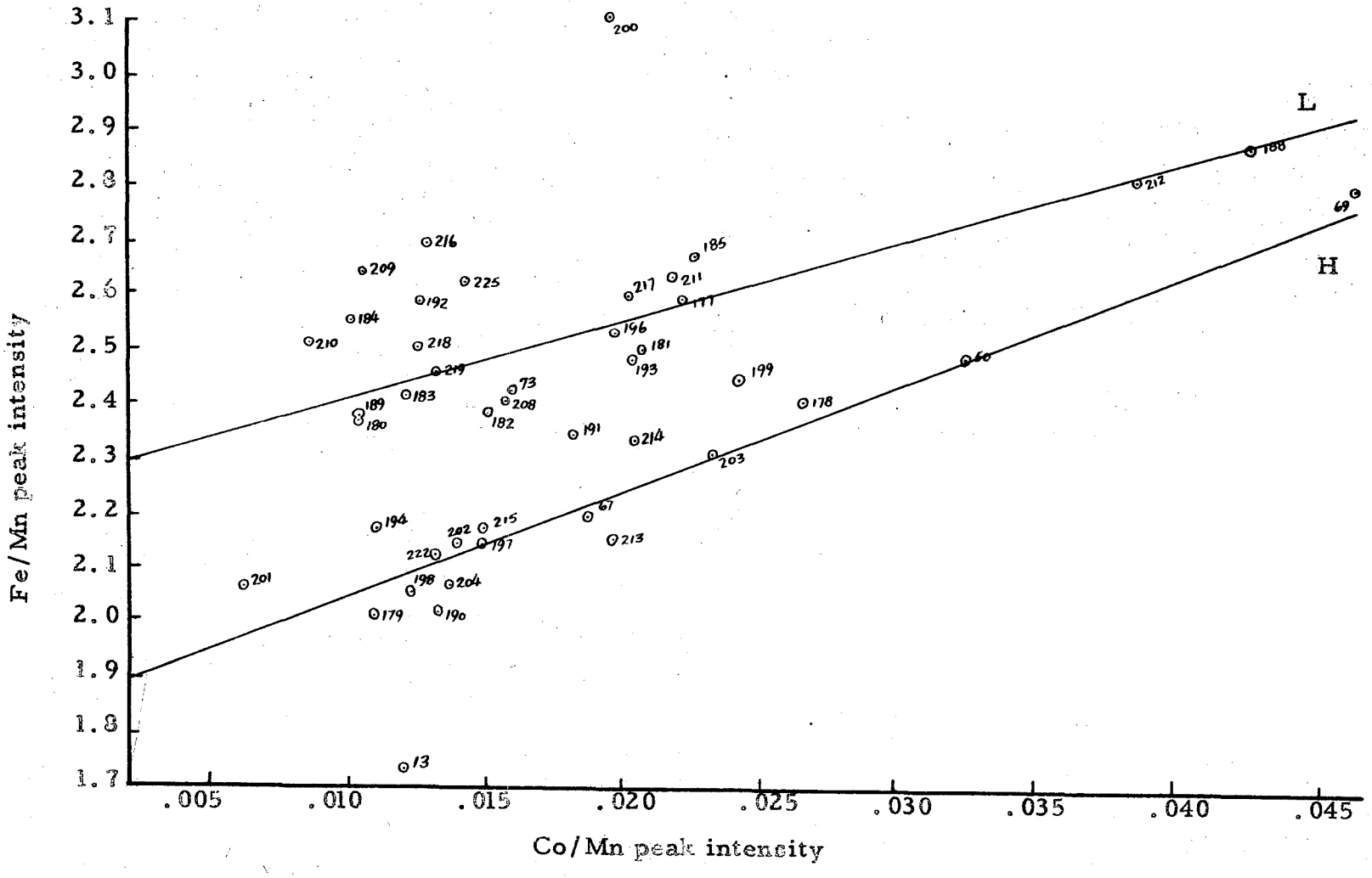

Figure 22. Relation between Fe/Mn and Co/Mn peak intensity ratios for chondrite falls.

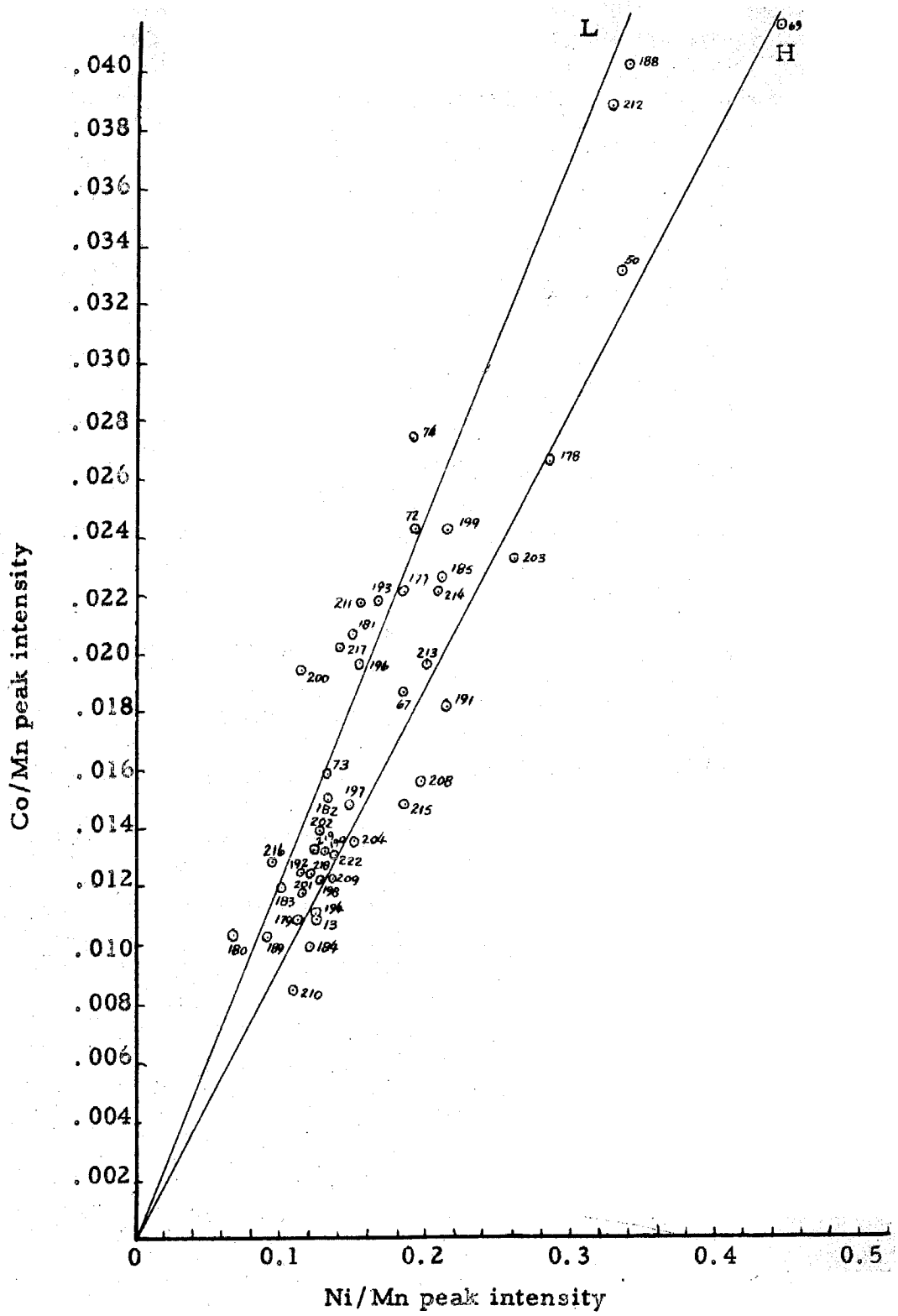

Figure 23. Relation between Co/Mn and Ni/Mn peak intensity ratios for chondrite falls.

The powdered chondrite falls were divided into magnetic and non-magnetic portions manually by passing a permanent alnico magnet over each sample. Ideally, the magnetic portion should be made up of only the metal phase and should only contain iron, nickel and cobalt. The non-magnetic phase should be made up of silicates and troilite. Inspection of both splits with a binocular microscope showed that the magnetic portion had a large amount of silicate and troilite contamination, while the non-magnetic portion was contaminated with metal to a much lesser degree. The data obtained when these splits were run in the X-ray fluorescence spectroscope are given in Table XXVIII.

If for each of the chondrites, a plot of the Fe/Mn vs Ni/Mn peak intensity ratios is made for the unsplit sample, the silicate split and the magnetic split, a straight line can be drawn through the three points. Figure 24 illustrates such a plot for the Olmedilla de Alarcon chondrite. If we assume that all the nickel is present in the metallic magnetic phase of the meteorite, we can extrapolate the line to the point where the Ni/Mn ratio is zero and there obtain the Fe/Mn peak intensity ratio in the pure non-magnetic portion of the chondrite. If there is no manganese present in the metal phase of the meteorite the slope of the line is equal to the Fe/Ni peak intensity ratio in the pure magnetic phase. Similar information can be obtained from a Fe/Mn vs Co/Mn plot.

The values of the Fe/Mn peak intensity ratios (non-magnetic) have been calculated for each chondrite from both the nickel and cobalt plots.

Table XXVIII. X-Ray Fluorescence Spectroscopic Data for Magnetic and Non-magnetic Splits of Chondrites

Number	Meteorite	Peak Intensities					Peak Intensity Ratios			
		Co	Fe	Ni	Cr	Mn	Co/Mn	Fe/Mn	Ni/Mn	Cr/Mn
M-213-N*	Alexandrovsky	5.70	2070	67.98	1059	1090	0.00523	1.90	0.0624	0.972
M-213-M		66.55	2710	648.1	789.8	610.3	0.1091	4.44	1.06	1.29
M-183-N	Alfianello	3.45	1879	32.24	655.5	832.2	0.00415	2.26	0.0387	0.788
M-183-M		43.47	1017	359.7	286.7	184.2	0.236	5.52	1.95	1.56
M-179-N	Allegan	2.21	1535	25.37	780.3	837.2	0.00264	1.88	0.0303	0.932
M-179-M		43.59	1410	287.9	375.8	273.9	0.159	5.15	1.05	1.37
M-67-N	Beardsley	4.98	1921	72.93	809.4	971.3	0.00513	1.98	0.0751	0.833
M-67-M		76.87	2498	543.4	587.8	458.5	0.167	5.45	1.19	1.28
M-181-N	Bjurbole	10.70	2331	67.07	889.8	983.9	0.0109	2.37	0.0631	0.904
M-181-M		70.41	1168	511.1	410.3	169.9	0.415	6.88	3.36	2.42
M-192-N	Chateau Renard	4.17	1636	38.27	1017	1020	0.00409	1.60	0.0375	0.996
M-192-M		45.65	2066	336.0	609.2	593.5	0.0769	3.48	0.566	1.03
M-184-N	Colby, Wisc.	5.04	2311	41.23	829.9	929.5	0.00542	2.49	0.0444	0.893
M-184-M		35.83	1203	308.9	396.8	323.8	0.111	3.72	0.954	1.23
M-180-N	Dhurmsala	7.61	2260	39.48	1082	967.3	0.00787	2.34	0.0408	1.12
M-180-M		14.95	256.1	102.6	240.5	70.62	0.212	3.63	1.45	3.41
M-210-N	Elenovka	3.08	2472	23.79	944.4	994.9	0.00310	2.49	0.0239	0.949
M-210-M		67.56	1761	540.9	415.0	394.1	0.171	4.47	1.37	1.05
M-69-N	Forest City	25.72	2137	266.3	811.5	895.3	0.0287	2.39	0.297	0.906
M-69-M		64.37	2991	531.6	984.5	823.2	0.0781	3.63	0.646	1.20

Table XXVIII(continued)

		Co	Fe	Ni	Cr	Mn	Co/Mn	Fe/Mn	Ni/Mn	Cr/Mn
M-214-N	Ichkala	6.40	2226	71.40	1034	1111	0.00576	2.00	0.0643	0.931
M-214-M		86.68	2661	674.5	478.0	381.6	0.227	6.97	1.77	1.28
M-193-N	Knyahinya	12.46	2403	102.6	1156	1002	0.0124	2.40	0.102	1.15
M-193-M		61.45	2079	590.6	724.3	633.3	0.0970	3.28	0.933	1.14
M-219-N	Kuleshovka	6.78	2482	29.34	985.0	1048	0.00647	2.37	0.0280	0.940
M-219-M		90.32	2355	631.6	496.7	510.7	0.177	4.61	1.24	0.973
M-209-N	Konashak	8.87	2644	69.39	991.0	1032	0.00859	2.56	0.0672	0.959
M-209-M		50.81	2496	478.3	785.8	755.5	0.0673	3.30	0.633	1.04
M-185-N	Marion	14.07	2277	123.4	865.8	910.5	0.0155	2.50	0.136	0.851
M-185-M		52.19	1149	391.7	340.0	191.3	0.273	6.01	2.05	1.78
M-189-N	Maxiba	4.17	2319	32.52	909.3	970.2	0.00430	2.39	0.0335	0.937
M-189-M		77.87	2093	628.0	453.3	457.7	0.170	4.57	1.37	0.990
M-73-N	Mocs	8.48	2364	64.11	922.1	1027	0.00826	2.30	0.0624	0.898
M-73-M		92.82	2105	629.4	408.1	369.9	0.251	5.69	1.70	1.10
M-188-N	Modoc	28.99	2400	194.4	606.3	867.7	0.0334	2.77	0.224	0.699
M-188-M		47.42	1745	416.8	506.3	469.0	0.101	3.72	0.889	1.08
M-212-N	Mordvinovka	34.05	2770	246.7	887.1	1012	0.0336	2.74	0.244	0.876
M-212-M		110.6	2125	993.7	400.6	298.2	0.371	7.13	3.33	1.34
M-190-N	Mount Browne	2.41	2003	35.89	1088	1101	0.00219	1.82	0.0326	0.988
M-190-M		52.27	1931	432.7	585.5	485.7	0.108	3.98	0.891	1.21
M-198-N	Nanjemoy	2.50	1800	31.57	934.0	972.8	0.00257	1.85	0.0325	0.960
M-198-M		54.49	1711	330.8	424.5	283.4	0.192	6.04	1.17	1.50
M-182-N	New Concord	5.33	2220	37.54	906.1	988.4	0.00539	2.25	0.0380	0.917
M-182-M		59.99	1377	356.4	343.1	242.4	0.248	5.68	1.47	1.42

Table XXVIII(continued)

		Co	Fe	Ni	Cr	Mn	Co/Mn	Fe/Mn	Ni/Mn	Cr/Mn
M-225-N	Nikolskoie	6.09	2635	45.67	982.2	1062	0.00573	2.48	0.0430	0.925
M-225-M		69.77	1792	621.1	448.3	352.0	0.198	5.09	1.76	1.27
M-194-N	Ochansk (1)	4.50	2114	56.40	1074	1057	0.00426	2.00	0.0534	1.02
M-194-M		88.68	2533	554.7	440.7	297.3	0.298	8.52	1.87	1.48
M-215-N	Ochansk (2)	6.17	2143	17.91	1115	1161	0.00531	1.85	0.0154	0.960
M-215-M		64.59	2071	545.5	531.6	346.0	0.187	5.99	1.58	1.54
M-200-N	Olivenza	8.49	2788	37.82	881.6	948.4	0.00895	2.94	0.0399	0.930
M-200-M		61.49	722.7	466.5	307.4	171.7	0.358	4.21	2.72	1.79
M-201-N	Olmedilla de	7.87	2074	31.65	1030	1066	0.00738	1.95	0.0297	0.966
M-201-M	Alarcon	66.75	2290	420.1	559.0	431.6	0.155	5.30	0.973	1.30
M-13-N	Pantar	4.99	2065	140.4	1044	1338	0.00373	1.54	0.105	0.780
M-13-M		79.05	2679	668.7	666.0	504.0	0.157	5.32	1.33	1.32
M-191-N	Parnallee	15.52	2424	154.5	1070	1110	0.0140	2.18	0.139	0.964
M-191-M		40.01	2059	453.0	801.5	643.5	0.0622	3.20	0.704	1.25
M-211-N	Pervomaisky	10.94	2766	83.54	993.0	1099	0.00995	2.52	0.0760	0.903
M-211-M		79.72	2346	595.5	517.9	507.5	0.157	4.62	1.17	1.02
M-204-N	Pultusk	7.86	2078.4	79.02	950.0	1048	0.00750	1.98	0.0754	0.907
M-204-M		64.01	2312.2	475.0	621.7	493.3	0.130	4.69	0.963	1.26
M-50-N	Richardton	21.72	1982	172.2	916.1	919.1	0.0236	2.16	0.187	0.997
M-50-M		88.63	3008	833.0	728.3	485.1	0.183	6.20	1.72	1.50
M-177-N	St. Michel	5.49	1884	46.02	800.0	799.8	0.00686	2.36	0.0575	1.00
M-177-M		33.79	1342	291.2	456.0	369.8	0.0914	3.63	0.788	1.23
M-208-N	Saratov	6.96	2447	95.38	1060	1085	0.00642	2.26	0.0879	0.978
M-208-M		51.34	2397	501.3	748.2	598.5	0.0858	4.01	0.838	1.25

Table XXVIII (continued)

		Co	Fe	Ni	Cr	Mn	Co/Mn	Fe/Mn	Ni/Mn	Cr/Mn
M-216-N	Savtschenskoje	6.76	2787	21.25	1025	1057	0.00640	2.64	0.0201	0.970
M-216-M		108.1	2004	904.7	695.7	493.5	0.219	4.06	1.83	1.41
M-217-N	Stavropol	10.65	2439	37.70	988.7	998.6	0.0107	2.44	0.0378	0.990
M-217-M		76.65	1790	504.2	372.1	323.6	0.237	5.53	1.56	1.15
M-196-N	Tane	11.84	2548	88.38	963.6	1049	0.0113	2.43	0.0842	0.918
M-196-M		89.81	2097	534.7	535.1	422.8	0.212	4.96	1.26	1.27
M-197-N	Uberaba	9.92	2109	75.64	1019	1002	0.00990	2.11	0.0755	1.02
M-197-M		73.87	1795	489.8	560.1	399.4	0.185	4.50	1.23	1.40
M-199-N	Weston	7.45	2003	65.82	969.0	1010	0.00738	1.98	0.0652	0.960
M-199-M		48.20	2697	382.6	982.0	820.7	0.0587	3.29	0.466	1.20
M-203-N	Yatoor	9.00	1939	121.4	935.7	924.1	0.00974	2.10	0.131	1.01
M-203-M		52.37	1795	460.2	454.5	306.1	0.171	5.87	1.50	1.49
M-202-N	Zhovtnevyi	3.72	2064	41.58	938.5	1068	0.00348	1.93	0.0389	0.879
M-202-M		68.54	2529	536.1	612.2	622.8	0.110	4.06	0.861	0.983

*M-No.-N non-magnetic split.

*M-No.-M magnetic split.

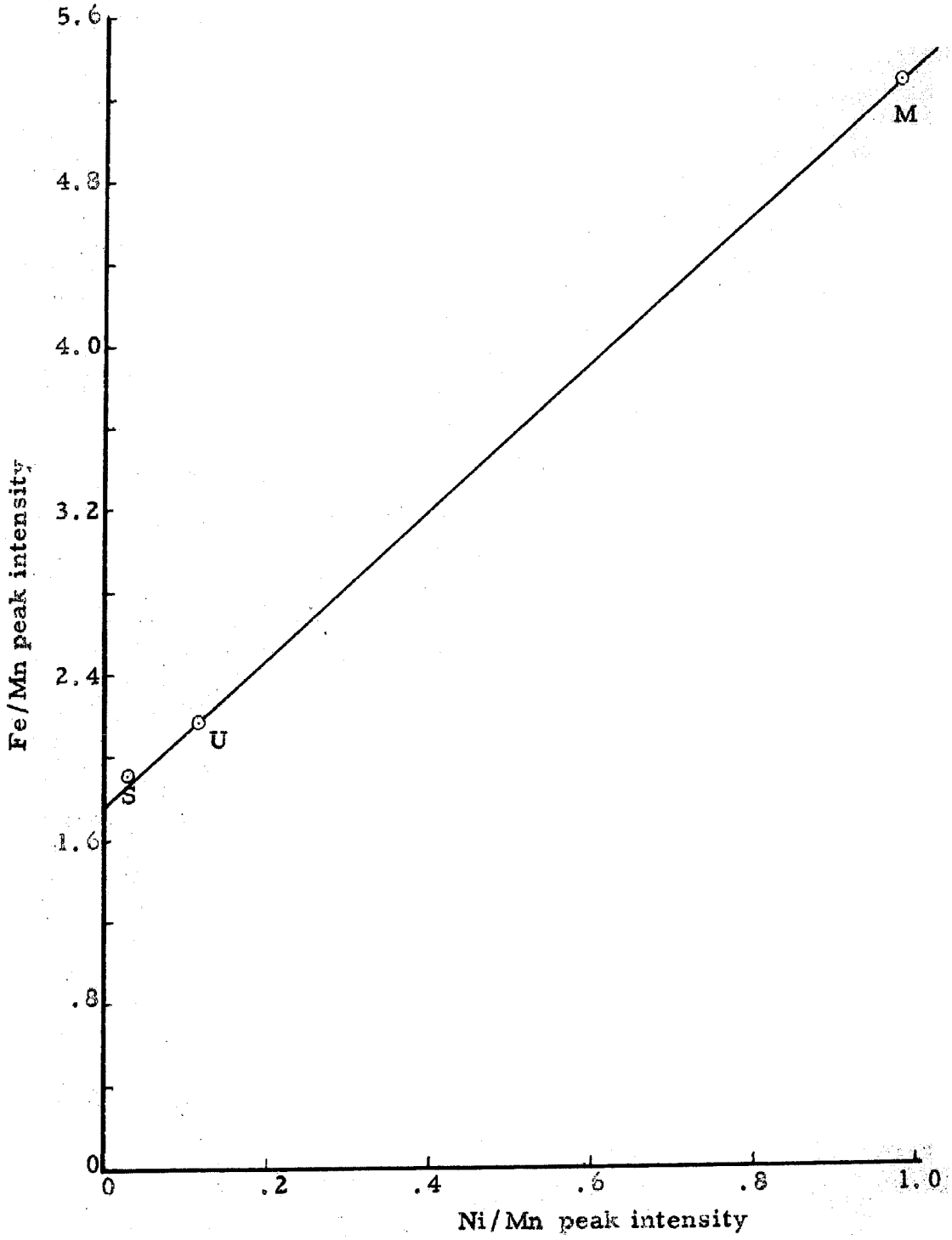

Figure 24. Plot of Fe/Mn vs Ni/Mn peak intensities for Olmedilla de Alarcon and its magnetic and non-magnetic splits.

The results and averages are given in Table XXIX, along with the Fe/Ni and Fe/Co peak intensity ratios in the pure magnetic phase.

Figure 25 shows plots of Fe/Mn vs Ni/Mn for both the unsplit chondrites and their non-magnetic splits. The joins for each of the meteorites tend to fall along one of two separate lines, indicating the presence of two major groups. The chondrite Olivenza (M-200) seems to form a unique join line of its own, and Pantar and Chateau Renard have joins which are at sharp angles to the general trends.

The two major groups correspond to the high and low iron groups of Urey and Craig. If a histogram showing the frequency of occurrence of the Fe/Mn peak intensity ratios in the non-magnetic phase is constructed, a bimodal distribution is found as shown in Figure 26. This distribution is the same as found by Urey and Craig for iron in the silicate phase. This similar distribution for non-magnetic Fe/Mn peak intensities is possible because both the manganese and troilite concentrations are relatively constant in most chondrites.

Histograms of the frequency of occurrence of metallic phase Fe/Co and Fe/Ni peak intensity ratios have bimodal distributions. A good separation between the modes can be made if the values of the metallic Fe/Co and Fe/Ni peak intensity ratios are plotted against each other. Figure 27 shows such a plot. The group with the higher Fe/Ni and Fe/Co ratios is a more highly reduced system. This group corresponds to the group in Figure 25 with the lower Fe/Mn ratio.

Included in Table XXIX is the apparent group for each chondrite fall as indicated by the data in Figures 23, 25, and 27. The designation of

Table XXIX. Peak Intensity Ratios for Metallic and Non-Metallic Splits and Apparent Group for Each Chondrite

Meteorite	Non-metal $\frac{Fe}{Mn}$ (Fe-Co)	Non-metal $\frac{Fe}{Mn}$ (Fe-Ni)	$\frac{Fe}{Mn}$ avg.	Metal $\frac{Fe}{Co}$	Metal $\frac{Fe}{Ni}$	This paper	Urey & Craig
Alexandrovsky	1.77	1.74	1.76	24.5	2.54	H	
Alfianello	2.20	2.19	2.20	14.1	1.71	L	
Allegan	1.83	1.79	1.81	11.3	3.20	H	H
Beardsley	1.87	1.74	1.81	21.4	3.13	H	
Bjurbole	2.26	2.28	2.27	10.5	1.38	L	L
Chateau Renard	1.50	1.47	1.48	25.6	3.55	?	
Colby, Wisc.	2.45	2.43	2.44	11.2	1.35	L	
Dhurmsala	2.28	2.29	2.29	7.24	1.03	L	
Elenovka	2.45	2.45	2.45	11.8	1.47	L	
Forest City	1.66	1.32	1.49	25.2	3.58	H	H
Ichkala	1.87	1.82	1.84	22.4	2.92	H	
Knyahinya	2.27	2.29	2.28	10.5	1.07	L	H
Krasnyi-Ugol	2.41	2.40	2.41	12.9	1.73	L	
Kuleshovka	2.28	2.31	2.29	13.2	1.87	L	
Kunashak	2.45	2.47	2.46	12.6	1.31	L	
Marion	2.29	2.25	2.27	13.6	1.83	L	
Maziba	2.34	2.34	2.34	13.0	1.63	L	
Mocs	2.19	2.17	2.18	14.0	2.07	L	
Modoc	2.29	2.44	2.37	14.1	1.44	L	L
Mordvinovka	2.30	2.31	2.30	13.0	1.43	L	
Mount Browne	1.86	1.73	1.80	18.8	2.51	H	H
Nanjemoy	1.79	1.73	1.76	22.1	3.69	H	
New Concord	2.17	2.15	2.16	14.2	2.40	L	
Nikolskoie	2.40	2.42	2.41	13.6	1.52	L	
Ochansk (1)	1.91	1.81	1.86	22.2	3.60	H	
Ochansk (2)	1.72	1.81	1.76	22.8	2.65	H	
Olivenza	2.91	2.92	2.91	3.63	0.47	L?	[L]
Olmedilla de Alarcon	1.78	1.84	1.81	22.8	3.56	H	H
Pantar	1.45	1.22	1.37	24.6	3.09	?	
Parnallee	1.89	1.93	1.91	21.1	1.80	H	
Pervomaisky	2.37	2.37	2.37	14.3	1.92	L	
Pultusk	1.82	1.75	1.79	22.1	3.05	H	
Richardton	1.56	1.66	1.61	25.4	2.64	H	
St. Michel	2.25	2.26	2.25	15.1	1.74	L	L
Saratov	2.11	2.05	2.08	22.4	2.38	H?	L
Savtschinskoje	2.59	2.62	2.60	7.98	2.62	L	
Stavropol	2.30	2.37	2.33	13.7	2.03	L	
Tane	2.29	2.25	2.33	12.6	2.14	L	
Uberaba	1.97	1.95	1.96	13.7	2.08	H?	
Weston	1.80	1.77	1.78	25.4	3.25	H	
Vatoor	1.87	1.83	1.85	20.0	2.59	H	
Zhovtnevyi	1.86	1.83	1.85	20.0	2.59	H	

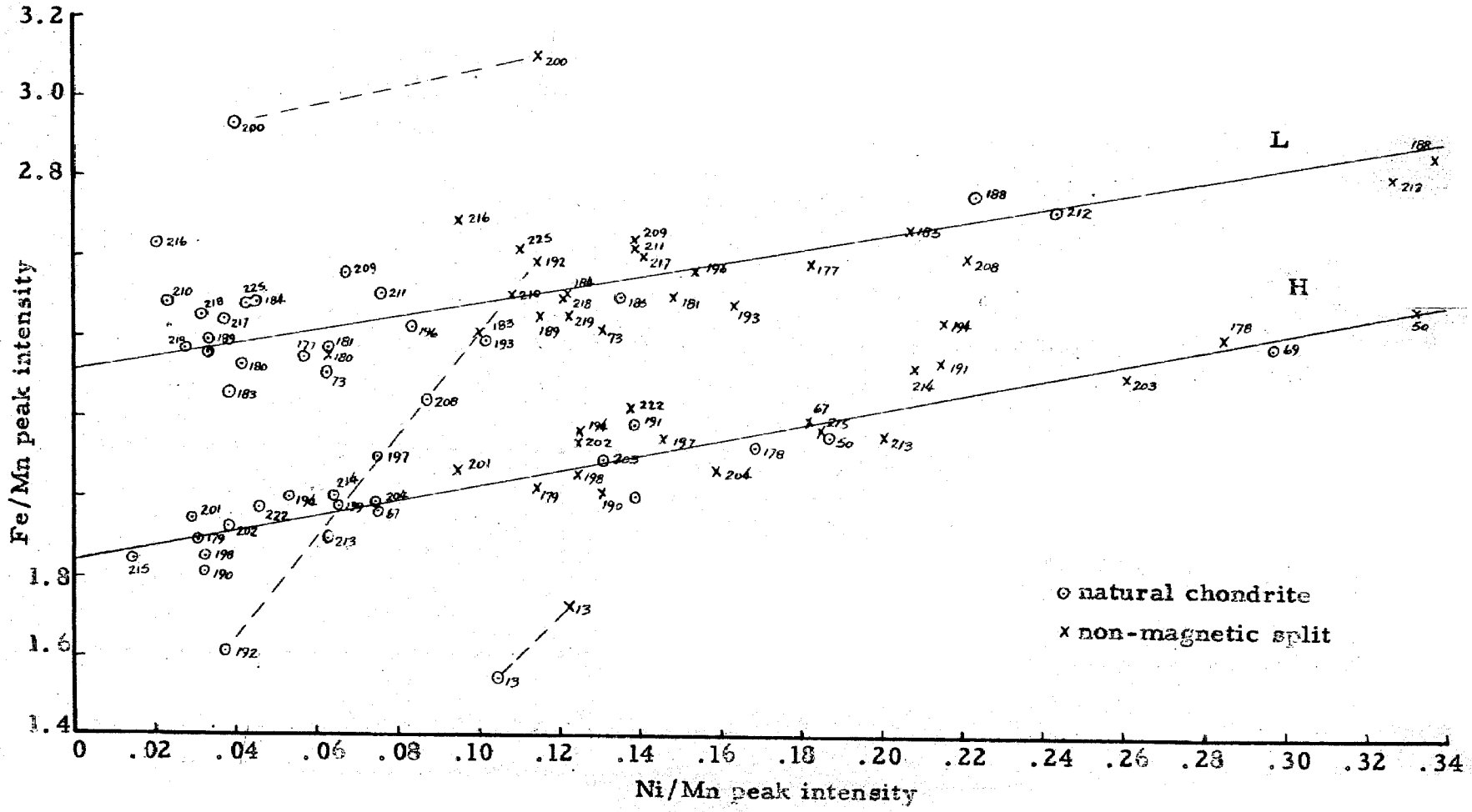

Figure 25. Relation between peak intensity ratios for chondrites and non-magnetic phase of chondrites.

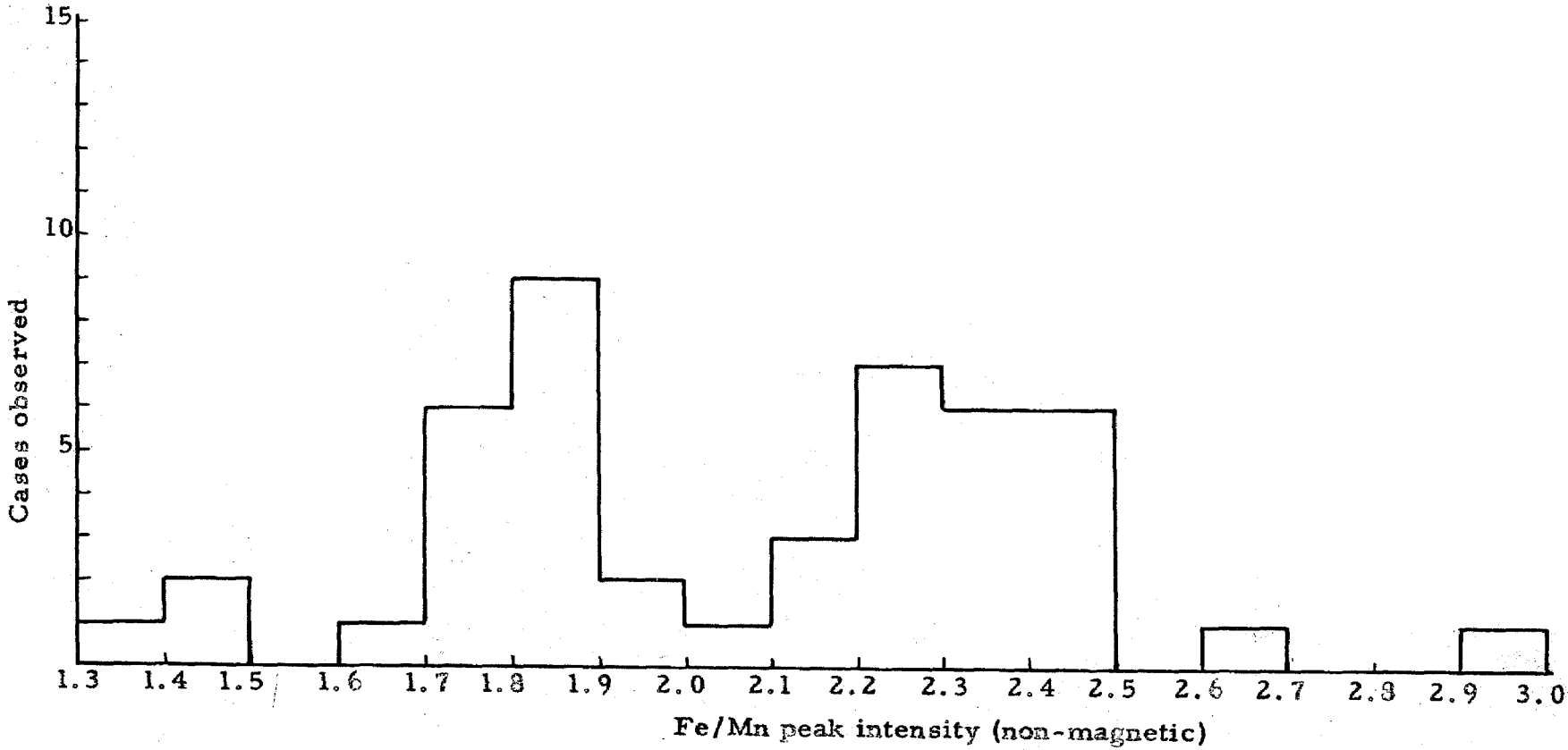

Figure 26. Frequency distribution of Fe/Mn peak intensity ratios in non-magnetic splits of chondrites.

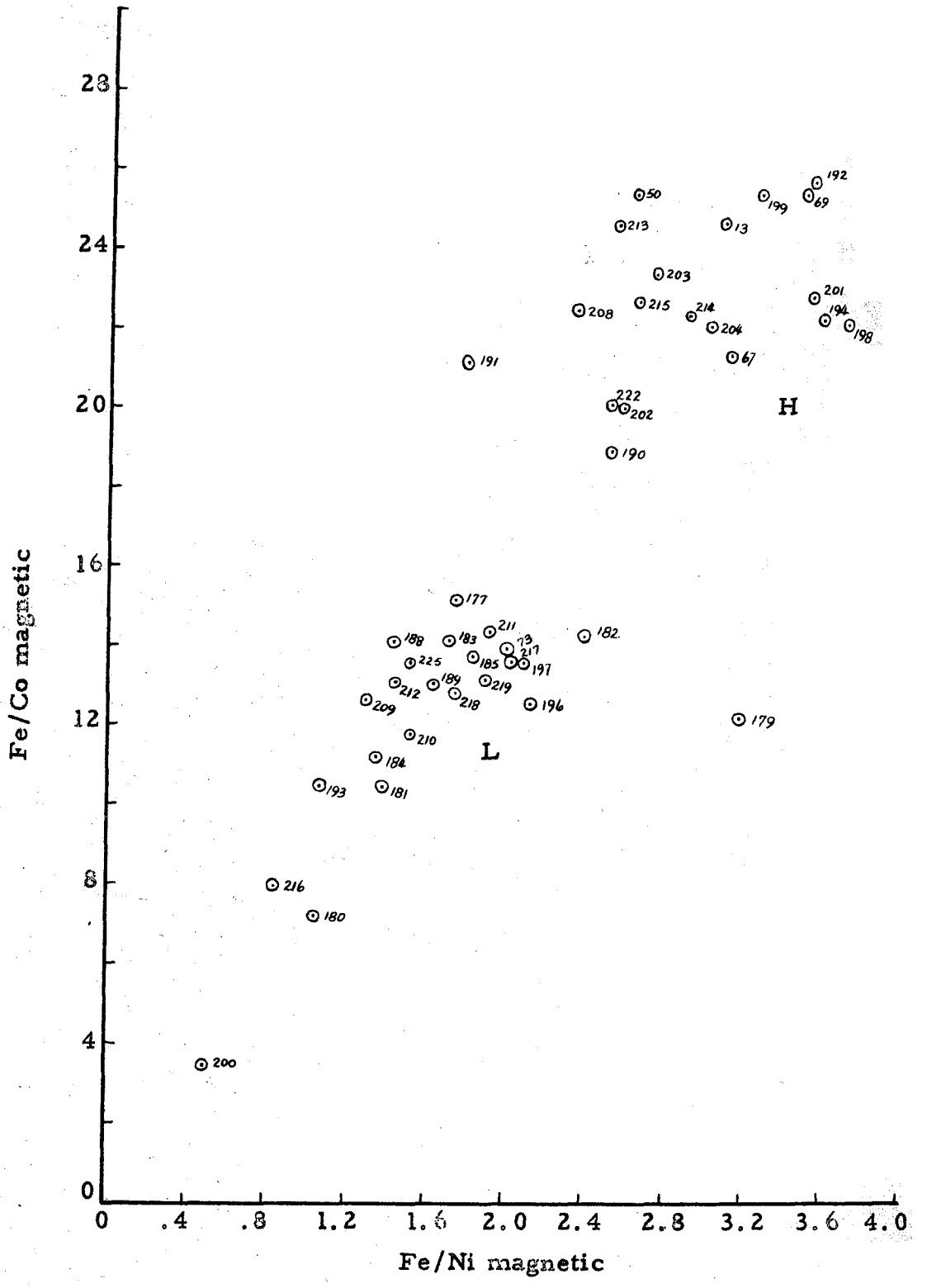

Figure 27. Magnetic phase peak intensity ratios for 43 chondrite falls.

high iron (H) or low iron (L) for a sample is the same as used by Urey and Craig. Also shown is the group designation given by Urey and Craig to the chondrites included in their compilation.

Conclusions

X-ray fluorescence spectroscopy has been used to confirm the presence of grouping in chondrites. Untreated chondrite falls can be classified into groups by determining their positions on peak intensity ratio plots of Ni/Mn vs Fe/Mn, Co/Mn vs Fe/Mn, and Co/Mn vs Ni/Mn.

Urey and Craig have shown that there is a difference between the Ni/Fe ratios in the two main chondrite groups. This investigation confirms this and indicates that there is also a difference in the Co/Fe ratios. The difference in the average Co/Ni peak intensity ratio for each group is probably not caused by differences in the chemical Co/Ni ratio, but is rather a secondary effect caused by other chemical and physical differences in the chondrites.

More reliable and consistent results can be obtained by classifying the chondrites on the basis of their Fe/Co and Fe/Ni peak intensity ratios in the metallic phase, and their Fe/Mn peak intensity ratios in the non-magnetic phase. There is good agreement between the chondrites placed in each group based on the X-ray fluorescence data and those classified by wet chemical analysis data.

The validity of extending the group trends found for the chondrite falls into the chondrite finds has not been fully investigated. Independent means of classification appear necessary to properly define group boundries. Preliminary inspection indicates that most of the chondrite

falls appear to be members of a single group.

Several chondrites do not fall in either of the two main groups. The Olivenza chondrite had unique results for all of the correlations presented. This fact lessens the probability that there was an error in treatment, and indicates that it is a member of a rarer group of chondrites. X-ray fluorescence spectroscopic data should be useful for indicating and checking odd chondrite compositions.

Chondrites are difficult to obtain in large quantities, so that any program requiring the analysis of a large number of chondrites would be limited in accuracy by the small samples available for each chondrite. The small samples generally available are not good samples of the total meteorite. For this reason the accuracy obtained in the above investigation seems to be practical for the problem at hand. It does not appear that a quantitative analysis of the untreated chondrites is possible by this method. It does appear possible to develop a method of quantitative analysis for chondrites if they are first treated in such a way as to put the sample into a more homogeneous chemical and physical state.

References

1. Swift, E. H., and Butler, E. A., Anal. Chem. 28, 146-154 (1956).

2. Butler, E.A., and Swift, E. H., Anal. Chem. 29, 491-495 (1957).

3. Cox, E. G., Wardlaw, W., and Webster, K. C., J. Chem. Soc., 775-81 (1936).

4. Buch, D. G., Zuehlke, C. W., Ballard, A. E., Anal. Chem. 31, 1368-1371 (1959).

5. Beale, R. S., Hutchison, A. W., and Chandlee, G. C., Anal. Chem. 13, 240-242 (1941).

6. Peters, D. G., and Swift, E. H., Talanta 1, 30-38 (1958).

7. Bowersox, D. F., and Swift, E. H., Anal. Chem. 30, 1288-1291 (1958).

8. Urey, H. C., and Craig, H., Geochim. et Cosmochim. Acta, 4, 36-82 (1953).

9. Von Engelhardt, W., Chem. Erde 10, 187-208 (1936).

10. Pinson, W. H., Ahrens, L. H., and Franck, M. L., Geochim. et Cosmochim. Acta 4, 251-259 (1953).

11. Hamaguchi, H., Reed, G. W., and Turkevich, A., Geochim. et Cosmochim. Acta 12, 337-339 (1957).

12. Rankama, K. and Sakama, T. G., Geochemistry, U. of Chicago Press, Chicago, 1950.

13. Brown, H., Rev. of Mod. Phys. 21, 625-634 (1949).

14. Urey, H. C., Phys. Rev. 88, 248-254 (1952).

15. Goldschmidt, V. M., Skrifter Norske Videnskaps-Akad. Oslo I. Mat-Naturv Klasse, 1937, No. 4, 120-121 (1938).

16. Wahl, W., and Wiik, H. B., Geochim et Cosmochim. Acta 1, 123-126 (1951).

17. Wahl, W., and Wiik, H. B., Bull. Comm. Geol. Finlande No. 150, 5-18 (1950).

18. Wiik, H. B., Comm. Socret. Scient. Fenn. Phys.-Math. 14, No. 14, 1-8 (1950).

19. Lovering, J. F., Nichiporuk, W., Chodos, A., and Brown, H., Geochim. et Cosmochim. Acta 11, 263-278 (1957).

20. Yavnell, A. A., Geochemistry, 78-92 (1956).

21. Foote, W. M., Am. J. Sci. 34, 437-456 (1912).

22. Pollack, E., and Brown, H., unpublished research.

23. Suess, H., and Urey, H. C., Rev. Mod. Phys. 28, 53-74 (1956).

24. Pollack, E., unpublished research.

Propositions

1. The complex compounds $\left[Au(SC(NH_2)CH_3)_2\right]$ Br and $\left[Cu(SC(NH_2)CH_3)_4\right]$ Br have been prepared (1). It is proposed that an attempt be made to investigate the reactions of Au(I) and Cu(I) with thioacetamide. A thioacetamide inhibition effect similar to that found with silver is expected.

2. Part of the Varpaisjarvi chondrite was destroyed by weathering in a very short time (2). A study of the physical strength and resistance to weathering of chondrites is proposed. An indication of the type of sample available from chondrite finds would result from this data.

3. Free energy data indicate that the phase In_5S_6 in the phase diagram In-In_2S_3, is not stable at room temperature. It is proposed that this possibility be investigated.

   ΔF for the reaction $In_2S + H_2 = 2In + H_2S$ should be determined as an aid in explaining inconsistencies in the literature regarding the occurrence and properties of In_2S, (3)(4).

4. A preliminary investigation of the germanium and cobalt concentrations in the metal phase of chondrites gave the following data:

Meteorite	% metal in magnetic sample	Conc. in metal Ge ppm	Co %
Knyahinya	44	155	0.87
Mocs	67	123	0.72
Ochansk	75	69	0.52
Olmedilla de Alarcon	62	58	0.55
Pantar	67	66	0.51
Pultusk	47	87	0.77
Zhovtnevyi	45	104	0.80

Several suggestions to account for the difference between these data and that predicted by Lovering et al are proposed (5).

5. A study of the nature of the silver-thioacetamide complex in solution is proposed.

6. Large quantities of shale are obtained as a by product at the U.S. Borax Corporation, Boron, California plant. This shale has been thoroughly investigated as an ore for several rare metals, but is not of a high enough grade to treat at the present time. An investigation of its direct use as a ceramic raw material is proposed.

7. The Nuevo Laredo stony meteorite contains unusually high concentrations of barium and uranium (6). The uranium contents of other high barium stony meteorites should be determined to see if there is a direct correlation between the barium and uranium contents.

8. A study of cosmic-ray induced radionuclides, with half lives from 100 to 10, 000 years, in meteorites is proposed. Data obtained could be used to indicate the terrestrial age of meteorite finds.

9. If there is a thallous ion-thioacetamide intermediate in the precipitation of thallous sulfide by thioacetamide, the reaction should have an ionic strength effect.

10. A simple method for the hydrostatic testing of bottles is proposed.

References for Propositions

1. Sidgwick, N. V., The Chemical Elements and Their Compounds, 142, London (1950).

2. Wahl, W. A., and Wiik, H. B., Bull. Comm. Geol. Finlande, 23, No. 150, 5-18 (1950).

3. Thomson, A. J., Stubbs, M. F., and Schufle, J. A., J. Am. Chem. Soc. 76, 341-343 (1954).

4. Stubbs, M. F., Schufle, J. H., Thomson, A. J., and Duncan, J. M., J. Am. Chem. Soc. 74, 1441-1443 (1952).

5. Lovering, J. F., Nichiporuk, W., Chodos, A. and Brown, H., Geochim. et Cosmochim. Acta 11, 277-278 (1957).

6. Hamaguchi, H., Reed, G. W., Turkevich, A., Geochim. et Cosmochim. Acta 12, 337-339 (1957).